Effects of an anthropogenic stressor on carbon biogeochemical processes and fluxes in water to land transition zones of ponds

By

Bai Houefa Caroline Bertille Ganglo

Accepted Dissertation thesis for the partial fulfillment of the requirements for a

Doctor of Natural Sciences

Fachbereich: Natur- und Umweltwissenschaften

Rheinland-Pfälzische Technische Universität Kaiserslautern-Landau

Thesis examiners:

Prof. Dr. Andreas Lorke, Landau

Dr. Clara Mendoza-Lera, Landau

Date of disputation

26.04.2023

Publications

This thesis is based on the following manuscript and publications (ordered by publication date):

Ganglo, C., Manfrin, A., Mendoza-Lera, C., & Lorke, A. (2022). Biocide treatment for mosquito control increases methane emissions in floodplain pond mesocosms. Frontiers in Water, *4*(9), 10.

https://doi.org/10.3389/frwa.2022.996898

Ganglo, C., Mendoza-Lera, C., Manfrin, A., Bolpagni R., Gerstle, V., Kolbenschlag S., Bollinger, E., Schulz, R. & Lorke, A. (2023). Does biocide treatment for mosquito control alter carbon dynamics in floodplain ponds? Science of the total environment , *872*(2), 161978.

https://doi.org/10.1016/j.scitotenv.2023.161978

Ganglo, C., Manfrin, A., Mendoza-Lera, C. & Lorke, A. (2023). Effects of chironomids density and mosquito biocide on methane dynamics in freshwater sediments. Plos One (resubmitted 30 June 2023)

Table of contents

List of figures

Summary

More than 2.4 % of the continental surface area is covered by shallow aquatic systems such as ponds. Despite occupying only a tiny fraction of the earth's surface area, ponds are globally significant sites of carbon cycling. They receive carbon, process it and emit large amounts of greenhouse gases into the atmosphere, the most potent among others are carbon dioxide (CO_2) and methane (CH_4). Tube-dwelling macroinvertebrates, such as chironomid larvae (Diptera: Chironomidae) change biogeochemical functions, particularly in shallow aquatic systems. Through bioturbation involving burrow ventilation and sediment particle reworking, tube-dwelling macroinvertebrates enhance solute exchange between sediment and water. Stimulate the benthic microbial community, and regulate organic matter decomposition. This doctoral project integrates aquatic carbon biogeochemical processes with the research field of ecology to relate knowledge of biogeochemical reaction dynamics upon application of the mosquito control biocide *Bacillus thuringiensis israelensis* (Bti), which is an entomopathogen that kills mosquitos larvae, but also reduces the abundance of chironomids. The interdisciplinary approach combines field measurements and laboratory experiments. First, an experiment was conducted in 12 outdoor floodplain ponds mesocosms (FPMs), where the effect of Bti application on carbon transformations, carbon pools, and carbon fluxes was monitored for one year. Half of the FPMs were Bti-treated and the remaining half were controls. The study revealed that seasonal variations governed changes in transformations, pools, and fluxes on the carbon components. Treated FPMs, for which a 26 % and 41% reduction in emerging merolimnic insects and macroinvertebrates abundance, respectively was reported (in companion studies) were higher CH_4 emitters (137% higher than in control mesocosms). The higher CH_4 emissions occurred specifically in the shallow zone where the macroinvertebrate reduction was also significant. In the same treated FPMs, a tendency towards less dissolved organic carbon in porewater (33% lower than in control mesocosms), was potentially caused by the reduction in bioturbation activities of chironomids, whereas the remaining measured components of the carbon budget were not affected by the treatment with Bti. Second, laboratory microcosm (LMs) experiments that excluded environmental constraints were developed, to clarify the findings of the FPMs experiment. Out of the 15 microcosms, 3 were treated (each set) with standard Bti dose, 5 times standard Bti dose, chironomid larvae with low and high areal density, and control. The findings demonstrated that bioturbation increased CH_4 and CO_2 efflux and sediment oxygen (O_2) consumption, while it did not affect the net production of CH_4 and CO_2. The negligible effect on net production rates in treatments with chironomids indicates that the increase in emissions rate was predominantly caused by bioturbation, which reduced the gas accumulation in the sediment. In the absence of chironomids, the application of any dose of Bti led to a three-fold higher net production rate of CH_4 and CO_2 (by up to 2.7 times than in control), due to the high addition of bioavailable carbon through the Bti excipients. However, the sole addition of carbon through the Bti excipients could not justify the high net production rate suggesting that the addition of Bti triggered a more robust carbon metabolism process. Both FPMs and LMs results suggested that the application of Bti may have functional implications on carbon biogeochemistry in affected aquatic systems beyond those mediated by changes in macroinvertebrate communities.

Structure of thesis

This thesis is based on the manuscript and published articles. A detailed description of the methodology can be found in the corresponding articles included in the appendices.

Chapter 1: Introduction, it provides background information on conditions underlying carbon processes and fluxes in targeted ecosystems (i.e., ponds). The role of ponds in carbon retention, transformation, and release, relevant environmental factors that condition carbon dynamics, the influence of benthic macroinvertebrates, and the implication of Bti on carbon processes and fluxes.

Chapter 2: Objective, it describes the knowledge gaps, objectives, research questions, and hypotheses of the thesis.

Chapter 3: Structure and contributions of the three articles, it highlights the contribution of the manuscripts, elaborated within the framework of my PhD program, to the objectives of the study.

Chapter 4: Discussion, it relates the results of the study to the research questions and hypotheses.

Chapter 5: Conclusions and outlook, it summarizes the study and its limitations and provides suggestions for the next steps.

The published and submitted manuscripts as well as additional data/information are listed in the appendices.

Chapter 1 – Introduction

> "*The environment is where we all meet; where all have a mutual interest; it is the one thing all of us share*."
>
> —Lady Bird Johnson

The global importance of shallow aquatic systems in carbon cycling and greenhouse gas emissions keeps on being enlightened (Vachon et al. 2021). Shallow aquatic systems such as small ponds (<0.001 square kilometers, depth < 3 meters) are major greenhouse gas sources contributing to a large extent to the global carbon budget (Downing & Duarte 2009; Downing 2010; Delsontro et al. 2016). They contribute about 41% and 15% to the diffusive carbon dioxide (CO_2) and methane (CH_4) emissions of lentic waters (Holgerson & Raymond 2016). Moreover, these systems have a great potential to accumulate large amounts of organic carbon in sediment, at up to 30 times higher rate than other ecosystems (Taylor et al. 2019). Besides greenhouse gas emissions, these shallow aquatic systems provide essential resources for both aquatic and terrestrial organisms (Cadotte & Williams 2014).

1.1 CH_4 production, oxidation, and emissions

In most aquatic systems, both CO_2 and CH_4 production results from the biological processing of organic matter. CH_4 is produced by methanogenic archaea in anoxic sediment (Borrel et al. 2011; Kelly et al. 2014; Bastviken 2022). The methanogens consist of a highly diverse group of microorganisms. They use a narrow range of substrates (such as H_2/CO_2, formate, acetate, methanol, methylated compound, CO, ethanol, and secondary alcohol), which are generally the end products of organic matter degradation through fermentative bacteria and eukarya (Borrel et al. 2011). The produced CH_4 is transported to the atmosphere through various emission pathways, which include direct transport from sediment to the atmosphere as a diffusive flux (Bastviken et al. 2004; Bastviken 2022), through plant roots as plant-mediated flux (Jeffrey et al. 2019; Bansal et al. 2020), or by ebullition through bubble release (Walter et al. 2007; Bastviken et al. 2004). The portion of CH_4 diffusing from sediments to the atmosphere depends on CH_4 oxidation (to CO_2) by methanotrophic bacteria, capable of oxidizing 30-99% of CH_4 produced in freshwaters (Sawakuchi et al. 2016). CH_4 production, oxidation, diffusion, ebullition, and plant mediated-emissions are controlled by many factors, among others are water depth (Gorsky et al. 2019), the ratio of the surface area to the volume (Holgerson and Raymond 2016), water temperature (Brown et al. 2004, Stadmark & Leonardson 2005), season (Bergen et al. 2019), sediment properties (Bodmer et al. 2020),

system productivity (Delsontro et al. 2016). A potentially overlooked processes affecting CH_4 dynamics in shallow aquatic systems are trophic and non-trophic interactions of methanogens and methanotrophs with benthic macroinvertebrates (Colina et al. 2021).

1.2 Role of macroinvertebrates in biogeochemical cycling

An important biological component of shallow aquatic systems are benthic macroinvertebrates, though considered as key engineers of carbon cycling in ponds (Hölker et al. 2015; Demars et al. 2021; Zhang et al. 2022). Benthic macroinvertebrates are majorly represented by tube-dwelling taxa such as chironomid larvae (Diptera: Chironomidae), which are among the most widely distributed and abundant tube-dwelling invertebrates in freshwater ecosystems (Leeper & Taylor 1998; Hölker et al. 2015). They often represent more than half of all aquatic macroinvertebrates in shallow aquatic systems by abundance (Hölker et al. 2015; Koenigs et al. 2018) and are considered an important element in the aquatic food web (Vasquez et al. 2022). Yet, their role in carbon budgets is largely underestimated (Covich et al. 1999; Benelli et al. 2018; Colina et al. 2021; Vadeboncoeur et al. 2002). Through direct or indirect pathways, benthic macroinvertebrates can affect a large range of carbon-related ecosystem functions, such as respiration, organic matter decomposition, and increase in greenhouse gas emissions (Kajan & Frenzel 1999; Baranov et al. 2016; Benelli & Bartoli 2021). Tube-dwelling invertebrates expand the sediment-water interfaces by constructing tunnels and U-shaped burrows in fine anoxic sediments (Bastviken et al. 2003; Sanseverino, et al. 2012; Van Hardenbroek et al. 2012; Adámek & Maršálek 2013; Nogaro & Steinman 2014). Through bioturbation and bioirrigation, they also facilitate the connection of the oxygenated surface waters with anoxic sediment layers modulating redox conditions and thus carbon processing (Mclachlan & Cantrell 1976; Hodkinson & Williams 1980; Hölker et al. 2015; Murniati et al. 2017; Colina et al. 2021). Chironomids' activities are strongly modulated by habitat suitability (De Haas et al. 2006) and seasons (Jackson & Mclachlan 1991; Frouz et al. 2003; Roskosch et al. 2012). Chironomids feed predominantly on sediment organic matter and methane-oxidizing bacteria (Deines et al. 2007; Grey 2016) and oxygenate the sediment, promoting aerobic decomposition of organic matter and sediment respiration (Lagauzère 2011; Baranov et al. 2016). During bioturbation, CO_2 and CH_4 fluxes can be affected by the transport of porewater rich in CO_2 and CH_4 (Booth et al. 2021; Colina et al. 2021). Therefore, the activities of tube-dwelling chironomids can influence carbon cycling by altering major components of the carbon budget, such as carbon transformations, carbon pools, and carbon fluxes. However, the important role of chironomids in aquatic ecosystems may be affected by biological agents used to control black flies and mosquitoes (Jakob & Poulin 2016).

1.3 Implication of biocide Bti on biogeochemical cycle

Due to its mostly targeted effect on mosquitoes and black flies, the biocide *Bacillus thuringiensis var israelensis* (Bti) is generally considered an "environmentally safe" alternative to traditional chemical pesticides (Boisvert & Boisvert 2000; Brühl et al. 2020) and thus is widely utilized to control the larval stage of black flies and mosquitoes. Yet, Bti ingredients are not fully known (Brühl et al. 2020). Globally, between 1992 to 2003, the quantity of Bti used per year increased from less than 4 tons per year to nearly 30 tons per year (Boisvert et al. 2005), and the requirement for its use was still amplified; especially in Germany (Becker et al. 2018). Bti is made of bacteria toxins that are activated in the midgut of chironomids larvae (Yiallouros et al. 1999; Becker 2003). Field experiments have observed a 88% and 50% decline in chironomids larvae by abundance and emergence respectively due to the application of the mosquito control agent Bti (Ali 1981; Allgeier et al. 2019). By reducing the abundance of chironomid larvae, Bti may affect several biogeochemical processes mediated by chironomids, such as anoxic sediment matrix reoxygenation, organic matter decomposition, and solute fluxes exchange. However, studies on Bti's effects have mostly been limited to aquatic macroinvertebrates (Highway 1998; Yiallouros et al. 1999; Theissinger et al. 2019; Bordalo et al. 2021) and nothing is known about its effect on carbon cycling (i.e. carbon processing and fluxes) in aquatic systems. Like other anthropogenic and microbial stressors, Bti could alter biodiversity and induce changes in ecosystem function such as CH_4 oxidation and CH_4 production (Griffiths et al. 2000; Tong & Xie 2019; Bollinger et al. 2021; Wang et al. 2021). In a microcosm experiment, Bti application led to alteration of the microbial communities (Duguma et al. 2015), while Bti's spores have a long-lasting regeneration effect when introduced in natural aquatic systems (Poulin et al. 2022; Tilquin et al. 2008). Therefore understanding its implication for carbon biogeochemistry is crucial.

Chapter 2 – Objectives

The general objective of my PhD project aimed to analyze the effect of Bti application on carbon dynamics in ponds. It seeks to fill the following knowledge gaps: In aquatic systems such as ponds, lakes, and floodplain, where Bti is applied for mosquito control purposes, an alteration in biogeochemical processes involved in carbon cycling, and greenhouse gas emissions can be envisioned due to the above-mentioned effect of Bti. Particularly, biological CH_4 production, and oxidation regulate CH_4 emissions in aquatic systems. These ecosystem functions are potentially modulated by tube-dwelling macroinvertebrates activities (largely represented by chironomid larvae) and could be affected by the application of Bti due to reduction of chironomid abundance.

Specifically, the project aimed to investigate the effect of application of Bti and change in chironomid density on:

- carbon transformation
- carbon pools
- carbon fluxes in ponds

This study aimed to investigate the following research questions (**Q**) and hypotheses (**H**):

- **Q1**: What is the effect of Bti application on carbon transformation through the changes in chironomids abundance in the systems?

H1.1: The reduced abundance of chironomids due to Bti results in a reduction of organic processing and reduction in CH_4 oxidation and increased CH_4 production in the sediment.

- **Q2**: Does the reduction of chironomids caused by Bti application affect the carbon pools in the FPMs?

H2.1: The reduced sediment aerobic organic matter processing increases the accumulation of particulate organic carbon in sediment inducing an increase in dissolved organic carbon in pore water and in surface water.

H2.2: The reduced CH_4 oxidation increases CH_4 accumulation in sediments and lead to increasing CH_4 concentration in water

H2.3: The degradation of Bti excipients in the sediment increases the production and concentrations of CH_4 and CO_2 in water.

- **Q3**: How does a change in chironomids abundance due to Bti affect CH_4 and CO_2 fluxes?

H3.1: Increased CH_4 concentration due to reduction in CH_4 oxidation and carbon addition by Bti increases the CH_4 flux from surface water to the atmosphere.

H3.2: Increased CO_2 concentration cause higher CO_2 flux from surface water to the atmosphere.

- **Q4**: What are the spatiotemporal factors that regulate the effect of treatment on carbon transformation, pools, and fluxes in the ponds?

H4.1: As habitat suitability regulates the abundance of chironomids, changes in the carbon budget components are more pronounced in the shallow zone (with sandy sediment) than in the deeper zone (with coarse sediment) of the ponds.

H4.2: Because chironomid activities depend on temperature, differences between treated and control systems will be larger in spring and summer than in autumn and winter.

Chapter 3 – Structure of the thesis

To test the objective on carbon transformation, pools, fluxes, and budgets in ponds, we used an ecosystem-scale mass balance approach as part of a joint outdoor mesocosm (FPMs) experiment. The FPMs experiment were used to mimick natural conditions in ponds (for one year from 2020 to 2021). Each FPM featured a shallow zone (aquatic-terrestrial), a deep zone (aquatic) and a terrestrial zone (riparian) (see highlighted zone in **Figure 1 A**, also see **Appendix I** & **II** for further details). Each FPM was flooded and Bti was applied to 6 non-adjacent FPMs following a common practice of mosquito control applications at the Upper Rhine Valley (Germany) (**Figure 1 B & C**). To fully understand the implications of changes in chironomid abundance (through Bti application) that occurred during the FPMs experiment, we developed a series of 15 laboratory microcosms (LMs) experiments. The LMs were closed system gas-tight microcosms allowing to access individual effect of treatment on carbon dynamics over a limited time period. The LMs volume were 1.83 L, with a large headspace volume of 0.61 L to enusure oxic conditions. The LMs were equipped with aerated tube that allow continuous water motion similar to natural conditions (**Figure 1 D-H**, **Appendix III**).

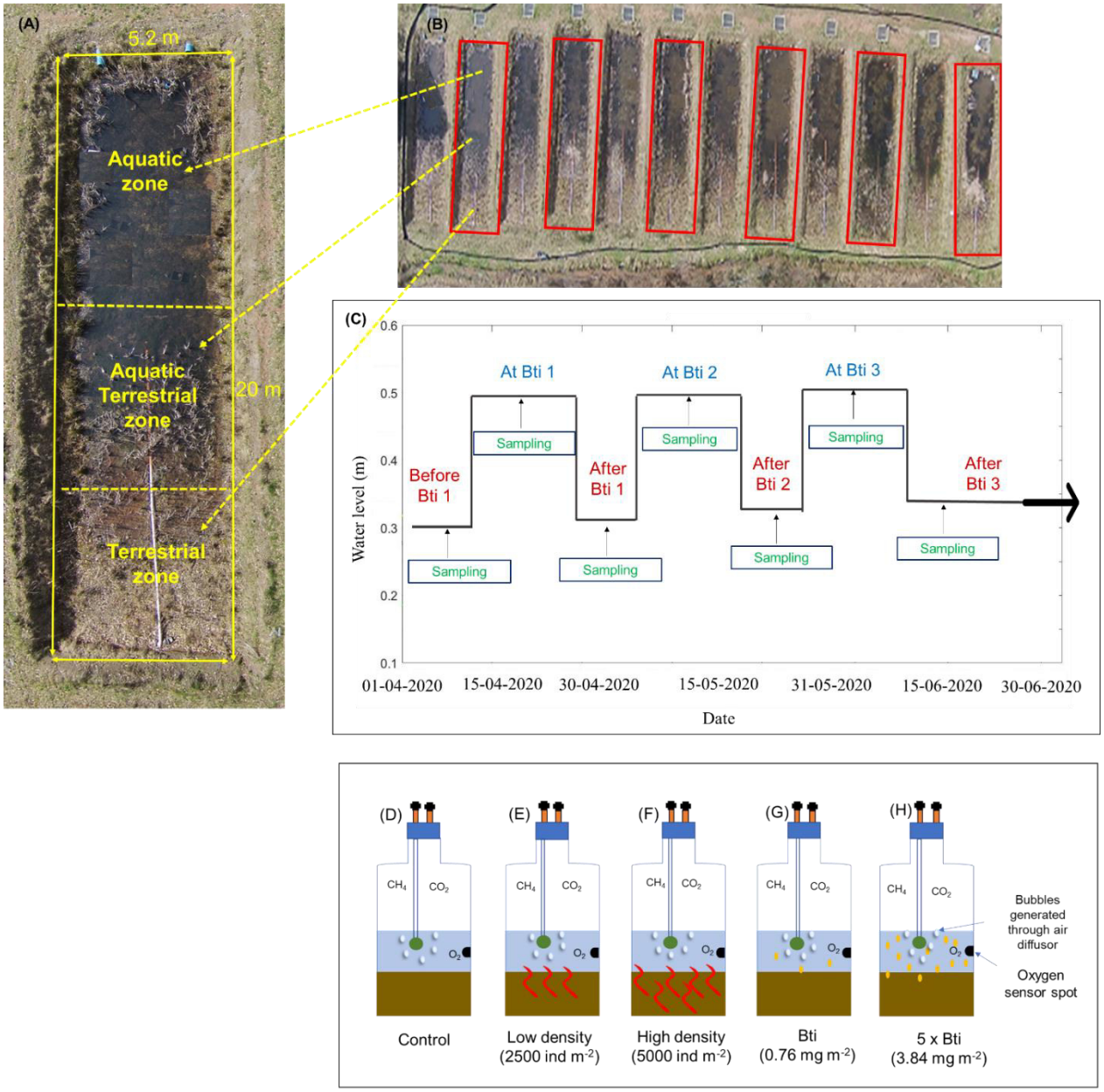

Figure 1: A. Detailed view of a single FPM with the aquatic zone and the aquatic-terrestrial transition zone and the terrestrial zone delimitated by yellow dashed lines. The area marked as the terrestrial zone was temporarily flooded during the three Bti applications. **B**. Areal image of the 12 experimental Floodplain Pond Mesocosms (FPM) at the Eusserthal Ecosystem Research Station, with Bti-treated FPMs highlighted in red and control FPMs labeled not highlighted. **C**. Illustration of flooding and Bti application events in the FPMs note that the dark arrow at the end of the third Bti application indicates that sampling continues until year-round. (Images **A, B & C** are extracted and modified from **Appendix I** & **II**). **D.** Image of experimental design showing control microcosms with bare sediment (n=3); **E**. treated microcosm with low chironomids larval density (n=3); **F**. treated microcosm with high chironomids larval density (n=3); **G**. treated microcosms with standard Bti dose (n=3); **H**. treated microcosms with 5 times the standard Bti dose (n=3) (**D**, **E**, **F**, **G** & **H** are extracted from **Appendix III**).

Two peer-reviewed publications and one manuscript contain the main findings supporting this doctoral project and are reported in appendices. A brief description of each publication highlighting their contributions to the research questions and hypotheses is next presented.

Biocide treatment for mosquito control increases methane emissions in floodplain pond mesocosms

Ganglo, C., Manfrin, A., Mendoza-Lera, C., & Lorke, A. (2022). Biocide treatment for mosquito control increases methane emissions in floodplain pond mesocosms. Frontiers in Water, *4*(9), 10. https://doi.org/10.3389/frwa.2022.996898 (**Appendix I**)

The effect of treatment on the CH_4 dynamic was accessed in the FPMs field experiment. CH_4 oxidative fraction was measured as a proxy of CH_4 oxidation using the carbon isotopic signature of CH_4 (δ13C-CH_4) determined from dissolved CH_4 in the surface water and gas in the sediment (**H1.1**). Dissolved CH_4 in the aquatic and aquatic-terrestrial zone transition zone was measured in surface water of FPMs (**H2.2**). CH_4 fluxes to the atmosphere were measured in both the aquatic and aquatic-terrestrial transition zones (**H3.1**).

Does biocide treatment for mosquito control alter carbon dynamics in floodplain ponds?

Ganglo, C., Mendoza-Lera, C., Manfrin, A., Bolpagni R., Gerstle, V., Kolbenschlag S., Bollinger, E., Schulz, R. & Lorke, A. (2023). Does biocide treatment for mosquito control alter carbon dynamics in floodplain ponds? Science of the total environment, *872*(2), 161978. https://doi.org/10.1016/j.scitotenv.2023.161978 (**Appendix II**)

The evaluation of the implication of Bti on carbon transformations, pools, and fluxes was as well monitored during the same FPMs experiment. For carbon transformation, teabag was deployed as a proxy for microbial decomposition of organic matter in water and sediment of shallow, deeper, and riparian zones (**H1.1**). For the pools of carbon, the amount of total organic carbon added as Bti (active component plus excipient) was estimated; total organic sediment was estimated (**H2.1**) and carbon in plant biomass and benthic macroinvertebrates biomass were estimated. Organic carbon in dissolved form as DOC was measured in porewater and surface water (**H2.1**). Inorganic carbon as CH_4 and CO_2 were measured in surface water of FPMs (**H2.2**). In addition to CH_4 fluxes, CO_2 fluxes were measured (**H3.1** & **H3.2**), and carbon leaving the systems as emergent insect flux was estimated. The carbon budget was completed by measurement of carbon input through wet deposition of total organic carbon (TOC). The differences in treatment among zones and seasons were evaluated on the measured variable using a statistical linear mixed effect model approach (**H4.1** & **H4.2** respectively).

Effects of chironomids density and mosquito biocide on methane dynamics in freshwater sediments.

Ganglo, C., Manfrin, A., Mendoza-Lera, C. & Lorke, A. (2023). Effects of chironomids density and mosquito biocide on methane dynamics in freshwater sediments. Plos One (submitted 07 February 2023) (**Appendix III**)

Based on the findings from the FPMs experiment, this study evaluated the individual effect of chironomids density and Bti on CH_4 dynamics in sediment using a small-scale LMs experiment. For that CH_4, CO_2, and O_2 concentration, emissions, and production were measured (**H2.3**).

Chapter 4 – Discussion

This chapter presents the overarching discussion of the results from the three articles presented in **Chapter 3**. The articles are referenced according to their respective location in the appendix section and present their contributions to rejected or accepted the raised hypotheses. Each subsection corresponds to a specific research question in the following order: carbon transformation, carbon pools, carbon fluxes, and carbon budgets.

4.1 Carbon transformation

This doctoral project is the first to evaluate the implication of mosquito control Bti on carbon dynamics in ponds. I hypothesized that the 41% reduction of chironomids abundance in the floodplain pond mesocosms (FPMs) reduced aerobic organic matter decomposition rate in sediment (**H1.1**) (**Appendix II**). However, the decomposition rate was not affected by treatment as predicted. I quantified the leachable carbon fraction in Bti's ingredients and suggest that they are made of labile organic carbon which could also have stimulated microbial organic matter decomposition in treated FPMs and masked potential differences between treated and untreated units. The mechanisms by which Bti's ingredients have contributed to the decomposition rate of organic matter could be explained by findings from the laboratory microcosms (LMs) experiment (**Appendix III**). CH_4 and CO_2 production have been up to 3 times higher for any Bti dose than in the controls during the incubation period. These findings imply that also in the FPMs, the supplied labile carbon are additional reactants which increased biogeochemical processes. Hence here there is not enough evidence to reject **H1.1**.

I cannot ignore that the reduced number of macroinvertebrates in treated FPMs may be an additional source of carbon (as detritus) that also may have been involved in decomposition and cover a potential treatment effect. These additional aspects should be considered when evaluating the carbon cycling in systems treated with Bti.

Other environmental factors that may have masked the overall effect of treatment in the FPMs can not be excluded . Organic matter decomposition rate varied mostly among seasons and was slower in anoxic sediment than in the water column of FPMs (**Appendix II**). The highest decomposition rate in water column in FPMs may have been stimulated by O_2 availability (Dauwe et al. 2001). Meanwhile, the slower decomposition rate in anoxic sediment indicates that the FPMs were intensive sites of organic matter accumulation, similar to other

inland waters (Wallin et al. 2016; Taylor et al. 2019; Vachon et al. 2021). It is worth noting that, the average decomposition rate in FPMs is in the same range as for peat and sandy lands as reported by Keuskamp et al. (2013). These environmental conditions should be integrated into the evaluation of the effect of microbial stressors in shallow freshwater systems.

4.2 Carbon pools

In general for carbon pools, a reduction in carbon transformation due to reducing chironomids abundance would result in a higher accumulation in the organic carbon pools leading to an increase in CH_4 and a decrease in CO_2 concentration in water. Among the measured carbon pools, only porewater DOC showed a tendency toward a 33 % reduction in treated FPMs than in control and this effect persisted over the year. The lower DOC in porewater of treated FPMs can be explained through non-trophic interactions of chironomids in sediment. The non-trophic interactions involved bioturbation and bioirrigation activities of chironomids that oxygenate sediment matrix, but increased solutes fluxes such as DOC across sediment-water boundaries (Cummins & Klug 1979; Parr et al. 2019). Hence **H2.1** is validated. A similar trend was observed in the LMs, showing that bioturbation by *Chironomus riparus* (at low and high density) induced higher CH_4 and CO_2 emissions. (**Figure 2 A & B**) (**Appendix III**). These findings are in line with the hypothesized links between bioturbation and greenhouse gas emissionsfound by Booth et al (2021), where more frequent bioturbation increase greenhouse gases emissions.

The mechanisms and processes by which the *Chironomus riparus* larvae have caused an increase in greenhouse gas emission rate may be explained by a combination of both trophic and non-trophic interactions as observed in laboratory experiments by Kajan and Frenzel (1999). Additionally, the bioturbation and bioirrigation by the chironomids oxygenate the sediment, which promotes CH_4 oxidation (Oliveira Junior et al. 2019), sediment respiration (Baranov et al. 2016; Murniati et al. 2017). These conditions explain the highest net O_2 consumption rate of 80 and 180 µmol O_2 per day for our low and high-density larvae treatments, respectively (**Appendix III**); and these values are in the reported range of O_2 consumption by chironomids (Murniati et al. 2017). Although high oxygen consumption rate was observed in presence of chironomids for LMs, the reduction in chironomids density did not affect CH_4 oxidative fraction for FPMs and may be obstructed by several factors. First oxidative fraction varied mainly as a function of the season, regardless of treatment. Second, dissolved CH_4 and O_2 concentrations were similar in deep and shallow zones of the FPMs and did not vary between treatments as expected. Third, horizontal mixing of the surface water could have covered a potential effect on oxidation (**Appendix I**). Horizontal mixing of surface

water in the FPMs may also have diluted differences in the isotopic signature of dissolved CH_4 and masked the identification of potential changes in CH_4 oxidation rates in the treated FPMs. Consequently, a potential effect on dissolved CO_2 concentration could also not be detected in the FPMs and maybe also be due to hydrodynamics conditions that governed shallow vegetated aquatic systems such as convective flows, which are generated by differential heating and cooling due to spatially varying water depths and light absorption properties of the water column and sediment surface (Nepf 2012). Here **H2.2** is rejected for both experiments; reduced CH_4 oxidation did not increase CH_4 concentration and decrease CO_2 concentration in water. Also, in the FPMs there were no changes in sediment carbon (the largest pool of carbon) detected. Under field conditions in the FPMs, the variability of processes that control carbon biogeochemistry as mentioned above may have covered a potential effect of treatment on the carbon pool in sediment.

Alternative mechanisms, which can explain the weak effect of treatment on carbon pools, were also attributed to labile carbon addition by the Bti source, although a very tiny addition to the carbon pool for treated FPMs (0.007% of the total carbon pool) (**Appendix II**). In the LMs Bti alone has promoted CH_4 and CO_2 production certainly by stimulating aerobic and anaerobic carbon metabolism in sediment. The produced gas remained accumulated in sediment and did not increase the input in water until bulk sediment was disturbed mechanically (**Figure 2 A & B**) (**Appendix III**). Note that in these conditions, a longer incubation time would have led to bubble formation in sediment and transport by ebullition, which in turn could have led to higher CH_4 fluxes over the long term**.** Because of the LMs findings, **H2.3** is partly accepted. Bti input increases the gas production but does not increase the concentration in water unless mechanical disturbance.

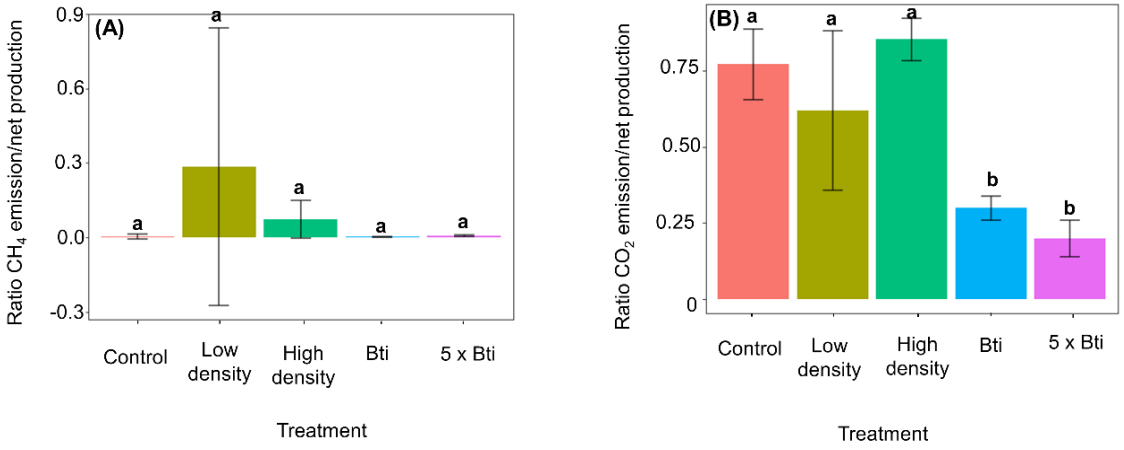

Figure 2: As described in **Appendix III** the figure represents mean values (bars) and standard deviation (error bars, *n* = 3) of the ratio of emission to net production rates of CH_4 (**A**) and CO_2 (**B**) measured during the LMs experiment. Different letters above each group of data indicate significant differences ($p \leq 0.05$).

4.3 Carbon fluxes

For carbon fluxes, I expected high CH_4 flux due to higher CH_4 concentration and lower CO_2 flux due to a reduction in CH_4 oxidation by reducing chironomids abundance (**H3.1**). In this case, the hypothesis is partially confirmed as CH_4 flux increased by 137% in treated FPMs, with a persistent trend over the year, validating **H3.1** for FPMs (**Figure 4 A**) (**Appendix I**). An increase in CH_4 flux was only observed in the aquatic-terrestrial zones of the FPMs, the area with sandy sediment, which is also the favorable habitat of chironomids (De Haas et al. 2006; Gerstle et al. 2022). These findings validate my assumptions that changes in carbon components are better reflected in the area with more chironomids (**H4.1**). Comparably, in the LMs incubation, an increase in chironomids larvae density also increased both CH_4 and CO_2 fluxes although the CH_4 production rate was not significantly affected by larvae density. In this case, the LMs findings do not give enough argument to validate **H3.1** as an increase in CH_4 emissions did not come from an increase in CH_4 production. Both results emphasized that chironomids can be cautiously integrated among regulators of greenhouse gas accumulation by increasing emission across sediment-water boundaries. Enhanced emissions potentially due to chironomids were observed in spring and summer than in winter in FPMs, which can be explained by temperature-dependent metabolic activities of chironomids (Jackson & Mclachlan 1991; Frouz et al. 2003; Roskosch et al. 2012). Due to plant mediated effect a potential effect of treatment on CO_2 emissions was not found in the aquatic-terrestrial zones of FPMs also because this zone was highly productive (**Appendix II**). Therefore **H4.2** can be accepted, rejecting **H3.2**.

High CH_4 emissions in the treated FPMs may be caused by a more direct functional implication of Bti on methanogenesis (**Appendix III**). As confirmed by the LMs experiments, Bti excipients represent a pulse of labile DOC, increasing carbon processing. In the LMs, the addition of Bti resulted in an increase in net CO_2 production rate by a factor of 2.7 and 3.4 for the standard Bti dose and the five times standard Bti dose, respectively (**Figure 3 B**). The increase in net CO_2 production rate in Bti treatments was comparable to that of the treatment with chironomids larvae, due to chironomid activities. Similarly to CO_2, the net production rates of CH_4 increased in the two treatments in which Bti was added, suggesting that both aerobic and anaerobic carbon metabolism in the LMs is boosted by labile carbon availability upon Bti addition. However, the amount of DOC added by Bti to fuel methanogenesis and respiration was relatively smaller compared to the produced greenhouse gases. This indicates that Bti' labile carbon might trigger the degradation of organic matter. These findings suggest that also in the FPMs more direct activities of Bti on microbial communities were promoting the higher CH_4 fluxes, suggesting the urgent need for future experiments to clarify the underlying implication of Bti in biogeochemical processes of carbon.

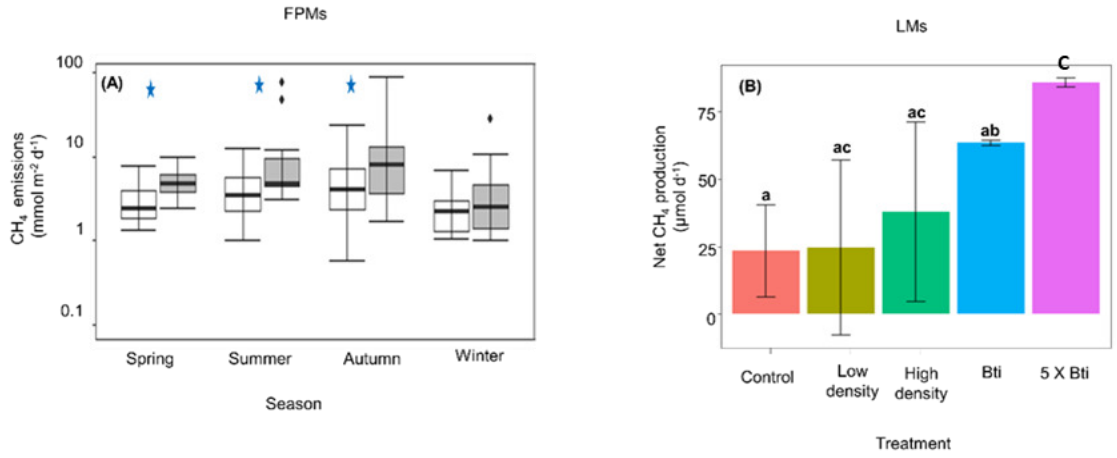

Figure 3: (**A**) Figure taken from **Appendix I** showing mean values (bars) and standard deviation (error bars, *n* = 3) of CH_4 emissions flux (mmol m^{-2} d^{-1}) in the aquatic-terrestrial zone of FPMs; Note blue stars denote significant difference between treated and control groups and (**B**) Figure taken from **Appendix III** representing net CH_4 production rates (µmol d^{-1}). Different letters above each group of data indicate significant differences ($p \leq 0.05$).

4.4 Carbon budget

It is more clear from the LMs that carbon biogeochemical processes and fluxes are regulated by the presence of chironomids larvae and Bti than it was shown in the FPMs. In the FPMs the processes and fluxes were mostly regulated by spatiotemporal factors, increasing the variability of carbon transformation, carbon pools, and carbon fluxes among seasons and

zones regardless of treatment (**Appendix II**). Thus studies in control systems (such as laboratory and microcosms experiments) may be more beneficial to fully understand biogeochemical dynamics in shallow aquatic systems.

The implication of Bti at the FPMs ecosystems level was limited to the observed changes such as carbon reduction in macroinvertebrates biomass and carbon addition by Bti in treated units contributing a very tiny change of 0.02 % to the total carbon pools; the higher CH_4 flux contributed up to 75% loss to the total carbon output to the FPMs (**Figure 4**). For the LMs most of the produce gases accumulated in sediment leading to less than 1% and less than 25 % loss of carbon through CH_4 and CO_2 emissions in the LMs' headspace. The carbon addition through Bti as DOC was less than 1 % of the resulting carbon produced as CO_2 and CH_4. All these results point out that systems treated with Bti are hotspots for greenhouse gases production.

Overall, the FPMs were net sinks of atmospheric carbon due to primary productivity. Sediment organic carbon is of biological detritus origin (Sobek et al. 2006). A total carbon pool of 1159.2 ± 314.3 g C m^{-2} (mean ± standard deviation) was concentrated in the sediment (**Figure 4**). The organic carbon content in sediment was in the same range as in constructed ponds (Ljung & Lin 2023). Sediment organic carbon was by far the largest pool, representing ~ 94% of the total carbon pool in the ponds. Part of the sediment organic carbon was broken down by biological processes and released back as dissolved organic carbon into the water column. Porewater and surface water total organic carbon (TOC) contributed respectively 0.1 and 0.2 % of the carbon pools. TOC in water was susceptible to a variety of in-water processes such as bacterial metabolism and dissolved gases exchange between FPMs' surface water and atmosphere (Sanches et al. 2019). The FPMs were year-round suppersaturaed in dissolved CH_4 with a mean saturation ratio of 6397 ± 5724%. A substantial fraction of dissolved CH_4, up to 77%, was oxidized to CO_2 by methanotrophs (**Appendix I**).

The dissolved CH_4 and CO_2 estimates were within reported values for temporary ponds in the temperate zone (Holgerson 2015). Among the biota, emergent macrophytes contributed the largest share (~5%) to the total carbon pool. Benthic macroinvertebrates contribute a relatively small proportion (~0.08 %) to the carbon pools. The FPMs received carbon influx (total input 3.24 ± 3.26 g C m^{-2} d^{-1}) from two sources: major atmospheric CO_2 uptake by plants during photosynthesis representing 99 % of the total carbon input flux and a very minor contribution of 0.1 % by TOC inflow of wet deposition (i.e.rain). The CO_2 influx rate in aquatic-terrestrial zones of FPMs was higher than in other two zones, indicating that these areas play

a key role in the FPMs system productivity. In addition, the aquatic-terrestrial zones of FPMs had finer sediment size and abundant aquatic vegetation, where both CH_4 and CO_2 fluxes may have been supported by plant-mediated transport (Maucieri et al. 2017; Bodmer et al. 2020). The most important carbon output (-0.23 ± 0.32 g C m^{-2} d^{-1}) was through CO_2 and CH_4 emissions, representing 75% and 24% respectively. The flux values are in the same order of magnitude as the average emission reported for urban and artificial ponds (Stadmark & Leonardson 2005; Bergen et al. 2019). The remaining carbon output fluxes are sourced by emergent insects (Kolbenschlag et al. 2023) but their contribution of 0.9% was of minor importance; which was potentially underestimated by the sampling method with emergence traps that could not entrap large insects (Cadotte & Williams 2014) .

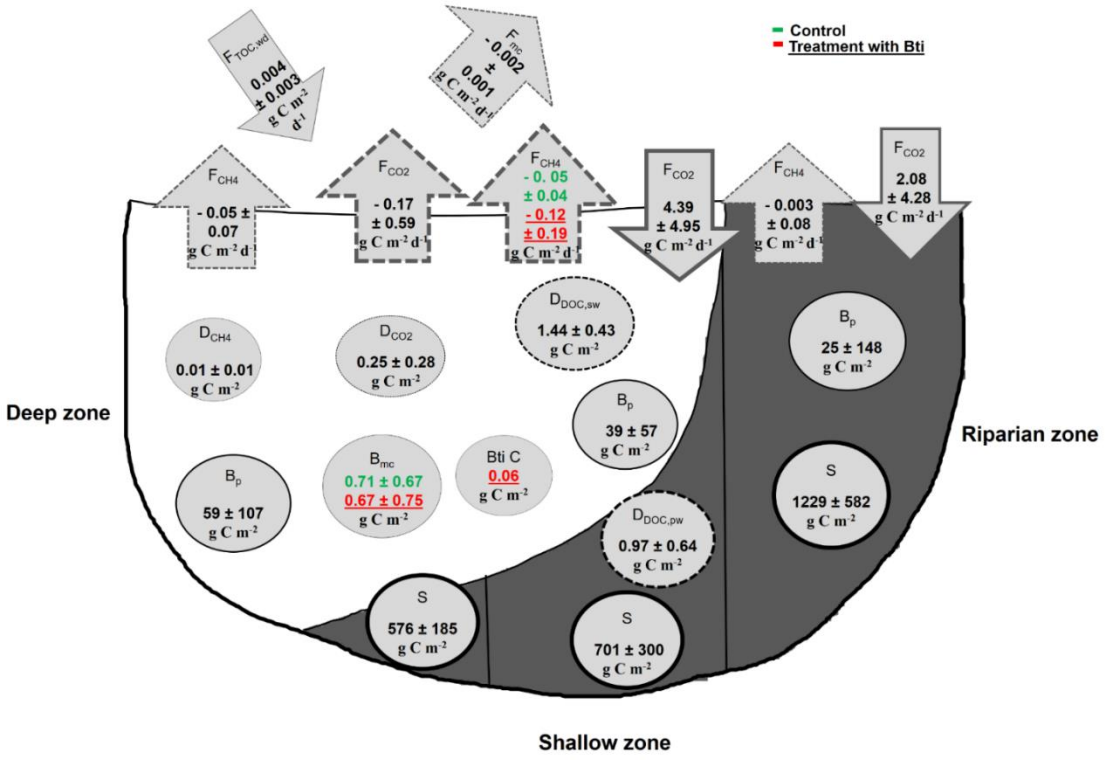

Figure 4: Graphical representation of the average carbon budget comprising the carbon pool components (numbers in circles in g C m^{-2}) and carbon flux components (numbers in arrows in g C m^{-2} d^{-1}) in the deep, shallow transition, and riparian zones of the 12 FPMs (mean values ± standard deviation). If significant differences were observed between FPMs treated with Bti and control FPMs, numbers in red (underlined) and green represent mean values for both treatments, respectively, while numbers in black represent the global average (if no significant differences were observed). Total carbon in plant biomass (B_p), and sediment organic carbon (S) were measured in all three zones. Macroinvertebrate carbon (B_{mc}) was measured in macrophytes and gravel zones of the FPMs. Surface water DOC ($D_{DOC,sw}$), porewater DOC ($D_{DOC,pw}$), dissolved CO_2 (D_{CO2}), and dissolved CH_4 concentration (D_{CH4}) were measured in between the deep aquatic and shallow transition zones, assuming horizontal homogeneity in the FPMs. Wet deposition TOC influx ($F_{TOC,wd}$) was obtained from precipitation water collection and annual precipitation data. CO_2 flux (F_{CO2}) and CH_4 flux (F_{CH4}) were measured in all three zones, and insect biomass efflux (F_{mc}) was measured in the deep and shallow zones of FPMs during spring and summer. Note that particulate carbon pools (in sediment, plants, Bti carbon, and macroinvertebrates) are outlined by solid lines, and dissolved carbon (in porewater and surface water, CO_2 and CH_4 concentration in water) are outlined with dashed lines. Arrows indicating carbon input (wet deposition DOC and CO_2 flux) are continuous and pointing downwards, whereas carbon output (CH_4 flux, CO_2 flux, and emerging insects) are shown as dashed arrows pointing upwards. The width of the circles and arrows indicates the magnitude of the contribution (not to scale) (**Appendix II**).

Chapter 5 – Conclusions and outlook

The goal of my doctoral study is to analyze the effect of Bti application on carbon dynamics in ponds through a 41% reduction of chironomids abundance and 26 % reduction of their emergence. The present doctoral project is the first to investigate the potential effects of the mosquito control biocide Bti on carbon dynamics in shallow lentic ecosystems. The implications of Bti on the processes and fluxes have been tested in open-field FPMs. The LMs study focused on individual effects of Bti and chironomids larvae density and clarify the underlying biogeochemical processes and fluxes of FPMs so that the four research questions are answered.

Q1: *What is the effect of Bti application on carbon transformation through the changes in chironomids abundance in the systems?* There was no effect of Bti found on organic matter decomposition rate in the FPMs. However, as suggested by the LMs experiment, the alone Bti's ingredients are labile carbon that affects carbon transformation potentially by increasing methanogenesis and sediment respiration independently of the chironomid's presence.

Q2: *How can the reduction of chironomids by Bti affect the carbon pools in the systems?* In the FPMs the reduction of bioturbation activities by chironomids reduced DOC in porewater. These effects were potentially caused by non-target adverse effects of Bti on chironomid larvae, which can affect carbon cycling by both trophic and non-trophic interactions. Whereas bioturbation increased CH_4 and CO_2 inputs in the water of LMs but did not affect the net balance of CH_4 (i.e production and oxidation).

Q3: *How does the occurring change in chironomids abundance due to Bti affect carbon fluxes?* CH_4 fluxes increase in response to Bti application, previously attributed to the reduction of chironomids larvae. However, the LMs experiment suggests that more direct effects of Bti on microbial communities and their activity were promoting the observed increase in fluxes. The findings prove that Bti has an adverse effect on carbon dynamics (by targeting CH_4 for example) in affected aquatic systems.

Q4: *What are the spatiotemporal factors that regulate the effect of treatment on carbon transformation, pools, and fluxes?* The effect of higher CH_4 fluxes was strong in the shallower

zone with sandy sediment than in deeper ones with coarse sediment, highlighting that habitat suitability is among others an important factor for carbon biogeochemistry. In addition, regardless of treatment, carbon components strongly varied between seasons and zones. However, the findings are limited to observation, and thus encourage more details experiments at both field and lab scales to reveal the functional implication of Bti in aquatic systems.

Summarizing, the doctoral project filled existing knowledge gaps in the mechanistic understanding of anthropogenic stressors on carbon biogeochemistry and open the floor to several questions among others:

1. Which microbial communities are impacted by Bti?
2. Does Bti facilitate the proliferation of methanogenic microorganisms?
3. What is the temporal extent of Bti's influence on methanogenesis?
4. What are the consequences of Bti exposure on CH_4 oxidation processes?
5. What is the ultimate fate of carbon compounds in aquatic ecosystems subjected to Bti treatment?
6. Can Bti be regarded as a regulatory factor in the CH_4 cycling dynamics within aquatic ecosystems?

To clarify these questions future studies could develop a novel experimental mesocosm system such as aquarium, which facilitates replicated laboratory experiments to study emissions and oxidation of CH_4 across the sediment-water interface, the production of CH_4 in sediments, and the characterization of methanogens communities. The mesocosm system could be tested and applied in a series of targeted experiments, which simulate natural environmental conditions in shallow aquatic systems, where overlying water above sediment will be exposed to continuous aeration conditions that allow oxygen flow ecosystems to mimic natural conditions. Future experiments could develop the following research objectives and hypotheses:

Objective 1 Experimental development of mesocosm systems that mimic natural conditions to measure methanogens communities and methane oxidation from aquatic sediment under environmental conditions that are reproducible and repeatable

Hypothesis 1 In the proposed mesocosm, methane components can be measured reproducibly under well-monitored environmental conditions.

The proposed systems allow the measurement of biogeochemical fluxes and processes, over prolonged (weeks) measurement times. Besides measuring all relevant biogeochemical components, the systems allow for the control of other abiotic and biotic parameters of water and sediments. Additional environmental variables, including stable isotope analysis could be carried on CH_4 gas, chironomids larvae, and sediment, and organic carbon content in water and sediment samples could be measured.

Objective 2 Estimate the variation of methanogens communities and methane oxidation under different treatment conditions

Hypothesis 2.1 Enhance methane production in presence of Bti is due to the proliferation of methanogens communities, whereas the increase in methane production also enhances methane oxidation.

Very few studies have invested the effect of Bti on methane dynamics (**Appendix I**). Recently we found that Bti‘s ingredients stimulate organic matter degradation that increases methane production (**Appendix III**). The application of Bti has been found to alter the microbial communities dynamics in the water column, and because methane is produced by methanogenic archaea (Bridgham et al. 2013), these bacterial communities are expected to be affected by Bti.

Hypothesis 2.2 Chironomids larvae by pumping oxygenated water in sediment and by feeding on organic matter, increase methane oxidation in sediment and prevent the proliferation of methanogens communities in sediment.

Few studies argue that bioturbation and bioirrigation by chironomids in sediment increase sediment respiration through the decomposition of organic matter and methane oxidation. Based on the experimental results, a process-based three dimensional coupled physical and biological model could be developed, which includes, relevant biogeochemical processes and fluxes.

Objective 3 Identify the major controlling factors for methanogens communities, and methane oxidation in shallow systems through a process-based model for aquatic sediments.

Hypothesis 3 The effect of different stressors can be incorporated into a process-based biogeochemical model.

References

Ali Arshad. (1981). Bacillus thuringiensis against and Some Nontarget Aquatic Invertebrates3. *Journal of Invertebrate Pathology*, *38*(2), 264–272. https://doi.org/10.1016/0022-2011(81)90132-4

Allgeier, S., Friedrich, A., & Brühl, C. A. (2019). Mosquito control based on Bacillus thuringiensis israelensis (Bti) interrupts artificial wetland food chains. *Science of the Total Environment*, *686*, 1173–1184. https://doi.org/10.1016/j.scitotenv.2019.05.358

Allgeier, S., Kästel, A., & Brühl, C. A. (2019). Adverse effects of mosquito control using Bacillus thuringiensis var. israelensis: Reduced chironomid abundances in mesocosm, semi-field and field studies. *Ecotoxicology and Environmental Safety*, *169*, 786–796. https://doi.org/10.1016/j.ecoenv.2018.11.050

Amani, M., Graça, M. A. S., & Ferreira, V. (2019). Effects of elevated atmospheric CO2 concentration and temperature on litter decomposition in streams: A meta-analysis. *International Review of Hydrobiology*, (September 2018), 14–25. https://doi.org/10.1002/iroh.201801965

Bansal, S., Johnson, O. F., Meier, J., & Zhu, X. (2020). Vegetation Affects Timing and Location of Wetland Methane Emissions. *Journal of Geophysical Research: Biogeosciences*, *125*(9), 1–14. https://doi.org/10.1029/2020JG005777

Baranov, V., Lewandowski, J., & Krause, S. (2016). Bioturbation enhances the aerobic respiration of lake sediments in warming lakes. *Biology Letters*, *12*(8), 8–11. https://doi.org/10.1098/rsbl.2016.0448

Baranov, V., Lewandowski, J., Romeijn, P., Singer, G., & Krause, S. (2016a). Effects of bioirrigation of non-biting midges (Diptera: Chironomidae) on lake sediment respiration. *Scientific Reports*, *6*(January), 1–10. https://doi.org/10.1038/srep27329

Baranov, V., Lewandowski, J., Romeijn, P., Singer, G., & Krause, S. (2016b). Effects of bioirrigation of non-biting midges (Diptera: Chironomidae) on lake sediment respiration. *Scientific Reports*, *6*(May), 1–10. https://doi.org/10.1038/srep27329

Bastviken, D., Cole, J., Pace, M., & Tranvik, L. (2004). Methane emissions from lakes: Dependence of lake characteristics, two regional assessments, and a global estimate. *Global Biogeochemical Cycles*, *18*(4), 1–12. https://doi.org/10.1029/2004GB002238

Bastviken, D., Ejlertsson, J., Sundh, I., & Tranvik, L. (2003). Methane as a Source of Carbon and Energy for Lake Pelagic Food Webs. *Ecology*, *84*(4), 969–981. https://doi.org/10.1890/0012-9658(2003)084[0969:MAASOC]2.0.CO;2

Bastviken, D., Ejlertsson, J., & Tranvik, L. (2002). Measurement of methane oxidation in lakes: A comparison of methods. *Environmental Science and Technology*, *36*(15), 3354–3361. https://doi.org/10.1021/es010311p

Becker, N. (1997). Microbial control of mosquitoes: Management of the upper rhine mosquito population as a model programme. *Parasitology Today*, *13*(12), 485–487. https://doi.org/10.1016/S0169-4758(97)01154-X

Becker, N. (2003). Ice granules containing endotoxins of microbial agents for the control of mosquito larvae - A new application technique. *Journal of the American Mosquito Control Association*, *19*(1), 63–66.

Becker, N. (2006). Biological control mosquitoes: Management of the upper rhine mosquito population as a model programme. *J. Eilenberg and H.M.T. Hokkanen (Eds.),An Ecological and Societal Approach to Biological Control Springer*, *2*, 227–245. https://doi.org/10.1007 › 978-1-4020-4401-4_11

Becker, N., Ludwig, M., & Su, T. (2018). Lack of Resistance in Aedes Vexans Field Populations After 36 the Upper Rhine Valley , Germany. *Journal of the American Mosquito Control Association*, *34*(2), 154–157. https://doi.org/https://doi.org/10.2987/17-6694.1

Benelli, S., & Bartoli, M. (2021). *Worms and submersed macrophytes reduce methane release and increase nutrient removal in organic sediments*. https://doi.org/10.1002/lol2.10207

Benjamini, Y., & Hochberg, Y. (1995). Controlling the False Discovery Rate: A Practical and Powerful Approach to Multiple Testing. *Journal of the Royal Statistical Society: Series B (Methodological)*, *57*(1), 289–300. https://doi.org/10.1111/j.2517-6161.1995.tb02031.x

Bergen, T. J. H. M., Barros, N., Mendonça, R., Aben, R. C. H., Althuizen, I. H. J., Huszar, V., … Kosten, S. (2019). Seasonal and diel variation in greenhouse gas emissions from an urban pond and its major drivers. *Limnology and Oceanography*, *64*(5), 2129–2139. https://doi.org/10.1002/lno.11173

Bodmer, P., Wilkinson, J., & Lorke, A. (2020). Sediment Properties Drive Spatial Variability of Potential Methane Production and Oxidation in Small Streams. *Journal of Geophysical Research: Biogeosciences*, *125*(1), 1–15. https://doi.org/10.1029/2019JG005213

Boisvert, M. (2005). Utilization of Bacillus thuringiensis var . israelensis (Bti) - Based Formulations for the Biological Control of Mosquitoes in Canada. *Victoria*, 87–93.

Boisvert, M., & Boisvert, J. (2000). Effects of bacillus thuringiensis var. israelensis on target and nontarget organisms: A review of laboratory and field experiments. *Biocontrol Science and Technology*, *10*(5), 517–561. https://doi.org/10.1080/095831500750016361

Booth, M. T., Urbanic, M., Wang, X., & Beaulieu, J. J. (2021). Bioturbation frequency alters methane emissions from reservoir sediments. *Science of the Total Environment*, *789*, 1–9. https://doi.org/https://doi.org/10.1016/j.scitotenv.2021.148033

Bordalo, M. D., Machado, A. L., Campos, D., Coelho, S. D., Rodrigues, A. C. M., Lopes, I., & Pestana, J. L. T. (2021). Responses of benthic macroinvertebrate communities to a Bti-based insecticide in artificial microcosm streams. *Environmental Pollution*, *282*. https://doi.org/10.1016/j.envpol.2021.117030

Borrel, G., Jezequel, D., Biderre-Petit, C., Morel-Desrosiers, N., Jean-Pierre Morel, Pierre Peyret, G. F., & Lehours, A.-C. (2011). Production and consumption of methane in freshwater lake ecosystems. *Research in Microbiology*, *162*, 832–847. https://doi.org/10.1016/j.resmic.2011.06.004

Boyero, L., Pearson, R. G., Hui, C., Gessner, M. O., Pérez, J., Alexandrou, M. A., … Yule, C. M. (2016). Biotic and abiotic variables influencing plant litter breakdown in streams: a global study. *Proceedings of the Royal Society B: Biological Sciences*, *283*(1829), 20152664. https://doi.org/10.1098/rspb.2015.2664

Bridgham, S. D., Cadillo-Quiroz, H., Keller, J. K., & Zhuang, Q. (2013). Methane emissions from wetlands: Biogeochemical, microbial, and modeling perspectives from local to

global scales. *Global Change Biology*, *19*(5), 1325–1346. https://doi.org/10.1111/gcb.12131

Brühl, C. A., Després, L., Frör, O., Patil, C. D., Poulin, B., Tetreau, G., & Allgeier, S. (2020). Environmental and socioeconomic effects of mosquito control in Europe using the biocide Bacillus thuringiensis subsp. israelensis (Bti). *Science of the Total Environment*, *724*, 1–16. https://doi.org/10.1016/j.scitotenv.2020.137800

Cadotte, T. A. S. M. W., & Williams, D. D. (2014). *How hydroperiod and species richness affect the balance of resource flows across aquatic-terrestrial habitats*. 131–143. https://doi.org/10.1007/s00027-013-0320-9

Colina, M., Meerhoff, M., Pérez, G., Veraart, A. J., Bodelier, P., Horst, A. Van Der, & Kosten, S. (2021). Trophic and non- - trophic effects of fish and macroinvertebrates on carbon emissions. *Freshwater Biology*, *66*(9), 1–15. https://doi.org/10.1111/fwb.13795

Covich, A. P., Palmer, M. A., & Crowl, T. A. (1999). The role of benthic invertebrate species in freshwater ecosystems: Zoobenthic species influence energy flows and nutrient cycling. *BioScience*, *49*(2), 119–127. https://doi.org/10.2307/1313537

Cummins, K. W., & Klug, M. J. (1979). Feeding Ecology of Stream Invertebrates. *Annual Review of Ecology and Systematics*, *10*(1), 147–172. https://doi.org/10.1146/annurev.es.10.110179.001051

Dauwe, B., Middelburg, J. J., & Herman, P. M. J. (2001). *Effect of oxygen on the degradability of organic matter in subtidal and intertidal sediments of the North Sea area*. *215*, 13–22. https://doi.org/10.3354/meps215013

De Haas, E. M., Wagner, C., Koelmans, A. A., Kraak, M. H. S., & Admiraal, W. (2006). Habitat selection by chironomid larvae: Fast growth requires fast food. *Journal of Animal Ecology*, *75*(1), 148–155. https://doi.org/10.1111/j.1365-2656.2005.01030.x

Deines, P., Grey, J., Richnow, H. H., & Eller, G. (2007). Linking larval chironomids to methane: Seasonal variation of the microbial methane cycle and chironomid δ13C. *Aquatic Microbial Ecology*, *46*(3), 273–282. https://doi.org/10.3354/ame046273

Delsontro, T., Boutet, L., St-pierre, A., Giorgio, P. A., & Prairie, Y. T. (2016). Methane ebullition and diffusion from northern ponds and lakes regulated by the interaction between temperature and system productivity. *Limnology and Oceanography*, *61*(S1), S62–S77. https://doi.org/10.1002/lno.10335

Demars, B. O. L., Kemp, J. L., Marteau, B., Friberg, N., & Thornton, B. (2021). Stream Macroinvertebrates and Carbon Cycling in Tangled Food Webs. *Ecosystems*, *24*(8), 1944–1961. https://doi.org/10.1007/s10021-021-00626-8

Ding, W., Cai, Z., & Tsuruta, H. (2004). Diel variation in methane emissions from the stands of Carex lasiocarpa and Deyeuxia angustifolia in a cool temperate freshwater marsh. *Atmospheric Environment*, *38*, 181–188. https://doi.org/10.1016/j.atmosenv.2003.09.066

Downing, J. A., & Duarte, C. M. (2009). Abundance and Size Distribution of Lakes, Ponds and Impoundments. *Encyclopedia of Inland Waters*, *51*(5), 469–478. https://doi.org/10.1016/B978-012370626-3.00025-9

Downing, John A. (2010). Emerging global role of small lakes and ponds: little things mean a lot. *Limnetica*, *29*(1), 9–24. https://doi.org/10.23818/limn.29.02

Duguma, D., Hall, M. W., Rugman-Jones, P., Stouthamer, R., Neufeld, J. D., & Walton, W. E. (2015). Microbial communities and nutrient dynamics in experimental microcosms are altered after the application of a high dose of Bti. *Journal of Applied Ecology*, *52*(3), 763–773. https://doi.org/10.1111/1365-2664.12422

Etminan, M., Myhre, G., Highwood, E. J., & Shine, K. P. (2016). Radiative forcing of carbon dioxide, methane, and nitrous oxide: A significant revision of the methane radiative forcing. *Geophysical Research Letters*, *43*(24), 12,614-12,623. https://doi.org/10.1002/2016GL071930

Fan, J., Zhong, H., Harris, W., Yu, G., Wang, S., Hu, Z., & Yue, Y. (2008). Carbon storage in the grasslands of China based on field measurements of above- and below-ground biomass. *Climatic Change*, *86*(3–4), 375–396. https://doi.org/10.1007/s10584-007-9316-6

Frouz, J., Matěna, J., & Ali, A. (2003). Survival strategies of chironomids (Diptera : Chironomidae) living in temporary habitats : a review. *European Journal of Entomology*, *100*, 459–465. https://doi.org/10.14411/eje.2003.069

Ganglo, C., Manfrin, A., Mendoza-lera, C., & Lorke, A. (2022). Biocide treatment for mosquito control increases CH4 emissions in floodplain pond mesocosms. *Frontiers in Water*, 10. https://doi.org/10.3389/frwa.2022.996898

Gerstle, V., Manfrin, A., Kolbenschlag, S., Gerken, M., Islam, A. S. M. M. U., Entling, M. H., … Brühl, C. A. (2022). Benthic macroinvertebrate community shifts based on Bti-induced chironomid reduction also decrease Odonata emergence. *Environmental Pollution*, *316*(P1), 2–8. https://doi.org/10.1016/j.envpol.2022.120488

Gorsky, A. L., Racanelli, G. A., Belvin, A. C., & Chambers, R. M. (2019). Greenhouse gas flux from stormwater ponds in southeastern Virginia (USA). *Anthropocene*, *28*, 100218. https://doi.org/10.1016/j.ancene.2019.100218

Griffiths, B. S., Ritz, K., Bardgett, R. D., Cook, R., Christensen, S., Ekelund, F., … Nicolardot,

B. (2000). Ecosystem response of pasture soil communities to fumigation-induced microbial diversity reductions: An examination of the biodiversity-ecosystem function relationship. *Oikos*, *90*(2), 279–294. https://doi.org/10.1034/j.1600-0706.2000.900208.x

Highway, M. T. (1998). *Effects of Bacillus Thuringiensis Israelensis (Bti) and Methophrene on nontarget macroinvertebrates in Minnesota wetlands*. *8*(1), 41–60. https://doi.org/10.1890/1051-0761(1998)008[0041:EOBTIB]2.0.CO;2

Hodkinson, I. D., & Williams, K. A. (1980). Tube Formation and Distribution of Chironomus Plumosus L. (Diptera : Chironomidae) in a Eutrophic Woodland Pond. *Chironomidae*, 331–337. https://doi.org/10.1016/b978-0-08-025889-8.50051-9

Holgerson, M. A. (2015). Drivers of carbon dioxide and methane supersaturation in small, temporary ponds. *Biogeochemistry*, *124*(1–3), 305–318. https://doi.org/10.1007/s10533-015-0099-y

Holgerson, M. A., & Raymond, P. A. (2016). Large contribution to inland water CO2 and CH4 emissions from very small ponds. *Nature Geoscience*, *9*(3), 222–226. https://doi.org/10.1038/ngeo2654

Hölker, F., Vanni, M. J., Kuiper, J. J., Meile, C., Grossart, H. P., Stief, P., … Lewandowski, J. (2015). Tube-dwelling invertebrates: Tiny ecosystem engineers have large effects in lake ecosystems. *Ecological Monographs*, *85*(3), 333–351. https://doi.org/10.1890/14-1160.1

International Hydropower Association (IHA). (2010). *GHG Measurement Guidelines for Freshwater Reservoirs*.

Jackson, J. M., & Mclachlan, A. J. (1991). Rain-pools on peat moorland as island habitats for midge larvae. *Hydrobiologia*, *209*, 59–65. https://doi.org/10.1007/BF00006718

Jakob, C., & Poulin, B. (2016). Indirect effects of mosquito control using Bti on dragonflies and damselflies (Odonata) in the Camargue. *Insect Conservation and Diversity*, *9*(2), 161–169. https://doi.org/10.1111/icad.12155

Jeffrey, L. C., Maher, D. T., Johnston, S. G., Kelaher, B. P., Steven, A., & Tait, D. R. (2019). Wetland methane emissions dominated by plant-mediated fluxes: Contrasting emissions pathways and seasons within a shallow freshwater subtropical wetland. *Limnology and Oceanography*, *64*(5), 1895–1912. https://doi.org/10.1002/lno.11158

Jones, R. I., & Grey, J. (2011). Biogenic methane in freshwater food webs. *Freshwater Biology*, *56*(2), 213–229. https://doi.org/10.1111/j.1365-2427.2010.02494.x

Kajan, R., & Frenzel, P. (1999). The effect of chironomid larvae on production, oxidation and fluxes of methane in a flooded rice soil. *FEMS Microbiology Ecology*, *28*(2), 121–129. https://doi.org/10.1016/S0168-6496(98)00097-X

Kästel, A., Allgeier, S., & Brühl, C. A. (2017). Decreasing Bacillus thuringiensis israelensis sensitivity of Chironomus riparius larvae with age indicates potential environmental risk for mosquito control. *Scientific Reports*, *7*(1), 1–7. https://doi.org/10.1038/s41598-017-14019-2

Kelly, C. A., & Chynoweth, D. P. (2014). The Contributions of Temperature and of the Input of Organic Matter in Controlling Rates of Sediment Methanogenesis. *American Society of Limnology and Oceanography*, *26*(5), 891–897. https://doi.org/https://doi.org/10.4319/lo.1981.26.5.0891

Keuskamp, J. A., Dingemans, B. J. J., Lehtinen, T., Sarneel, J. M., & Hefting, M. M. (2013). Tea Bag Index: A novel approach to collect uniform decomposition data across ecosystems. *Methods in Ecology and Evolution*, *4*(11), 1070–1075. https://doi.org/10.1111/2041-210X.12097

Knoblauch, C., Spott, O., Evgrafova, S., Kutzbach, L., & Pfeiffer, E. M. (2015). Regulation of methane production, oxidation, and emission by vascular plants and bryophytes in ponds of the northeast Siberian polygonal tundra. *Journal of Geophysical Research: Biogeosciences*, *120*(12), 2525–2541. https://doi.org/10.1002/2015JG003053

Koenigs, R., Sturgeon, W., & Biologist, P. (2018). *Chironomid (Lake Fly) Relative Abundance Assessment Report*.

Kolbenschlag, S., Gerstle, V., Eberhardt, J., Bollinger, E., Schulz, R., Brühl, C. A., & Bundschuh, M. (2023). A temporal perspective of aquatic subsidy: Bti affects the emergence of Chironomidae. *Ecotoxicology and Environmental Safety*, *250*, 114503. https://doi.org/10.1016/j.ecoenv.2023.114503

Lagauzère, S., Moreira, S., & Koschorreck, M. (2011). Influence of bioturbation on the biogeochemistry of littoral sediments of an acidic post-mining pit lake. *Biogeosciences*, *8*(2), 339–352. https://doi.org/10.5194/bg-8-339-2011

Leeper, D. A., & Taylor, B. E. (1998). Insect emergence from a South Carolina (USA) temporary wetland pond, with emphasis on the Chironomidae (Diptera). *Chicago Journals*, *17*(1), 54–72. https://doi.org/10.2307/1468051

Leonte, M., Kessler, J. D., Kellermann, M. Y., Arrington, E. C., Valentine, D. L., & Sylva, S. P. (2017). Rapid rates of aerobic methane oxidation at the feather edge of gas hydrate stability in the waters of Hudson Canyon, US Atlantic Margin. *Geochimica et Cosmochimica Acta*, *204*, 375–387. https://doi.org/10.1016/j.gca.2017.01.009

Ljung, K., & Lin, S. (2023). Organic Carbon Burial in Constructed Ponds in Southern Sweden. *Earth Science, Systems and Society*, *3*(January), 1–13. https://doi.org/10.3389/esss.2023.10061

Maeck, A., Hofmann, H., & Lorke, A. (2014). Pumping methane out of aquatic sediments – Ebullition forcing mechanisms in an impounded river. *Biogeosciences*, *11*(11), 2925–2938. https://doi.org/10.5194/bg-11-2925-2014

Maucieri, C., Barbera, A. C., Vymazal, J., & Borin, M. (2017). A review on the main affecting factors of greenhouse gases emission in constructed wetlands. *Agricultural and Forest Meteorology*, *236*, 175–193. https://doi.org/10.1016/j.agrformet.2017.01.006

Mclachlan, A. J., & Cantrell, M. A. (1976). Sediment development and its influence on the distribution and tube structure of Chironomus plumosus L. (Chironomidae, Diptera) in a new impoundment. *Freshwater Biology*, *6*(5), 437–443. https://doi.org/10.1111/j.1365-2427.1976.tb01632.x

Murniati, E., Gross, D., Herlina, H., Hancke, K., & Lorke, A. (2017). Effects of bioirrigation on the spatial and temporal dynamics of oxygen above the sediment-water interface. *Freshwater Science*, *36*(4), 784–795. https://doi.org/10.1086/694854

Nepf, H. M. (2012). Flow and Transport in Regions with Aquatic Vegetation. *Annual Review of Fluid Mechanics of Fluid Mechanics*, *44*, 123–142. https://doi.org/10.1146/annurev-fluid-120710-101048

Nogaro, G., & Steinman, A. D. (2014). Influence of ecosystem engineers on ecosystem processes is mediated by lake sediment properties. *Oikos*, *123*(4), 500–512. https://doi.org/10.1111/j.1600-0706.2013.00978.x

Oliveira Junior, E. S., Temmink, R. J. M., Buhler, B. F., Souza, R. M., Resende, N., Spanings, T., … Kosten, S. (2019). Benthivorous fish bioturbation reduces methane emissions, but increases total greenhouse gas emissions. *Freshwater Biology*, *64*(1), 197–207. https://doi.org/10.1111/fwb.13209

Parr, T. B., Capps, K. A., Inamdar, S. P., & Metcalf, K. A. (2019). Animal-mediated organic

matter transformation: Aquatic insects as a source of microbially bioavailable organic nutrients and energy. *Functional Ecology*, *33*(3), 524–535. https://doi.org/10.1111/1365-2435.13242

Peacock, M., Audet, J., Bastviken, D., Cook, S., Evans, C. D., Grinham, A., … Futter, M. N. (2021). Small artificial waterbodies are widespread and persistent emitters of methane and carbon dioxide. *Global Change Biology*, *27*(20), 5109–5123. https://doi.org/10.1111/gcb.15762

Peters, V., & Conrad, R. (1996). Sequential reduction processes and initiation of CH4 production upon flooding of oxic upland soils. *Soil Biology and Biochemistry*, *28*(3), 371–382. https://doi.org/0038-0717(95)00146-8

Pinheiro, J., Bates, D., DebRoy, S., & Sarkar, D. (2022). *nlme: Linear and Nonlinear Mixed Effects Models*. https://doi.org/https://CRAN.R-project.org/package=nlme

Poindexter, C. M., Baldocchi, D. D., Matthes, J. H., Knox, S. H., & Variano, E. A. (2016). The contribution of an overlooked transport process to a wetland's methane emissions. *Geophysical Research Letters*, *48*(12), 6276–6284. https://doi.org/10.1002/2016GL068782.Received

Poulin, B., Lefebvre, G., Hilaire, S., & Després, L. (2022). Long-term persistence and recycling of Bacillus thuringiensis israelensis spores in wetlands sprayed for mosquito control. *Ecotoxicology and Environmental Safety*, *243*(8). https://doi.org/10.1016/j.ecoenv.2022.114004

Rosentreter, J. A., Borges, A. V, Deemer, B. R., Holgerson, M. A., Liu, S., Song, C., … Eyre, B. D. (2021). Half of global methane emissions come from highly variable aquatic ecosystem sources. *Nature Geoscience*, *14*, 225–230. https://doi.org/10.1038/s41561-021-00715-2

Roskosch, A., Hette, N., & Hupfer, M. (2012). Alteration of Chironomus plumosus ventilation activity and bioirrigation-mediated benthic fluxes by changes in temperature , oxygen concentration , and seasonal variations. *Freshwater Science*, *31*(2), 269–281. https://doi.org/10.1899/11-043.1

Sanches, L. F., Guenet, B., Marinho, C. C., Barros, N., & de Assis Esteves, F. (2019). Global regulation of methane emission from natural lakes. *Scientific Reports*, *9*(1), 1–10. https://doi.org/10.1038/s41598-018-36519-5

Sanseverino, A. M., Bastviken, D., Sundh, I., Pickova, J., & Enrich-Prast, A. (2012). Methane carbon supports aquatic food webs to the fish level. *PLoS ONE*, *7*(8). https://doi.org/10.1371/journal.pone.0042723

Saunois, M., Stavert, A. R., Poulter, B., Bousquet, P., Canadell, J. G., Jackson, R. B., … Houweling, S. (2020). The Global Methane Budget 2000 – 2017. *Earth System Science Data*, *12*, 1561–1623. https://doi.org/https://doi.org/10.5194/essd-12-1561-2020

Sawakuchi, H. O., Bastviken, D., Sawakuchi, A. O., Ward, N. D., Borges, C. D., Tsai, S. M., … Krusche, A. V. (2016). Oxidative mitigation of aquatic methane emissions in large Amazonian rivers. *Global Change Biology*, *22*(3), 1075–1085. https://doi.org/10.1111/gcb.13169

Sawakuchi, O., Ward, N. D., Borges, C. D., Tsai, S. I. U. M., Richey, J. E., Centen, A., … Sciences, G. (2016). *Oxidative mitigation of aquatic methane emissions in large Amazonian rivers*. 1075–1085. https://doi.org/10.1111/gcb.13169

Segers, R. (1998). Methane production and methane consumption : a review of processes underlying wetland methane fluxes. *Springer*, *41*(1), 23–51. Retrieved from http://www.jstor.org/stable/1469307 .

Sobek, S., Söderbäck, B., Karlsson, S., Andersson, E., & Brunberg, A. K. (2006). A Carbon Budget of a Small Humic Lake: An Example of the Importance of Lakes for Organic Matter Cycling in Boreal Catchments. *Ambio*, *35*(8), 469–475. https://doi.org/10.1579/0044-7447(2006)35[469:ACBOAS]2.0.CO;2

Stadmark, J., & Leonardson, L. (2005). Emissions of greenhouse gases from ponds constructed for nitrogen removal. *Ecological Engineering*, *25*(5), 542–551. https://doi.org/10.1016/j.ecoleng.2005.07.004

Taylor, S., Gilbert, P. J., Cooke, D. A., Deary, M. E., & Jeffries, M. J. (2019). High carbon burial rates by small ponds in the landscape. *Frontiers in Ecology and the Environment*, *17*(1), 25–31. https://doi.org/10.1002/fee.1988

Theissinger, K., Röder, N., Allgeier, S., Beermann, A. J., Brühl, C. A., Friedrich, A., … Schwenk, K. (2019). Mosquito control actions affect chironomid diversity in temporary wetlands of the Upper Rhine Valley. *Molecular Ecology*, *28*(18), 4300–4316. https://doi.org/10.1111/mec.15214

Thottathil, S. D., Reis, P. C. J., del Giorgio, P. A., & Prairie, Y. T. (2018). The Extent and

Regulation of Summer Methane Oxidation in Northern Lakes. *Journal of Geophysical Research: Biogeosciences*, *123*(10), 3216–3230. https://doi.org/10.1029/2018JG004464

Tilquin, M., Paris, M., Reynaud, S., Despres, L., Ravanel, P., Geremia, R. A., & Gury, J. (2008). Long lasting persistence of Bacillus thuringiensis subsp. israelensis (Bti) in mosquito natural habitats. *PLoS ONE*, *3*(10). https://doi.org/10.1371/journal.pone.0003432

Vachon, D., Sponseller, R. A., & Karlsson, J. (2021). Integrating carbon emission, accumulation and transport in inland waters to understand their role in the global carbon cycle. *Global Change Biology*, *27*(4), 719–727. https://doi.org/10.1111/gcb.15448

Vadeboncoeur, Y., Vander Zanden, M. J., & Lodge, D. M. (2002). Putting the lake back together: Reintegrating benthic pathways into lake food web models. *BioScience*, *52*(1), 44–54. https://doi.org/10.1641/0006-3568(2002)052[0044:PTLBTR]2.0.CO;2

Van Der Nat, F. J. W. A., & Middelburg, J. J. (1998). Effects of two common macrophytes on methane dynamics in freshwater sediments. *Biogeochemistry*, *43*, 79–104. https://doi.org/10.1023/A:1006076527187

Van Hardenbroek, M., Lotter, A. F., Bastviken, D., Duc, N. T., & Heiri, O. (2012). Relationship between δ13C of chironomid remains and methane flux in Swedish lakes. *Freshwater Biology*, *57*(1), 166–177. https://doi.org/10.1111/j.1365-2427.2011.02710.x

Vasquez, A. A., Bonnici, B. L., Yusuf, S. H., Cruz, J. I., Hudson, P. L., & Ram, J. L. (2022). Improved Chironomid Barcode Database Enhances Identification of Water Mite Dietary Content. *Diversity*, *14*(2). https://doi.org/10.3390/d14020065

Velthuis, M., Kosten, S., Aben, R., Kazanjian, G., Hilt, S., Peeters, E. T. H. M., … Bakker, E. S. (2018). Warming enhances sedimentation and decomposition of organic carbon in shallow macrophyte-dominated systems with zero net effect on carbon burial. *Global Change Biology*, *24*(11), 5231–5242. https://doi.org/10.1111/gcb.14387

Wallin, M. B., Chmiel, H. E., Kokic, J., Denfeld, B. A., Sobek, S., Koehler, B., … Eve, M.-. (2016). *The role of sediments in the carbon budget of a small boreal lake I*. 1814–1825. https://doi.org/10.1002/lno.10336

Walter, K. M., Smith, L. C., & Chapin, F. S. (2007). Methane bubbling from northern lakes: Present and future contributions to the global methane budget. *Philosophical Transactions of the Royal Society A: Mathematical, Physical and Engineering Sciences*, *365*(1856), 1657–1676. https://doi.org/10.1098/rsta.2007.2036

Wang, C., Lai, D. Y. F., Sardans, J., Wang, W., Zeng, C., & Peñuelas, J. (2017). Factors related with CH4 and N2O emissions from a paddy field: Clues for management implications. *PLoS ONE*, *12*(1), 1–23. https://doi.org/10.1371/journal.pone.0169254

Yavitt, J. B., Angel, L. L., Fahey, T. J., Cirmo, C. P., & Driscoll, C. T. (1992). Methane fluxes , concentrations , and production Adirondack beaver impoundments. *Limnology and Oceanography*, *37*(5), 1057–1066. https://doi.org/10.4319/lo.1992.37.5.1057

Yiallouros, M., Storch, V., & Becker, N. (1999). Impact of Bacillus thuringiensis var. israelensis on Larvae of Chironomus thummi thummi and Psectrocladius psilopterus (Diptera: Chironomidae). *Journal of Invertebrate Pathology*, *74*(1), 39–47. https://doi.org/10.1006/jipa.1999.4852

Zhang, Y., Wang, J., Tao, J., Zhou, Y., Yang, H., Yang, X., … Jeppesen, E. (2022). Concentrations of dissolved organic matter and methane in lakes in Southwest China: Different roles of external factors and in-lake biota. *Water Research*, *225*(September), 119190. https://doi.org/10.1016/j.watres.2022.119190

Zuur, A. F., Ieno, E. N., & Elphick, C. S. (2010). A protocol for data exploration to avoid common statistical problems. *Methods in Ecology and Evolution*, *1*(1), 3–14. https://doi.org/10.1111/j.2041-210x.2009.00001.x

Authors contributions

The present thesis is based on three research articles provided in Appendix A1-A3. The author's contribution in all the appendices is detailed. I was lead author in all research articles.

Appendix A1

Ganglo, C., Manfrin, A., Mendoza-Lera, C., & Lorke, A. (2022). Biocide treatment for mosquito control increases methane emissions in floodplain pond mesocosms. Frontiers in Water. https://doi.org/10.3389/frwa.2022.996898

Conceptualization: Caroline Ganglo, Clara Mendoza-Lera, Andreas Lorke

Methodology: Caroline Ganglo, Clara Mendoza-Lera, Andreas Lorke

Data collection: Caroline Ganglo

Data curation: Caroline Ganglo

Data analysis: Caroline Ganglo, Alessandro Manfrin Clara Mendoza-Lera, Andreas Lorke

Writing: Caroline Ganglo, Alessandro Manfrin Clara Mendoza-Lera, Andreas Lorke

Appendix A2

Ganglo, C., Mendoza-Lera, C., Manfrin, A., Bolpagni R., Gerstle, V., Kolbenschlag S., Bollinger, E., Schulz, R. & Lorke, A. (2023). Does biocide treatment for mosquito control alter carbon dynamics in floodplain ponds? Science of the total environment https://doi.org/10.1016/j.scitotenv.2023.161978

Conceptualization: Caroline Ganglo, Verena Gerstle, Sara Kolbenschlag, Clara Mendoza-Lera, Andreas Lorke

Experiment design: : Caroline Ganglo, Verena Gerstle, Sara Kolbenschlag, Clara Mendoza-Lera, Andreas Lorke

Methodology: Caroline Ganglo, Clara Mendoza-Lera, Andreas Lorke

Data collection: Caroline Ganglo, Verena Gerstle, Sara Kolbenschlag, Eric Bollinger

Data analysis: Caroline Ganglo, Alessandro Manfrin Clara Mendoza-Lera, Andreas Lorke

Writing: Caroline Ganglo, Alessandro Manfrin Clara Mendoza-Lera, Rossano Bolpagni, Verena Gerstle, Sara Kolbenschlag , Eric Bollinger, Ralf Schulz, Andreas Lorke

Appendix A3

Ganglo, C., Manfrin, A., Mendoza-Lera, C. & Lorke, A. (2023). Effects of chironomids density and mosquito biocide on methane dynamics in freshwater sediments. Plos One (submitted 07 February 2023)

Conceptualization: Caroline Ganglo, Clara Mendoza-Lera, Andreas Lorke

Methodology: Caroline Ganglo, Clara Mendoza-Lera, Andreas Lorke

Data collection: Caroline Ganglo

Data analysis: Caroline Ganglo, Alessandro Manfrin Clara Mendoza-Lera, Andreas Lorke

Writing: Caroline Ganglo, Alessandro Manfrin Clara Mendoza-Lera, Andreas Lorke

Declaration

I independently conducted the work presented in this thesis entitled

"**Effects of an anthropogenic stressor on carbon biogeochemical processes and fluxes in water to land transition zones of ponds**".

All used assistances are mentioned and involved contributors are either co-authors of or are acknowledged in the respective publication.

This thesis has never been submitted elsewhere for an examination, as a thesis, or for evaluation in a similar context to any department of this university or any scientific institution. I am aware that a violation of the aforementioned conditions can have legal consequences.

27.02.2023	Caroline Ganglo
Place, date	Signature

Curriculum Vitae

Caroline Ganglo

WORK EXPERIENCE

Germany 10. 2019 - 03. 2023	**Graduate Researcher**: Graduate College Systemlink University of Koblenz Landau Germany **Project founded by Deutsche Forschungsgemeinschaft**
China 09. 2017 - 07. 2019	**Graduate Researcher** : Nanjing University of Information Science and Technology, China **Project founded by Nanjing University of Information Science and Technology China**
United State of America 05. 2015 - 07. 2015	**Research Training in Biodiversity**: Kansas University, United States of America

EDUCATION

Germany 09.2019 - 03.2023	University of Kaiserslautern-Landau • **Doctoral degree**: Natural sciences
China 09.2017 - 07.2019	Nanjing University of Information Science and Technology • **Master degree**: Environmental Science and Engineering
Republic of Benin 01.2011 - 11.2014	University of Abomey-Calavi • **Bachelor degree**: Environmental Science

Acknowledgment

I wish to express my sincere gratitude to the Deutsche Forschungsgemeinschaft (DFG, German Research Foundation) for their support and funding under grant number −326210499/GRK2360, SystemLink. Your contribution has been instrumental in the success of this work.

I would like to extend my heartfelt gratitude to my main mentor, Andreas Lorke, who graciously accepted the role of supervising my Ph.D. study. His invaluable advice and guidance were a cornerstone of my journey. I am also deeply thankful to Clara Mendoza-Lera for her unwavering support and guidance throughout my Ph.D. program. Alessandro Manfrin deserves special mention for introducing me to the world of statistics and for providing support, advice, and words of encouragement during my Ph.D. journey. I extend my sincere appreciation to Rossano Bolpagni for undertaking the challenging task of proofreading my thesis within a tight timeframe. I would also like to thank Viktor Baranov and Rossano Bolpagni for providing invaluable insights that greatly enriched my understanding and helped me address various confusions. I am also indebted to Ralf Schulz for his exceptional support.

I must express my gratitude to my colleagues at Systemlink for fostering a wonderful family-like work environment. Special thanks to Anja Knäbel and Simone von Schlichtegroll for their unwavering support and encouragement. I would like to convey my thanks to the Environmental Physics Group at the university for their support in setting up experiments and for engaging in collaborative efforts. This journey has been enriched by the wisdom, support, and collaboration of these individuals and groups, for which I am truly grateful.

I am grateful to myself for dedicating the time and effort to complete this incredible journey. I also want to extend my heartfelt thanks to my parents, Jean Cossi Ganglo, and, in particular, my mother, Marie-Rose Hamahouzo, for their unwavering love and support. Additionally, my heartfelt appreciation goes out to my siblings for their tremendous support and affection.

I extend my utmost gratitude to my Creator, who has never forsaken me. Your boundless grace and blessings surpass my ability to express gratitude.

Appendix I

Published paper

(Ganglo, C., Manfrin, A., Mendoza-lera, C., & Lorke, A. (2022). Biocide treatment for mosquito control increases CH_4 emissions in floodplain pond mesocosms. *Frontiers in Water*, *4*(9), 10. https://doi.org/10.3389/frwa.2022.996898)

frontiers | Frontiers in Water

TYPE Original Research
PUBLISHED 12 September 2022
DOI 10.3389/frwa.2022.996898

OPEN ACCESS

EDITED BY
Congsheng Fu,
Nanjing Institute of Geography and Limnology (CAS), China

REVIEWED BY
Pedro Maia Barbosa,
Université du Québec à Montréal, Canada
Alain Isabwe,
Institute of Urban Environment (CAS), China

*CORRESPONDENCE
Caroline Ganglo
carolineganglo20@gmail.com

SPECIALTY SECTION
This article was submitted to Water and Climate, a section of the journal Frontiers in Water

RECEIVED 18 July 2022
ACCEPTED 22 August 2022
PUBLISHED 12 September 2022

CITATION
Ganglo C, Manfrin A, Mendoza-Lera C and Lorke A (2022) Biocide treatment for mosquito control increases CH_4 emissions in floodplain pond mesocosms. *Front. Water* 4:996898. doi: 10.3389/frwa.2022.996898

Biocide treatment for mosquito control increases CH_4 emissions in floodplain pond mesocosms

Caroline Ganglo*, Alessandro Manfrin, Clara Mendoza-Lera and Andreas Lorke

Institute for Environmental Sciences, University of Koblenz-Landau, Landau, Germany

Shallow lentic freshwater aquatic systems are globally important emitters of methane (CH_4), a highly potent greenhouse gas. Previous laboratory studies indicated that bioturbation by chironomids can reduce CH_4 production and increase CH_4 oxidation by enhancing oxygen transport into sediment. Thus, reduction in chironomid density by application of biocides for mosquito control, such as *Bacillus thuringinesis* var. *israelensis* (Bti), have the potential to affect CH_4 emissions. We evaluated the effect of a 41% reduction in chironomid larvae abundance due to Bti applications on CH_4 dynamics in the aquatic and aquatic-terrestrial transition zones of 12 floodplain pond mesocosms (FPMs) (half treated, half control). We evaluated short-term (2 months) and seasonal effects by measuring CH_4 emissions, dissolved concentrations, and oxidation rates in spring, summer, autumn, and winter. On average, CH_4 emissions from the aquatic-terrestrial transition zone of the treated FPMs were 137 % higher than those of the control FPMs. The lack of differences in mean oxidation rates between the treated and control mesocosms suggests that a reduction in bioturbation and the associated decreased oxygen transport into the sediment promoted CH_4 production in the treated FPMs. Our findings point to potential effects of Bti on CH_4 biogeochemistry through alterations of the chironomid abundance, and highlight the underestimated role of invertebrates in biogeochemical cycling in these ecosystems.

KEYWORDS

Bti, biogeochemistry, methane, lentic shallow water, bioturbation

Introduction

Methane (CH_4) is a potent greenhouse gas, and the increase in its atmospheric concentration has been contributing about 23% of the additional radiative forcing accumulated in the lower atmosphere since preindustrial times (Etminan et al., 2016; Saunois et al., 2020). Nearly 50% of the total global CH_4 emissions are from aquatic ecosystems, with the largest contributions from small (<0.001 km^2) and shallow lentic aquatic system (Bergen et al., 2019; Rosentreter et al., 2021).

CH_4 is mainly produced by methanogenic archaea in anoxic sediments during the breakdown of organic matter (Segers, 1998). Its production rate is mainly controlled by redox conditions, quantity and quality of organic matter, and temperature (Yavitt et al., 1992; Peters and Conrad, 1996; Kelly and Chynoweth, 2014). On the other hand, CH_4 oxidation to carbon dioxide (CO_2) by methanotrophic bacteria under oxic conditions in sediment or in the water column is the major sink of CH_4 (Borrel et al., 2011). Up to 90% of the CH_4 produced can be oxidized before reaching the atmosphere as diffusive emission (Bastviken et al., 2004; Knoblauch et al., 2015; Sawakuchi et al., 2016). However, CH_4 oxidation in oxic aquatic compartments can be efficiently bypassed by non-diffusive emission pathways that directly transport CH_4 from anoxic sediments to the atmosphere, including bubble-mediated transport (ebullition) (Bastviken et al., 2004; Walter et al., 2007), and plant-mediated transport (Jeffrey et al., 2019; Bansal et al., 2020).

CH_4 production, oxidation, and emission (both diffusive and non-diffusive) in shallow aquatic systems are regulated by numerous factors, including water depth (Gorsky et al., 2019), the ratio of surface area to volume (Holgerson and Raymond, 2016), water temperature (Stadmark and Leonardson, 2005), sediment properties (Bodmer et al., 2020), system productivity (Delsontro et al., 2016), and vegetation (Bansal et al., 2020). The most overlooked processes affecting CH_4 dynamics are trophic and non-trophic interactions of methanogens and methanotrophs with benthic macroinvertebrates (Colina et al., 2021). In shallow, lentic ecosystems, benthic macroinvertebrate communities are often dominated by sediment-dwelling groups such as chironomid larvae (Diptera: Chironomidae) (Leeper and Taylor, 1998; Hölker et al., 2015). They construct U-shaped burrows (tubes) in areas of fine sediment (De Haas et al., 2006; Nogaro and Steinman, 2014), which they actively ventilate with surface water connecting the water column with anoxic sediment layers (Mclachlan and Cantrell, 1976; Hodkinson and Williams, 1980; Murniati et al., 2017). On the one hand, chironomids can promote CH_4 emissions by feeding on CH_4 oxidizing bacteria (Jones and Grey, 2011) and trigger the release of CH_4 gas bubbles (Booth et al., 2021). On the other hand, they may promote CH_4 oxidation by oxygenating the sediment (Kajan and Frenzel, 1999). Due to the seasonal variations in burrowing activity (Jackson and Mclachlan, 1991; Frouz et al., 2003), and the lack of *in situ* studies, it remains unclear how chironomid activity affects CH_4 dynamics at ecosystem scale (Kajan and Frenzel, 1999).

As most macroinvertebrates, chironomids are affected by anthropogenic stressors. A particular threat to chironomids are biological agents used to control larval stages of various nematocerous dipterans (i.e. black flies and mosquitoes) (Jakob and Poulin, 2016), such as *Bacillus thuringiensis* var. *israelensis* (Bti) (Boisvert and Boisvert, 2000; Brühl et al., 2020). Bti is widely used in Europe in in other parts of the world (Brühl et al., 2020). In Germany, up to 5000 tons of Bti formulations were applied to 400,000 ha in the Upper Rhine Valley between 1981 and 2016 (Becker et al., 2018). Due to its targeted effect on mosquitos and black flies, Bti is generally considered an "environmentally safe" alternative to traditional chemical pesticides (Brühl et al., 2020). Chironomid larvae were the most severely affected aquatic invertebrates and experienced abundance reductions by 50–87% in Bti-treated mesocosms and field studies in Germany (Allgeier et al., 2019a,b), which potentially also affects CH_4 dynamics in these ecosystems.

Here we tested whether the application of Bti has implications for CH_4 emission, concentration, and oxidation through reduction of the chironomid abundance. We measured dissolved CH_4 concentrations, CH_4 emission and oxidation rates from 12 floodplain pond mesocosms (FPMs), half of which were treated with Bti. A companion study carried out in parallel at the same FPMs revealed a reduction in chironomid larvae abundance in the treated FPMs by 41% compared to controls (Gerstle et al., 2022). We hypothesized that the reduced chironomid density would result in a decrease in CH_4 oxidation, higher concentrations of dissolved CH_4 in water, and in higher emissions to the atmosphere in the treated FPMs. We expected this effect to be most pronounced in the aquatic-terrestrial transition zone of the FPMs, which featured more favorable conditions for chironomids than the deeper areas of the FPMs with coarser sediment.

Materials and methods

Study site

The experiment was conducted in 12 identical FPMs, located at the Eusserthal Ecosystems Research Station in south-western (EERES; Germany 49°15'14" N, 7°57'42" E). The FPMs were constructed in 2018, have a surface area of ∼104 m^2 and can contain a water volume up to ∼25 m^3. The FPMs are separated from groundwater by a flexible rubber foil, can be fed on demand with water from the nearby stream, Sulzbach, and the water level can be adjusted to mimic flooding events (Stehle et al., 2022). Each FPM comprises a gradient in water depth with an aquatic-terrestrial transition zone (surface area: ∼30 m^2, water volume: ∼6 m^3, water depth: ∼0.20 m), and an aquatic zone (surface area: ∼43 m^2, water volume: ∼13 m^3, water depth: ∼0.30 m) (Supplementary Figure S1). The aquatic-terrestrial transition zone is characterized by a 15 cm thick layer of medium to coarse sand (diameter: ∼0.05 cm) and is covered by submerged macrophytes (∼28 % areal coverage) and emerged plants (∼46 %). In the aquatic zone, the bed consists of a 13 cm thick layer of coarse pebbles (diameter: ∼1-3 cm) and is colonized by submerged macrophytes (*Elodea* MICHX. and *Ceratophyllum* L. ∼35 % areal coverage), and by emergent plants (*Typha L.* ∼40 %) along the banks.

Experimental set-up

Flooding and Bti application

Following common practice of mosquito control applications at the Upper Rhine Valley, Bti was applied three times during elevated water levels (i.e., flooding) (Becker, 2006). Before each application, flooding was mimicked by gradually increasing the water level in all FPMs by 0.25 m (from 0.30 ± 0.02 m to 0.50 ± 0.02 m at the deepest location) over a period of two days (water level was continuously monitored in each FPM over the study period using pressure loggers (U20-001-03, Onset Computer Corporation, Hobo, USA). The water level was kept at high level for 10 days, before it was lowered over two days to its initial value. The flooding periods were from 11 to 22 April, 2 to 13 May, and 23 May to 3 June 2020 after which the water level slowly reduced to non-flooding levels over two days (see Supplementary Table S1 for more detail). On the third day of each flood, Bti was applied to every other FPM (n=6; referred to as treated FPMs in the following, Supplementary Figure S2). The untreated FPMs are considered as controls. Bti was applied as a suspension (VectoBac WG; Valent Biosciences, Illinois, USA) at maximum field rate (2.88 × 10^9 ITU ha^{-1} according to the manufacturer) using a knapsack sprayer (Prima 5, Gloria, Germany). The maximum field rate of Bti is usually applied when the water is deeper than 10 cm (Becker, 1997). The areal application rate (118 mg VectoBac® WG m^{-2}) was calculated using the surface area of the FPMs during flooding (~104 m^2). Bti granules quickly sink to the bottom of the pond (within an hour). Its ingredients and metabolites can therefore have accumulated in the treated ponds over the three applications.

Sampling design

To test the short-term effect of Bti applications, CH_4 emissions were measured 4 days before the first flooding (06 April 2020), and 3–5 days after each time the water level was decreased to its regular level (28 April, 14 May, 08 June) (Supplementary Figure S2). Dissolved CH_4 concentration was measured during seven sampling campaigns: 3 days before the first flooding (09 April 2020), 3–7 days after each Bti applications (20 April, 09 May, 28 May), and 3–5 days after each time the water level was decreased to its regular level (27 April, 14 May, 08 June).

To assess seasonal effects of Bti application, additional measurements of emissions and dissolved CH_4 concentrations were performed in spring (April 2020 and May 2020), summer (June 2020 and July 2020), autumn (September 2020 and November 2020), and winter (January 2020 and March 2021). In addition, a 2 days sampling campaigns in aquatic compartment of three FPMs (one treated FPM and two control FPMs) occurred in July (from 21 to 22) to assess daily variation in CH_4 emissions. These data were added to the summer measurement.

As a proxy for CH_4 oxidation, the isotopic signature of carbon in CH_4 ($\delta^{13}C$-CH_4) was measured in gas bubbles collected from the sediment and in dissolved gas in the surface water of the aquatic zone in May 2020 [2 days after the second Bti application (Spring)], June 2020 [2 days after the third flooding (Summer)] and in September 2020 (Autumn), as well as in February 2020 and March 2021 (Winter). Microbial CH_4 oxidation results in enrichment of ^{13}C in the remaining CH_4 (sampled in surface water) in comparison to freshly produced CH_4 (sampled as bubbles) (Bastviken et al., 2002).

CH_4 emissions

CH_4 emissions to the atmosphere were measured in both the aquatic and aquatic-terrestrial transition zones using transparent, floating, static chambers made of plastic polyethylene foil (allflex. E, 300µm, PA/EVOH/PA/PE, allvac Folien GmbH, Germany) (Supplementary Figure S3). Two chambers of different size were used to include vegetation: 72.5 cm x 72.5 cm x 54.6 cm and 72 cm x 72.5 cm x147.2 cm (LxWxH). Two battery-powered fans were placed inside each chamber to ensure uniform gas mixing. The chambers were connected in closed-loop with a gas analyzer (Ultra-portable Greenhouse Gas Analyzer; UGGA, Los Gatos Research Inc., Mountain View, CA, USA) using 2 m Tygon tubing. Relative humidity and temperature in the chamber was monitored *in-situ* (blueDan clima 4.0, ESYS GmbH, Berlin, Germany). Each chamber deployment lasted for about 5 min, or shorter if the relative humidity inside the chamber reached 90%.

CH_4 emissions were calculated based on the slope of a linear regression of the CH_4 mole fraction in the chamber headspace over time (S in ppm s^{-1})

$$F = S\left(\frac{V}{A}\right)\left(\frac{P}{RT}\right)t \quad (1)$$

where F represents the CH_4 flux (mmol m^{-2} d^{-1}), V is the chamber volume (m^3), A is the chamber surface area (m^2), p is atmospheric pressure (atm), R is the universal gas constant (0.0821 atm K^{-1} mol^{-1}), T is the temperature in the chamber headspace (K), and t is a unit conversion factor (t=86,400 s d^{-1}).

Dissolved CH_4

Dissolved CH_4 in the aquatic and aquatic-terrestrial transition zone was measured using the headspace method (International Hydropower Association, 2010). Water samples were collected at 5–10 cm depth using 1.2 l Schott glass bottles (sample volume: ~0.9 l, headspace volume: ~0.3 l) avoiding bubbling. Once closed, the bottle was vigorously shaken for 2 min to ensure gas equilibration between the water sample and the headspace. The bottle headspace was connected to a gas analyzer (Ultra-portable Greenhouse Gas Analyzer; UGGA, Los

Gatos Research Inc., Mountain View, CA, USA) in a closed-loop to measure the molar fraction of CH_4. Dissolved CH_4 in the water samples (c_{CH4} in $\mu mol\ l^{-1}$) was calculated as:

$$c_{CH4} = (X_{Final} - X_{Initial})(V_{HS}/V_s)(p/RT) + P_{Final}K_{CH4} \quad (2)$$

where X_{Final} and $X_{Initial}$ (in parts per million; ppm) are the mole fractions of CH_4 in the sample at equilibrium and the mole fraction of CH_4 in the atmosphere at the sampling time, respectively; V_{HS} and Vs (in l) are headspace volume and sample volume; K_{CH4} is the Henry coefficient of CH_4 (in mol l^{-1} atm^{-1}) at the sampling temperature T (in K); p is the atmospheric pressure (assumed constant at 1 atm) and R is the universal gas constant (0.0821 atm K^{-1} mol^{-1}). The temperature-dependent Henry coefficient was calculated following:

$$K_{CH4} = \left(\frac{\rho_w}{M_w}\right) \exp(-115.6477 + \frac{155.5756}{\frac{T}{100}} + 65.2533 \ln\left(\frac{T}{100}\right) - 6.1698\ T/100) \quad (3)$$

with ρ_w being water density (1,000 g l^{-1}) and M_w the molar mass of water (18.02 g $mole^{-1}$) (International Hydropower Association, 2010).

We also measured dissolved oxygen concentration and temperature using a multiprobe (WTW 82362 Weilheim, multi 3430 Germany) in the surface water of the aquatic and aquatic-terrestrial zone during the dissolved CH_4 concentration measurements.

CH_4 oxidative fraction

The carbon isotopic signature of methane ($\delta^{13}C$-CH_4) was determined from dissolved CH_4 in the surface water and from gas in the sediment. The gas dissolved in surface water was measured using the headspace method (water volume ~30 ml, headspace ~10 ml). The sediment surface was stirred to force ebullition and captured gas bubbles were collected using a handheld funnel. 2.5 ml of gas sample (both from headspace of the surface water and gas bubbles) was transferred to helium flushed exetainers (17 ml), which were analyzed using a PDZ Europa TGII trace gas analyzer and continuous on-line flow Europa 20/20 isotope ratio mass spectrometer (IRMS) at the Biology Center CASNa Sádkách Ceské Budějovice, Czech Republic. Isotopic data reported in δ units (‰) are relative to the Pee Dee belemnite (PDB) standard according to

$$\delta^{13}C = 1000(\frac{R_{sample}}{R_{standard}} - 1) \quad (4)$$

where R is the relative isotope abundance ratio $^{13}C/^{12}C$.

The fraction of CH_4 oxidized (f_{open}) was estimated using an open system, steady-state isotope mixing model (Leonte et al., 2017):

$$f_{open} = \frac{\alpha}{1-\alpha}\left(\frac{\delta_B + 1000}{\delta_{SW} + 1000} - 1\right) \quad (5)$$

where δ_{SW} and δ_B are the $\delta^{13}C$ values of dissolved CH_4 in surface water and in gas bubbles, respectively, α is the fractionation factor for aerobic CH_4 oxidation [$\alpha = 1.02$ (Bastviken et al., 2002)], and f_{open} is the fraction of the diffusive CH_4 flux from the sediment to the water column that becomes oxidized and is not emitted to the atmosphere. f_{open} was multiplied by 100 to obtain the CH4 oxidative fraction in percentage (%). As the model does not account for ebullition and plant-mediated emissions that bypass oxidation, the calculation may underestimate the fraction of the total CH_4 production that is oxidized. However, differences in estimates of the fraction oxidized between treatment and control FPMs can be considered as indicators for differences in oxidation rates.

We additionally calculated the oxidative fraction using the Rayleigh closed system model, which does not rely on steady-state conditions (Thottathil et al., 2018):

$$\ln(1 - f_{close}) = \frac{\ln(\delta_B + 1000) - \ln(\delta_{SW} + 1000)}{\alpha - 1} \quad (6)$$

where f_{close} is the fraction of the diffusive CH_4 flux from the sediment to the water column that becomes oxidized and is not emitted to the atmosphere. f_{close} was multiplied by 100 to obtain the CH_4 oxidative fraction in percentage (%).

Statistical analysis

All data are reported as mean ± standard error. Short term changes in CH_4 emissions and dissolved CH_4 concentration were assessed with linear mixed effect models (LMEMs) using the lme function in the package nlme (Pinheiro et al., 2017) for R (R Core Team, 2013). The model included zone (aquatic and aquatic-terrestrial), treatment (treated and control FPMs), time (before the experiment started, at Bti applications and after Bti applications for dissolved CH_4; before the experiment started and after Bti applications for CH_4 emissions, Supplementary Figure S2), and their interaction as fixed factors. FPM number was used as random factor to account for repeated sampling. In both models, a backward selection was applied using likelihood ratio tests against reduced models following Zuur et al., 2010 chapter 5. The residuals of the initial and of the final selected model were assessed using qq-plots and model residual-fitted values plots. When necessary, dependent variables were log-transformed to meet normality and homogeneity of residual assumptions (Zuur et al., 2010). Potential serial correlation was also considered by fitting the initial model with different autocorrelation structures (Zuur et al., 2010) and using Akaike Information Criterion assessment

to select the best model (Zuur et al., 2010). In case of significant effects of model interactions ($p \leq 0.05$), a contrast analysis was run using linear models with adjusted p-values after Benjamini-Hochberg correction to decrease false discovery rate due to multiple testing (Benjamini and Hochberg, 1995).

Longer-term (seasonal) effect of Bti application were assessed using LMEMs for CH_4 emissions, CH_4 dissolved concentrations and CH_4 oxidative fraction, similarly to the short-term analysis described above (short term analysis). Because sampling for CH_4 oxidative fraction started 2 days after the second Bti application, we analyzed these data for the long-term effect. For the longer-term effect, treatment, season (Spring (but excluding the time before the first Bti application) Summer, Autumn and Winter), and their interactions were considered as fixed factors and FPM as a random factor. The model selection and validation followed the same procedure as previously described.

Results

CH_4 emissions

During the short-term sampling, all FPMs were a source of CH_4 to the atmosphere with an overall mean emission of 4.06 ± 0.42 mmol m^{-2} d^{-1}. Before the Bti application, CH_4 emission was comparable among FPMs (Supplementary Table S3). During the Bti application period, CH_4 emissions did not differ between sampling times, treatment and zone (Supplementary Table S3; Figures 1A,B), except for a single sampling time (After Bti 2) (Figure 1B), when the emissions from the aquatic-terrestrial transition zone were higher in FPMs treated with Bti in comparison to the control FPMs (Tables 1, 2; Supplementary Table S4; Figure 1B).

CH_4 emissions after treatment were comparable among seasons and overall were consistently higher in the aquatic-terrestrial transition zone than in the aquatic one (Supplementary Table S3; Figures 1C,D). In the aquatic-terrestrial transition zone, we measured significantly higher CH_4 emissions from treated FPMs compared to the control units in spring, summer and autumn (Tables 1, 2; Supplementary Table S4; Figure 1D) (although slightly above significance). In the aquatic zone, CH_4 emissions were comparable between treatments and seasons (Table 1; Supplementary Table S4; Figure 1C).

Dissolved CH_4 concentrations

Overall, the FPMs were oxygen saturated with annual mean values of 98.0 ± 1.0% and mean annual temperature of 15.2 ± 0.3°C (Supplementary Figures S5, S6). All FPMs were supersaturated in dissolved CH_4 with respect to atmospheric equilibrium concentration throughout the year, with a mean saturation ratio of 6,311 ± 291%. Dissolved CH_4 was similar among FPMs before the first Bti application (Supplementary Tables S3, S4) and did not vary neither between treatment and control, nor between zones (Figures 2A,B). During the Bti application period (short-term sampling), dissolved CH_4 in surface water tended to increase and the concentration became significantly different from the previous times after the second Bti application (Supplementary Table S4). Seasonally, all FPMs had the highest dissolved CH_4 in summer (2.45 ± 0.20 μmol l^{-1}) and the lowest in autumn (0.85 ± 0.07 μmol l^{-1}) (Supplementary Table S4; Figures 2A,B).

CH_4 oxidative fraction

The average mixing ratio of CH_4 in gas bubbles was 12.7 ± 1.1 % and the δ^{13}C-CH_4 in bubble gas (−61.1 ± 0.6 ‰) was consistently lower than in surface water (−48.8 ± 0.5 ‰) (Supplementary Table S2). Overall, 57–77 % and 45–53 % of the diffusive flux of CH_4 from the sediment was oxidized from the open system and closed system models, respectively (Supplementary Table S2). In some cases, oxidative fractions estimated using the open system, steady-state model were > 1 (in total 10 out of 48 samples). In those samples, δ^{13}C-CH_4 values of surface water were strongly depleted (<-43 ‰). As f_{open}>1 indicates violation of the assumptions of isotope mixing model (Leonte et al., 2017), these data were not considered in the further analyses. Neither treatment nor season had a significant effect on the estimated CH_4 oxidative fractions from both models (Supplementary Table S3; Supplementary Figure S4).

Discussion

The present study is the first, to the best of our knowledge, to assess the biogeochemical implications of the application of the biocide Bti in floodplain pond mesocosms (FPM). We hypothesized that the reduced density of chironomids would lower CH_4 oxidation, leading to higher concentrations of dissolved CH_4 concentrations and emissions in treated FPMs, especially in the aquatic-terrestrial transition zone. In this zone, the CH_4 emissions from the treated FPMs were significantly higher during spring, summer and autumn compared to the untreated controls (Table 2). On average, the emissions from the aquatic-terrestrial transition zone were enhanced by 137 % during these samplings. This finding suggests a long-lasting effect of the application of Bti on chironomid density and therefore FPM CH_4 emissions, potentially related to reduction in chironomids. In a companion study (Gerstle et al., 2022) ~41% less chironomid larvae were found in Bti-treated FPMs compared to control ones (Supplementary Figure S7; Supplementary Table S5) for an overview on collected taxa and

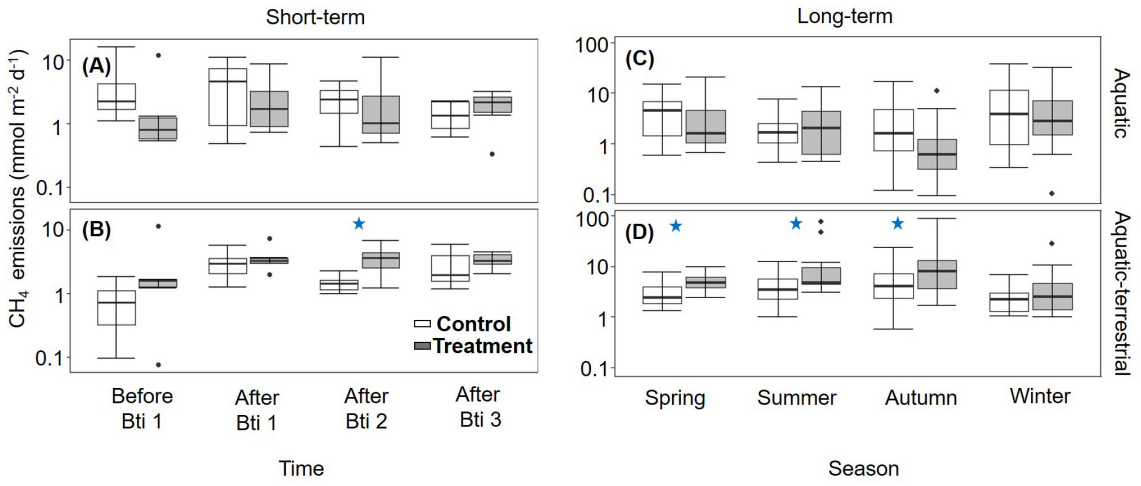

FIGURE 1
Box plots for CH_4 emissions ($n = 6$) measured in control (open boxes) and treated (filled boxes) FPMs. Data are presented for the short-term sampling during the Bti application period in the **(A)** aquatic and **(B)** aquatic-terrestrial compartments, and for the seasonal (long term) sampling in the **(C)** aquatic and **(D)** aquatic-terrestrial compartments. The lower and upper limits of the boxes show the 25th and 75th percentiles, respectively; the horizontal line inside the box is the median, and lower and upper whiskers show the 10th and 90th percentiles, respectively. Filled black circles are data falling outside the 10th and 90th percentiles. Blue stars denote significant difference between treated and control groups. Note that the *y*-axes are log-scaled.

TABLE 1 Significant effect of single factors and their interaction ($p \leq 0.05$) on dissolved CH_4 concentrations, emissions, and oxidative fraction (*F*-stat) after linear mixed effect model analysis.

Variables	Factors	numDF	denDF	F-value	*p*-value
CH_4 emissions -Short term	Zone × Treatment	1	82	5.88	0.02
CH_4 emissions -Seasonal	Zone	1	223	48.6	< 0.0001
	Zone × Treatment	1	223	16.80	0.0001
	Zone × Season	3	223	5.63	0.0001
CH_4 dissolved concentrations – Short term	Time	6	198	11.57	<0.0001
CH_4 dissolved concentrations – Seasonal	Season	3	349	38.30	<0.0001

numDF, numerator degrees of freedom; denDF, denominator degrees of freedom.
Full statistical report (including non-significant factors) available in Supplementary Tables S2, S3.

TABLE 2 Areal emission rates of CH_4 in the aquatic-terrestrial transition zone of untreated (Control) FPMs and those treated with Bti (Treatment), and the relative enhancement of CH_4 emissions from treated units.

FPMs	Control				Treatment			
Time/season	After Bti 2	Spring	Summer	Autumn	After Bti 2	Spring	Summer	Autumn
CH_4 emission (mmol m^{-2} d^{-1})	2.01 ± 0.26	3.10 ± 0.55	4.34 ± 0.59	5.43 ± 1.21	5.13 ± 1.00	5.26 ± 0.67	12.46 ± 4.71	12.97 ± 4.78
Relative enhancement in treated FPMs (%)	-	-	-	-	155	70	187	139

All numbers are presented as mean ± and standard error.

abundance). The chironomids in treated and control FPMs were sampled two weeks after our last CH_4 measurement, after the third and last application of Bti, in two different habitats: macrophytes and gravel, which respectively correspond to the aquatic-terrestrial and aquatic zone in our study. Chironomid larvae were by far the most abundant taxa and showed 72% higher abundance of all benthic macroinvertebrates' community (Gerstle et al., 2022).

Although our measurements cannot provide a causal relationship between observed changes in CH_4 emissions, in combination with the measured reduction in chironomid density, they support a previously hypothesized link between

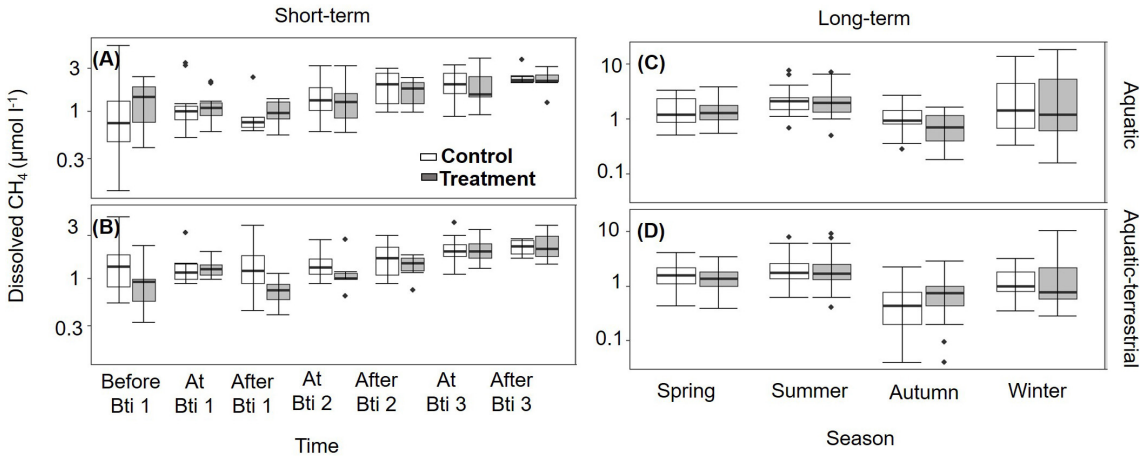

FIGURE 2
Box plots for dissolved CH_4 concentration ($n = 6$) measured in control (open boxes) and treated (filled boxes) FPMs. Data are presented for the short-term sampling during the Bti application period in the **(A)** aquatic and **(B)** aquatic-terrestrial compartments, and for the seasonal (long term) sampling in the **(C)** aquatic and **(D)** aquatic-terrestrial compartments. The lower and upper limits of the boxes show the 25th and 75th percentiles, respectively; the horizontal line inside the box is the median, and lower and upper whiskers show the 10th and 90th percentiles, respectively. Filled black circles are data falling outside the 10th and 90th percentiles. Note that *y*-axes are log-scaled.

chironomid abundance and CH_4 emissions (Hölker et al., 2015). Higher CH_4 emissions in Bti-treated FPMs were not detected immediately after Bti application, but in the long term. These findings might be explained by a different sensitivity to Bti depending on the chironomid developmental larval stage (Kästel et al., 2017). A stronger effect of Bti has been found in early instar chironomid larvae compared to mature larvae. As only mature larvae create burrows and thus bioturbate (Baranov et al., 2016), the reduction of mostly early instar larvae might explain why the effect on CH_4 dynamics was only detected when those larvae generations, after some time, developed the ability to burrow. Furthermore, we found that increased CH_4 emissions were only observed in the aquatic-terrestrial transition zone that is, in the area of the FPMs with finer sediment deposits (~0.05 cm grain size) and abundant aquatic vegetation (mostly macrophytes). This area is the preferred habitat for tube dwelling chironomids (De Haas et al., 2006; Gerstle et al., 2022), while densities of chironomids in the gravel bed sediment (~1-3 cm grain size) of the aquatic zone were much lower than in the aquatic-terrestrial transition zone (Supplementary Figure S7). The higher abundance of chironomids and their burrowing activity in the aquatic-terrestrial transition zone compared to the aquatic zone can explain why the effect was detected only in the aquatic-terrestrial transition zone. Finally, we observed significantly higher emissions during spring, summer and autumn, but not in winter, when the lower temperature (4 ± 0.4 °C) can have caused a decrease in chironomid metabolism (Jackson and Mclachlan, 1991; Frouz et al., 2003; Roskosch et al., 2012). All these results point toward an important role of chironomids in CH_4 dynamics and implications of Bti applications that are modulated by the sediment properties and the temporal dynamics of the chironomid population.

The exact mechanisms and processes by which the reduction in chironomid abundance may have caused the increase in emissions cannot be identified by our results, and remain an open question. We suggest a combination of trophic and non-trophic interactions of chironomids affecting CH_4 dynamics in FPMs, which is additionally influenced by FPM hydrodynamics: On the one hand, the increase of CH_4 emissions in the aquatic-terrestrial transition zone of treated FPMs was potentially caused by a reduction in grazing pressure on methane-oxidizing bacteria by chironomids, as observed by Kajan and Frenzel (1999) in laboratory experiments. On the other hand, the activity of the chironomids oxygenates the sediment, which reduces methanogenesis and promotes oxidation (Hölker et al., 2015; Murniati et al., 2017; Oliveira Junior et al., 2019; Booth et al., 2021), thus reducing CH_4 emissions as a consequence of non-trophic effects. However, this oxygenation pathway was not reflected in the oxidative fraction, which varied mainly as a function of the season, regardless of treatment. The dissolved CH_4 and oxygen concentrations were similar in both zones of the FPMs, indicating horizontal mixing of the surface water. Exchange flows and hydrodynamic conditions in small, shallow, and partially vegetated aquatic systems are expected to be governed by convective flows, which are generated by differential heating and cooling due to spatially varying water depths and light absorption properties of the water column and sediment surface (Nepf, 2012). Horizontal mixing of surface water in the FPMs may also have diluted differences in the isotopic signature of dissolved CH_4 and masked the

identification of potential changes in CH_4 oxidation rates in the aquatic-terrestrial transition zone of the treated FPMs. With similar dissolved CH_4 concentrations and comparable hydrodynamic conditions, CH_4 emissions across the air-water interface can be expected to be of similar magnitude in both zones, suggesting that the higher emissions in the aquatic-terrestrial transition zone of the treated FPMs were supported by higher ebullition rates and/or plant-mediated emissions. As these emissions pathways mostly bypath CH_4 oxidation (Bastviken et al., 2004; Walter et al., 2007), their modification by chironomid activity would not necessarily be associated with changes in the isotopic composition of dissolved CH_4 nor in its concentration in surface water.

However, alternative mechanisms for the increase in CH_4 emissions from Bti treated FPMs that are not related to chironomid declines cannot be ruled out. Bti has been demonstrated to have long-lasting effects on the composition of microbial communities in the water column of microcosms that were treated with a high dose of Bti (about 10 times higher than the recommended field rate used in our experiments) (Duguma et al., 2015). Moreover, Bti is applied as a formulated suspension of toxin crystals, along with ingredients of unknown composition (Brühl et al., 2020). Parts of these ingredients, or their transformation products, may become available as a carbon source for methanogenesis. However, the applied areal rate of Bti application adds a relatively small amount of carbon. Assuming a carbon mass fraction in the Bti of about 50 % (as for sucrose), the total amount of applied Bti (3x 118 mg m^{-2}) would correspond to a total addition of 14.75 mmol C m^{-2}. This amount, if completely converted to CH_4, could fuel the average emission rate during spring (3.1 mmol m^{-2} d^{-1}, Table 2) for only 4 days, thus may not explain the enhanced emissions during summer and autumn.

The measurements analyzed in the present study provide only snapshots of the highly dynamic CH_4 emissions. Unresolved variations include diurnal changes in air-water gas exchange due to nocturnal mixing (Holgerson and Raymond, 2016; Poindexter et al., 2016), physiological activity of plants (Bansal et al., 2020), and episodically enhanced ebullition rates in response to atmospheric pressure changes (Walter et al., 2007; Maeck et al., 2014). Although the measured CH_4 emissions are in the range of fluxes reported for ponds in the temperate zone (Bergen et al., 2019; Peacock et al., 2021), the observed fluxes may not provide robust estimates of the overall CH_4 emissions from the FPMs due to the above-mentioned sampling limitations. Yet our findings indicate a potential effect of Bti application through chironomid reduction over extended periods and suggest seasonally enhanced ecosystem-scale CH_4 emissions by 137 %. In view of the widespread global use of Bti for mosquito control (Boisvert, 2005; Kästel et al., 2017), and the important role of the targeted aquatic ecosystems, such as lakes, ponds, FPMs, and freshwater wetlands, as the largest natural source of atmospheric CH_4 (Rosentreter et al., 2021), the effects at ecosystem scale need urgent evaluation in future studies. Additionally more detailed experiments that analyze the role of chironomids and other benthic invertebrates, and that of Bti in CH_4 dynamics at the sediment-water interface under controlled environmental or laboratory conditions are required.

Data availability statement

The data used to produce the results of this paper will be provided upon request.

Author contributions

CG: conceptualization, methodology, data collection, data curation, data analysis, and writing. AM: data analysis and writing. CM-L and AL: conceptualization, methodology, data analysis, and writing. All authors contributed to the article and approved the submitted version.

Funding

This work was funded by the Deutsche Forschungsgemeinschaft (DFG, German Research Foundation) −326210499/GRK2360, Systemlink.

Acknowledgments

We acknowledge the support of Rossano Bolpagni, Verena Gerstle, Sara Koblenschlag, Housam Ismaeli, Christoph Bors, Eliana Bohorquez Bedoya, and Sandhya Magesh during the planning and implementation of the experiment. Carsten A. Brühl provided valuable comments on earlier drafts of the manuscript. We thank the two anonymous reviewers for their comments that improved the manuscript.

Conflict of interest

The authors declare that the research was conducted in the absence of any commercial or financial relationships that could be construed as a potential conflict of interest.

Publisher's note

All claims expressed in this article are solely those of the authors and do not necessarily represent those

of their affiliated organizations, or those of the publisher, the editors and the reviewers. Any product that may be evaluated in this article, or claim that may be made by its manufacturer, is not guaranteed or endorsed by the publisher.

Supplementary material

The Supplementary Material for this article can be found online at: https://www.frontiersin.org/articles/10.3389/frwa.2022.996898/full#supplementary-material

References

Allgeier, S., Friedrich, A., and Brühl, C. A. (2019a). Mosquito control based on Bacillus thuringiensis israelensis (Bti) interrupts artificial wetland food chains. *Sci. Total Environ.* 686, 1173–1184. doi: 10.1016/j.scitotenv.2019.05.358

Allgeier, S., Kästel, A., and Brühl, C. A. (2019b). Adverse effects of mosquito control using Bacillus thuringiensis var. israelensis: reduced chironomid abundances in mesocosm, semi-field and field studies. *Ecotoxicol. Environ. Safety* 169, 786–796. doi: 10.1016/j.ecoenv.2018.11.050

Bansal, S., Johnson, O. F., Meier, J., and Zhu, X. (2020). Vegetation affects timing and location of wetland methane emissions. *J. Geophy. Res. Biogeosci.* 125, 1–14. doi: 10.1029/2020JG005777

Baranov, V., Lewandowski, J., and Krause, S. (2016). Bioturbation enhances the aerobic respiration of lake sediments in warming lakes. *Biol. Lett.* 12, 8–11. doi: 10.1098/rsbl.2016.0448

Bastviken, D., Cole, J., Pace, M., and Tranvik, L. (2004). Methane emissions from lakes: Dependence of lake characteristics, two regional assessments, and a global estimate. *Global Biogeochem. Cycles* 18, 1–12. doi: 10.1029/2004GB002238

Bastviken, D., Ejlertsson, J., and Tranvik, L. (2002). Measurement of methane oxidation in lakes: A comparison of methods. *Environ. Sci. Technol.* 36, 3354–3361. doi: 10.1021/es010311p

Becker, N. (1997). Microbial control of mosquitoes: management of the upper rhine mosquito population as a model programme. *Parasitol. Today* 13, 485–487. doi: 10.1016/S0169-4758(97)01154-X

Becker, N. (2006). Biological control mosquitoes: Management of the upper rhine mosquito population as a model programme. Eilenberg, J., and Hokkanen, H. M. T., editors. *An Ecological and Societal Approach to Biological Control.* New York, NY: Springer. p. 227–245.

Becker, N., Ludwig, M., and Su, T. (2018). Lack of resistance in aedes vexans field populations after 36 the upper Rhine Valley, Germany. *J. Am. Mosq. Control Assoc.* 34, 154–157. doi: 10.2987/17-6694.1

Benjamini, Y., and Hochberg, Y. (1995). Controlling the false discovery rate: a practical and powerful approach to multiple testing. *J. R. Stat. Soc. Series B* 57, 289–300. doi: 10.1111/j.2517-6161.1995.tb02031.x

Bergen, T. J. H. M., Barros, N., Mendonça, R., Aben, R. C. H., Althuizen, I. H. J., and Huszar, V., et al. (2019). Seasonal and diel variation in greenhouse gas emissions from an urban pond and its major drivers. *Limnol. Oceanogr.* 64, 2129–2139. doi: 10.1002/lno.11173

Bodmer, P., Wilkinson, J., and Lorke, A. (2020). Sediment properties drive spatial variability of potential methane production and oxidation in small streams. *J. Geophy. Res. Biogeosci.* 125, 1–15. doi: 10.1029/2019JG005213

Boisvert, M., and Boisvert, J. (2000). Effects of *Bacillus thuringiensis var.* israelensis on target and nontarget organisms: a review of laboratory and field experiments. *Biocont. Sci. Technol.* 10, 517–561. doi: 10.1080/095831500750016361

Boisvert, M. (2005). Utilization of *Bacillus thuringiensis var. israelensis* (Bti) - based formulations for the biological control of mosquitoes in Canada. *Victoria* 87–93.

Booth, M. T., Urbanic, M., Wang, X., and Beaulieu, J. J. (2021). Bioturbation frequency alters methane emissions from reservoir sediments. *Sci. Total Environ.* 789, 1–9. doi: 10.1016/j.scitotenv.2021.148033

Borrel, G., Jezequel, D., Biderre-Petit, C., Morel-Desrosiers, N., Morel, J-. P., and Pierre Peyret, G. F. (2011). Production and consumption of methane in freshwater lake ecosystems. *Res. Microbiol.* 162, 832–847. doi: 10.1016/j.resmic.2011.06.004

Brühl, C. A., Després, L., Frör, O., Patil, C. D., Poulin, B., and Tetreau, G., et al. (2020). Environmental and socioeconomic effects of mosquito control in Europe using the biocide Bacillus thuringiensis subsp. *israelensis (Bti). Sci. Total Environ.* 724, 1–16. doi: 10.1016/j.scitotenv.2020.137800

Colina, M., Meerhoff, M., Pérez, G., Veraart, A. J., Bodelier, P., and Horst, A., et al. (2021). Trophic and non- - trophic effects of fish and macroinvertebrates on carbon emissions. *Freshw. Biol.* 66, 1–15. doi: 10.1111/fwb.13795

De Haas, E. M., Wagner, C., Koelmans, A. A., Kraak, M. H. S., and Admiraal, W. (2006). Habitat selection by chironomid larvae: Fast growth requires fast food. *J. Anim. Ecol.* 75, 148–155. doi: 10.1111/j.1365-2656.2005.01030.x

Delsontro, T., Boutet, L., St-pierre, A., Giorgio, P. A., and Prairie, Y. T. (2016). Methane ebullition and diffusion from northern ponds and lakes regulated by the interaction between temperature and system productivity. *Limnol. Oceanogr.* 61, S62–S77. doi: 10.1002/lno.10335

Duguma, D., Hall, M. W., Rugman-Jones, P., Stouthamer, R., Neufeld, J. D., and Walton, W. E. (2015). Microbial communities and nutrient dynamics in experimental microcosms are altered after the application of a high dose of Bti. *J. Appl. Ecol.* 52, 763–773. doi: 10.1111/1365-2664.12422

Etminan, M., Myhre, G., Highwood, E. J., and Shine, K. P. (2016). Radiative forcing of carbon dioxide, methane, and nitrous oxide: a significant revision of the methane radiative forcing. *Geophys. Res. Let.* 12, 614–612, 623. doi: 10.1002/2016GL071930

Frouz, J., Matěna, J., and Ali, A. (2003). Survival strategies of chironomids (Diptera : Chironomidae) living in temporary habitats : a review. *Eur. J. Entomol.* 100, 459–465. doi: 10.14411/eje.2003.069

Gerstle, V., Manfrin, A., Kolbenschlag, S., Gerken, M., Mufachcher Ul Islam, A. S. M., Entling, M. H., et al. (2022). *Benthic macroinvertebrate community shifts induced by Bti also reduce Odonata emergence.* Environmental Pollution, Elsevier.

Gorsky, A. L., Racanelli, G. A., Belvin, A. C., and Chambers, R. M. (2019). Greenhouse gas flux from stormwater ponds in southeastern Virginia (USA). *Anthropocene* 28, 100218. doi: 10.1016/j.ancene.2019.100218

Hodkinson, I. D., and Williams, K. A. (1980). Tube formation and distribution of *Chironomus Plumosus L.* (Diptera : Chironomidae) in a eutrophic woodland pond. *Chironomidae.* 331–37. doi: 10.1016/B978-0-08-025889-8.50051-9

Holgerson, M. A., and Raymond, P. A. (2016). Large contribution to inland water CO2 and CH4 emissions from very small ponds. *Nat. Geosci.* 9, 222–226. doi: 10.1038/ngeo2654

Hölker, F., Vanni, M. J., Kuiper, J. J., Meile, C., Grossart, H. P., and Stief, P., et al. (2015). Tube-dwelling invertebrates: tiny ecosystem engineers have large effects in lake ecosystems. *Ecol. Monogr.* 85, 333–351. doi: 10.1890/14-1160.1

International Hydropower Association. (2010). *GHG Measurement Guidelines for Freshwater Reservoirs*. London: International Hydropower Association.

Jackson, J. M., and Mclachlan, A. J. (1991). Rain-pools on peat moorland as island habitats for midge larvae. *Hydrobiologia* 209, 59–65. doi: 10.1007/BF00006718

Jakob, C., and Poulin, B. (2016). Indirect effects of mosquito control using Bti on dragonflies and damselflies (Odonata) in the Camargue. *Insect Conserv. Divers.* 9, 161–169. doi: 10.1111/icad.12155

Jeffrey, L. C., Maher, D. T., Johnston, S. G., Kelaher, B. P., Steven, A., and Tait, D. R. (2019). Wetland methane emissions dominated by plant-mediated fluxes: Contrasting emissions pathways and seasons within a shallow freshwater subtropical wetland. *Limnol. Oceanogr.* 64, 1895–1912. doi: 10.1002/lno.11158

Jones, R. I., and Grey, J. (2011). Biogenic methane in freshwater food webs. *Freshw. Biol.* 56, 213–229. doi: 10.1111/j.1365-2427.2010.02494.x

Kajan, R., and Frenzel, P. (1999). The effect of chironomid larvae on production, oxidation and fluxes of methane in a flooded rice soil. *FEMS Microbiol. Ecol.* 28, 121–129. doi: 10.1111/j.1574-6941.1999.tb00567.x

Kästel, A., Allgeier, S., and Brühl, C. A. (2017). Decreasing Bacillus thuringiensis israelensis sensitivity of Chironomus riparius larvae with age

indicates potential environmental risk for mosquito control. *Sci. Rep.* 7, 1–7. doi: 10.1038/s41598-017-14019-2

Kelly, C. A., and Chynoweth, D. P. (2014). The Contributions of Temperature and of the Input of Organic Matter in Controlling Rates of Sediment Methanogenesis. *Am. Soc. Limnol. Oceanography*, 26, 891–897. doi: 10.4319/lo.1981.26.5.0891

Knoblauch, C., Spott, O., Evgrafova, S., Kutzbach, L., and Pfeiffer, E. M. (2015). Regulation of methane production, oxidation, and emission by vascular plants and bryophytes in ponds of the northeast Siberian polygonal tundra. *J. Geophy. Res. Biogeosci.* 120, 2525–2541. doi: 10.1002/2015JG003053

Leeper, D. A., and Taylor, B. E. (1998). Insect emergence from a South Carolina (USA) temporary wetland pond, with emphasis on the Chironomidae (Diptera). *Chicago J.* 17, 54–72. doi: 10.2307/1468051

Leonte, M., Kessler, J. D., Kellermann, M. Y., Arrington, E. C., Valentine, D. L., and Sylva, S. P. (2017). Rapid rates of aerobic methane oxidation at the feather edge of gas hydrate stability in the waters of Hudson Canyon, US Atlantic Margin. *Geochim. Cosmochim. Acta* 204, 375–387. doi: 10.1016/j.gca.2017.01.009

Maeck, A., Hofmann, H., and Lorke, A. (2014). Pumping methane out of aquatic sediments andndash; Ebullition forcing mechanisms in an impounded river. *Biogeosciences* 11, 2925–2938. doi: 10.5194/bg-11-2925-2014

Mclachlan, A. J., and Cantrell, M. A. (1976). Sediment development and its influence on the distribution and tube structure of *Chironomus plumosus* L. (Chironomidae, Diptera) in a new impoundment. *Freshwater Biology* 6, 437–443. doi: 10.1111/j.1365-2427.1976.tb01632.x

Murniati, E., Gross, D., Herlina, H., Hancke, K., and Lorke, A. (2017). Effects of bioirrigation on the spatial and temporal dynamics of oxygen above the sediment-water interface. *Freshwater Sci.* 36, 784–795. doi: 10.1086/694854

Nepf, H. M. (2012). Flow and transport in regions with aquatic vegetation. *Annu. Rev. Fluid Mech. Fluid Mech.* 44, 123–142. doi: 10.1146/annurev-fluid-120710-101048

Nogaro, G., and Steinman, A. D. (2014). Influence of ecosystem engineers on ecosystem processes is mediated by lake sediment properties. *Oikos* 123, 500–512. doi: 10.1111/j.1600-0706.2013.00978.x

Oliveira Junior, E. S., Temmink, R. J. M., Buhler, B. F., Souza, R. M., Resende, N., and Spanings, T., et al. (2019). Benthivorous fish bioturbation reduces methane emissions, but increases total greenhouse gas emissions. *Freshw. Biol.* 64, 197–207. doi: 10.1111/fwb.13209

Peacock, M., Audet, J., Bastviken, D., Cook, S., Evans, C. D., and Grinham, A., et al. (2021). Small artificial waterbodies are widespread and persistent emitters of methane and carbon dioxide. *Glob. Chang. Biol.* 27, 5109–5123. doi: 10.1111/gcb.15762

Peters, V., and Conrad, R. (1996). Sequential reduction processes and initiation of CH4 production upon flooding of oxic upland soils. *Soil Biol. Biochem.* 28, 371–382. doi: 10.1016/0038-0717(95)00146-8

Pinheiro, J., Bates, D., DebRoy, S., Sarkar, D., Heisterkamp, S., van Willigen, B., et al. (2017). *Package 'nlme.' Linear and Nonlinear Mixed Effects Models, Version*, 3.

Poindexter, C. M., Baldocchi, D. D., Matthes, J. H., Knox, S. H., and Variano, E. A. (2016). The contribution of an overlooked transport process to a wetland's methane emissions. *Geophys. Res. Lett.* 48, 6276–6284. doi: 10.1002/2016GL068782

R Core Team. (2013). *R: A Language and Environment for Statistical Computing.*

Rosentreter, J. A., Borges, A. V., Deemer, B. R., Holgerson, M. A., Liu, S., and Song, C., et al. (2021). Half of global methane emissions come from highly variable aquatic ecosystem sources. *Nat. Geosci.* 14, 225–230. doi: 10.1038/s41561-021-00715-2

Roskosch, A., Hette, N., and Hupfer, M. (2012). Alteration of Chironomus plumosus ventilation activity and bioirrigation-mediated benthic fluxes by changes in temperature, oxygen concentration, and seasonal variations. *Freshw. Sci.* 31, 269–281. doi: 10.1899/11-043.1

Saunois, M., Stavert, A. R., Poulter, B., Bousquet, P., Canadell, J. G., and Jackson, R. B., et al. (2020). The global methane budget 2000 – 2017. *Earth Syst. Sci. Data* 12, 1561–1623. doi: 10.5194/essd-12-1561-2020

Sawakuchi, H. O., Bastviken, D., Sawakuchi, A. O., Ward, N. D., Borges, C. D., and Tsai, S. M., et al. (2016). Oxidative mitigation of aquatic methane emissions in large Amazonian rivers. *Glob. Chang. Biol.* 22, 1075–1085. doi: 10.1111/gcb.13169

Segers, R. (1998). *Methane Production and Methane Consumption: A Review of Processes Underlying Wetland Methane Fluxes*. Berlin: Springer. p. 41, 23–51.

Stadmark, J., and Leonardson, L. (2005). Emissions of greenhouse gases from ponds constructed for nitrogen removal. *Ecol. Eng.* 25, 542–551. doi: 10.1016/j.ecoleng.2005.07.004

Stehle, S., Manfrin, A., Feckler, A., Graf, T., Joschko, T. J., and Jupke, J., et al. (2022). Structural and functional development of twelve newly established floodplain pond mesocosms. *Ecol. Evol.* 12, 1–15. doi: 10.1002/ece3.8674

Thottathil, S. D., Reis, P. C. J., del Giorgio, P. A., and Prairie, Y. T. (2018). The extent and regulation of summer methane oxidation in Northern Lakes. *J. Geophy. Res. Biogeosci.* 123, 3216–3230. doi: 10.1029/2018JG004464

Walter, K. M., Smith, L. C., and Chapin, F. S. (2007). Methane bubbling from northern lakes: Present and future contributions to the global methane budget. *Philos. Trans. R. Soc. A Math. Phy. Eng. Sci.* 365, 1657–1676. doi: 10.1098/rsta.2007.2036

Yavitt, J. B., Angel, L. L., Fahey, T. J., Cirmo, C. P., and Driscoll, C. T. (1992). Methane fluxes, concentrations, and production Adirondack beaver impoundments. *Limnol. Oceanogr.* 37, 1057–1066. doi: 10.4319/lo.1992.37.5.1057

Zuur, A. F., Ieno, E. N., and Elphick, C. S. (2010). A protocol for data exploration to avoid common statistical problems. *Methods Ecol. Evol.* 1, 3–14. doi: 10.1111/j.2041-210X.2009.00001.x

Supplemental information for:

Biocide Bti treatment increases CH_4 emissions in floodplain pond mesocosms

Caroline Ganglo[a*], Alessandro Manfrin[a], Clara Mendoza-Lera[a], Andreas Lorke[a]

[a]*Institute for Environmental Sciences, University of Koblenz-Landau, 76829, Landau, Germany*

[*]Email: carolineganglo20@gmail.com

Frontiers in water

15 pages, 3 Tables, 1551 words, 7 Figures

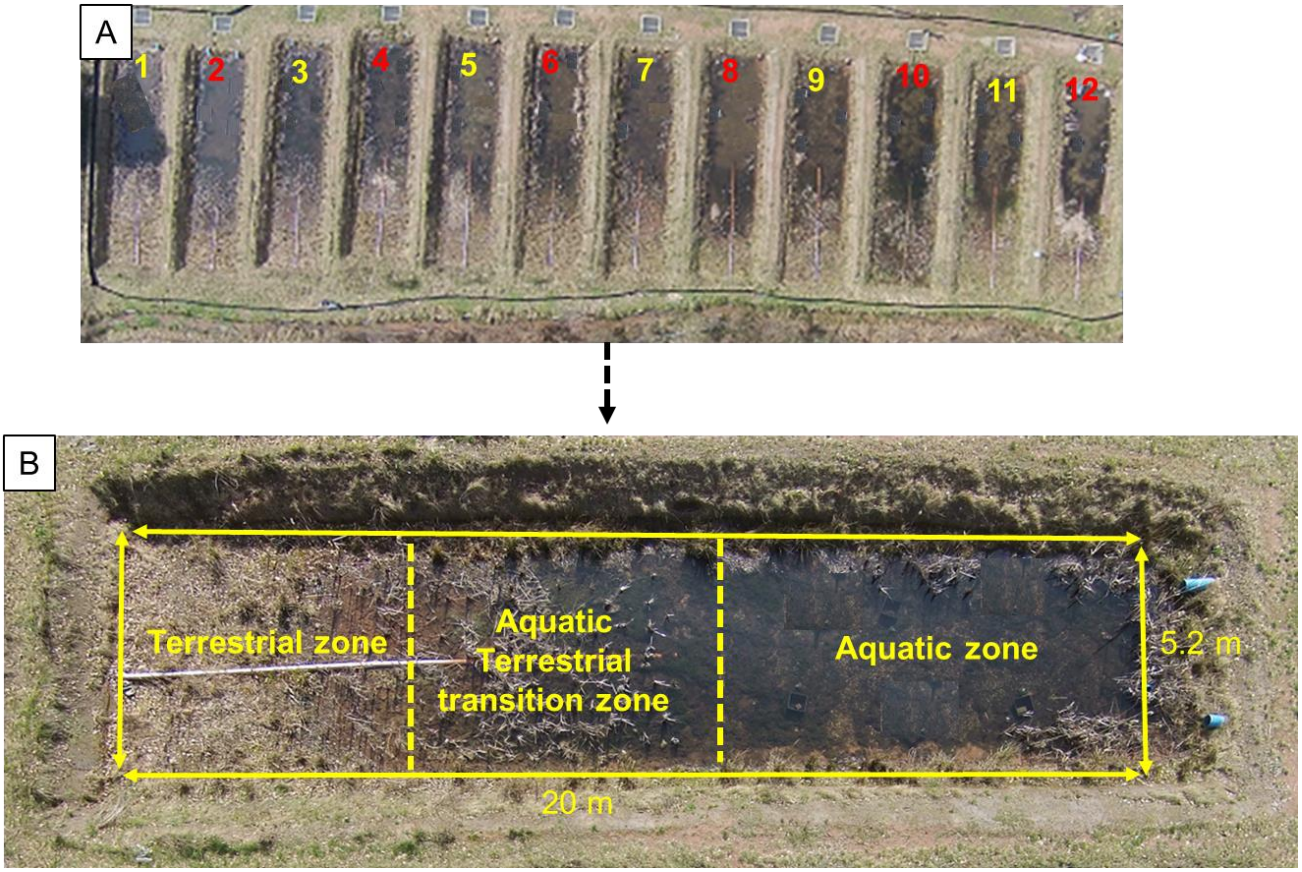

SI Figure S1 (A) Areal image of the 12 experimental Floodplain Pond Mesocosms (FPM) at the Eusserthal Ecosystem Research Station, with Bti treated FPMs labeled with yellow numbers and control FPMs labeled in red. **B**. Detailed view of a single pond with the aquatic zone and the aquatic-terrestrial transition zone delimitated by yellow dashed lines. The area marked as the terrestrial zone was temporarily flooded during the three Bti applications (see **SI Figure S2**).

SI Table S1: Dates of flooding, Bti application during the year of the experiment.

Date	Flooding/ Bti	Water level (m)
11 April 2020	Flooding	0.3 → 0.4
12 April 2020	Flooding	0.4 → 0.5
14 April 2020	**1st Bti application**	
21 April 2020	Drawdown	0.5 → 0.4
22 April 2020	Drawdown	0.4 → 0.3
02 May 2020	Flooding,	0.3 → 0.4
03 May 2020	Flooding,	0.4 → 0.5
04 May 2020	**2nd Bti application**	
12 May 2020	Drawdown	0.5 → 0.4
13 May 2020	Drawdown	0.4 → 0.3
23 May 2020	Flooding,	0.3 → 0.4
24 May 2020	Flooding,	0.4 → 0.5
25 May 2020	**3rd Bti application**	
02 June 2020	Drawdown	0.5 → 0.4
03 June 2020	Drawdown	0.4 → 0.3

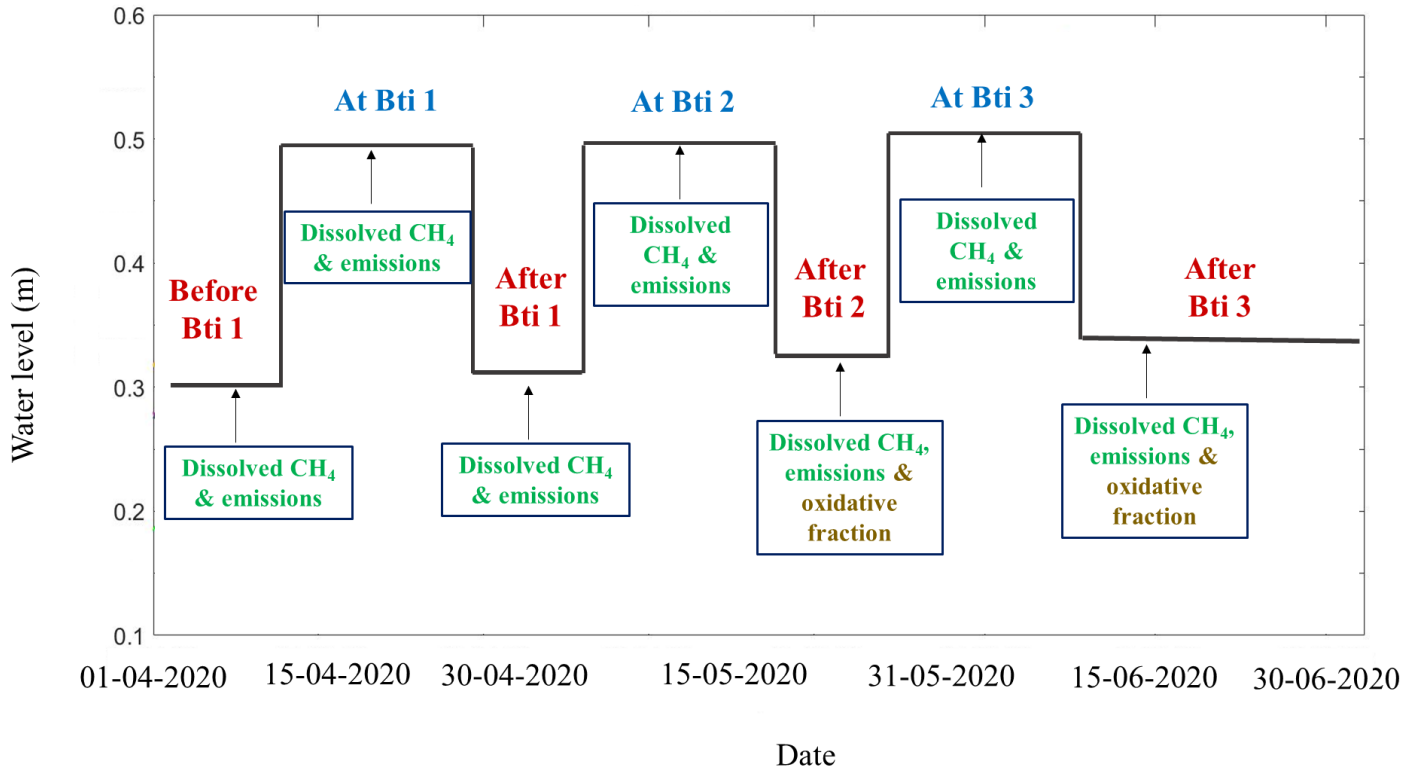

SI Figure S2 Time series of water level in the 12 FPMs during the Bti application (short-term sampling). Three sequential floods were generated and Bti was applied to six selected FPMs during each flood. Experimental phases are denoted as Before Bti 1, At and After each Bti. Sampling times for dissolved CH_4, concentrations, emissions, and oxidative fraction are indicated by labeled arrows.

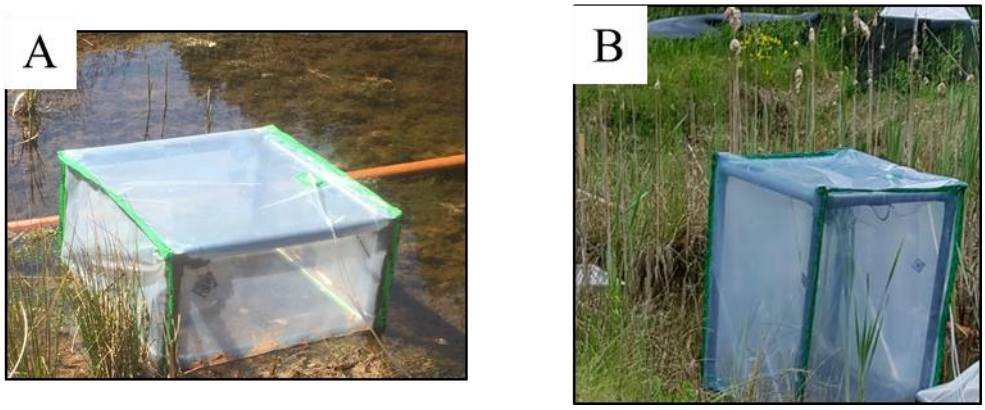

SI Figure S3 Images of the transparent chambers used for CH_4 emissions measurements in the aquatic zone (**A**) and in the aquatic-terrestrial transition zone (**B**) of the FPMs.

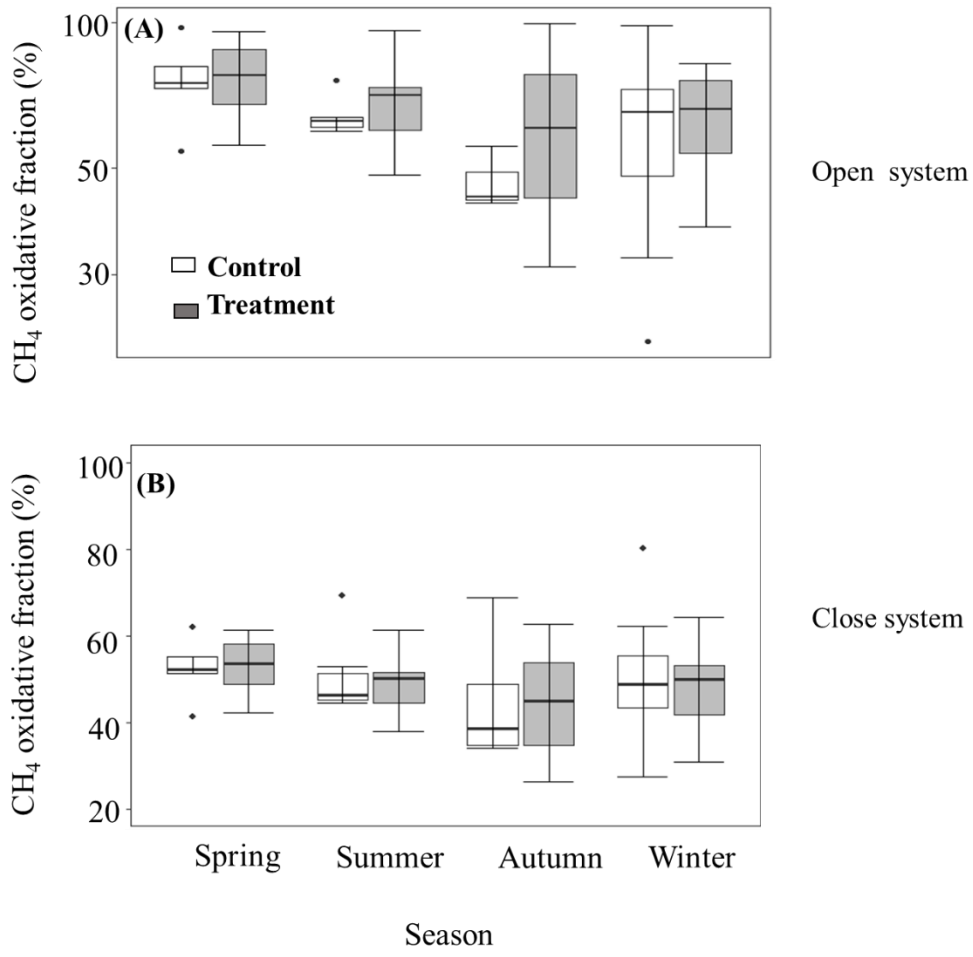

SI Figure. **S4** Box plot of percentage CH_4 oxidative fraction of (**A**) open system model and (**B**) close system model from FPMs treated with Bti (filled boxes) and in the control FPMs (open boxes). Lower and upper box boundaries show the 25th and 75th percentiles, respectively, the horizontal line inside the box shows the median, and the whiskers show 10th and 90th percentiles, respectively. Filled black circles show data falling outside 10th and 90th percentiles (*n*= 6).

SI Table S2: Mean ± and standard error of Isotopic signatures ($\delta^{13}C$ in CH_4) from gas bubbles released from the sediment and in dissolved gas in the surface water, and the oxidized fraction of diffusive CH_4 fluxes in the twelve FPMs. *n* = 12

	FPMs			
Season	Spring	Summer	Autumn	Winter
$\delta^{13}C$ in dissolved CH_4 (‰)	-51.99 ± 0.67	-49.87 ± 0.92	-47.33 ± 0.89	-47.30 ± 0.76
$\delta^{13}C$ in bubble gas (‰)	-66.27 ± 0.51	-62.38 ± 0.71	-57.94 ± 0.86	-59.11 ± 0.77
Mixing ratio of CH_4 in bubble gas (in %)	19.76 ± 1.64	4.92 ± 0.33	19.22 ± 1.83	9.74 ± 1.68
CH_4 oxidative fraction (open system model)	0.77 ± 0.04	0.67 ± 0.04	0.57 ± 0.08	0.63 ± 0.04
CH_4 oxidative fraction (close system model)	0.53 ± 0.02	0.50 ± 0.03	0.45 ± 0.05	0.48 ± 0.03

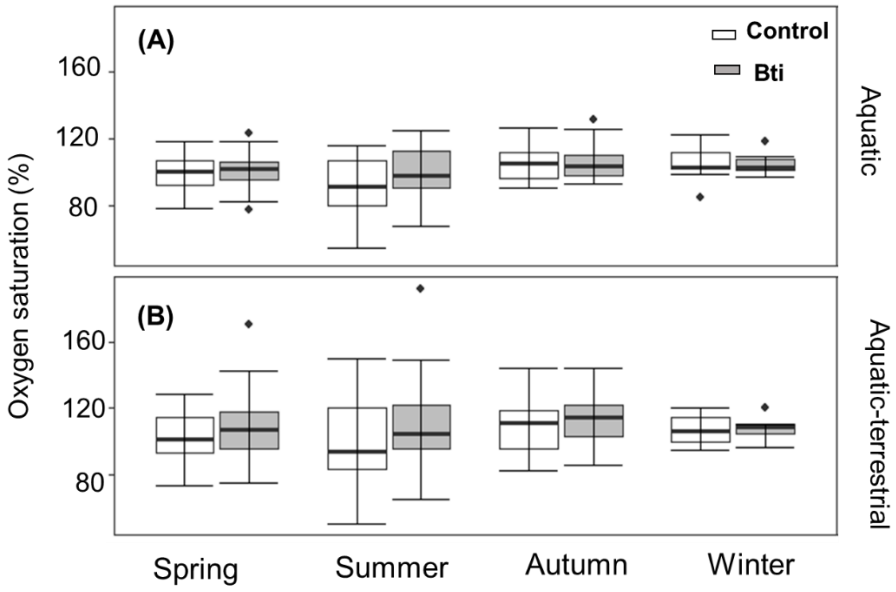

SI Figure. **S5** Box plot of oxygen saturation measured in aquatic (**A**) and aquatic-terrestrial (**B**) during seasonal sampling in treated (filled boxes) and in the control FPMs (open boxes). Lower and upper box boundaries show the 25th and 75th percentiles, respectively, the horizontal line inside the box shows the median, and the whiskers show 10th and 90th percentiles, respectively. Filled black circles show data falling outside 10th and 90th percentiles (*n*= 6).

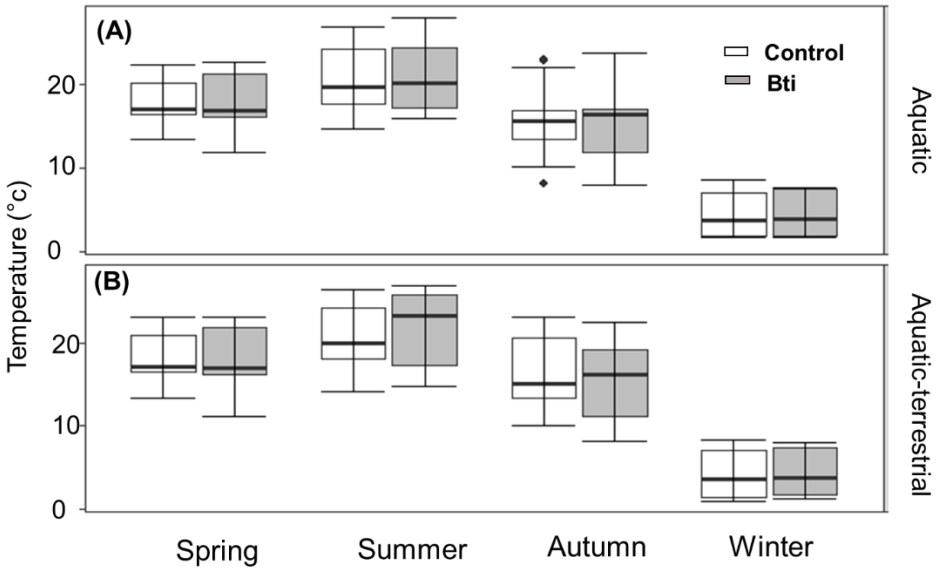

SI Figure. **S6** Box plot of temperature measured in aquatic (**A**) and aquatic-terrestrial (**B**) during seasonal sampling in treated (filled boxes) and in the control FPMs (open boxes). Lower and upper box boundaries show the 25th and 75th percentiles, respectively, the horizontal line inside the box shows the median, and the whiskers show 10th and 90th percentiles, respectively. Filled black circles show data falling outside 10th and 90th percentiles (*n*= 6).

SI Table S3: Linear mixed effect models selection using likelihood ratio tests (LRT) against reduced models report: interactions among individual factors (×), effect of individual factor and

significant factor of the final model on CH_4 concentration, emissions, and oxidative fraction. Numbers marked in bold highlight significant effects.

Variables	Model	R^2 marginal	Factors	Statistical test	p-value
CH_4 concentration - Short term	Full model	0.26		LRT	
			Zone × Timepoint × Treatment	8.54	0.20
			Zone × Treatment	0.64	0.42
			Timepoint × Treatment	1.85	0.93
			Zone × Timepoint	4.47	0.61
			Treatment	0.24	0.62
			Zone	0.02	0.88
	Final model	0.24		F-stat	
			Timepoint	**$F_{6,198}$= 11.57**	**<0.0001**
CH_4 concentration - seasonal	Full model	0.2		LRT	
			Zone × Season × Treatment	3.27	0.35
			Zone × Treatment	0.06	0.81
			Season × Treatment	1.16	0.76
			Zone × Season	5.87	0.12
			Treatment	0.05	0.83
			Zone	2.16	0.14
	Final model	0.18		F-stat	
			Season	**$F_{3,349}$ = 38.30**	**<0.0001**
CH_4 emissions -Short term	Full model	0.20		LRT	
			Zone × Timepoint × Treatment	2.9	0.41
			Timepoint × Treatment	1.52	0.68
			Zone × Timepoint	7.48	0.06
			Timepoint	6.40	0.09

Variables	Model	R^2 marginal	Factors	Statistical test	p-value
	Final model	0.07		F-stat	
			Zone	$F_{1, 82} = 0.34$	0.56
			Treatment	$F_{1, 10} = 0.52$	0.47
			Zone × Treatment	**$F_{1, 82} = 5.88$**	**0.02**
CH_4 emissions -seasonal	Full model	0.23		LRT	
			Zone × Season × Treatment	2.46	0.48
			Season × Treatment	2.40	0.49
	Final model	0.21		F-stat	
			Zone	**$F_{1, 223} = 48.6$**	**< 0.0001**
			Season	$F_{3, 223} = 0.38$	0.77
			Treatment	$F_{1, 10} = 3.53$	0.09
			Zone × Treatment	**$F_{1, 223} = 16.80$**	**0.0001**
			Zone × Season	**$F_{3, 223} = 5.63$**	**0.0001**
CH_4 oxidative fraction	Full model	0.14		LRT	
			Season × Treatment	0.97	0.81
			Treatment	1.07	0.3
	Final model	0.12		F-stat	
			Season	$F_{3, 36} = 2.30$	0.094

SI Table S4: Post-hoc pairwise comparisons of factors or interaction on CH_4 concentration and emissions using linear model (lm)/ linear mixed effect model (lme)/. Estimate represents the mean difference between pairwise factors and t-ratio is the ratio of Estimate to standard error. Statistically significant values are marked in bold.

Variables	Contrast					
CH_4 concentration - Short term	Pairwise structure	Contrasts analysis (lm)	Estimate	t value	p	p-adj
	Timepoint	At Bti1-Before Bti 1	0.01	0.11	0.916	0.916
		After1-Before Bti 1	-0.08	-0.53	0.601	0.742
		At Bti2-Before Bti 1	0.04	0.31	0.754	0.792
		After2-Before Bti 1	0.13	0.92	0.368	0.512
		At Bti3-Before Bti 1	**0.32**	**3.09**	**0.004**	**0.015**
		After3-Before Bti 1	**0.39**	**2.82**	**0.009**	**0.03**
		After1-At Bti1	-0.08	-0.72	0.477	0.626
		At Bti2-At Bti1	0.042	0.409	0.685	0.777
		After2-At Bti1	0.123	1.255	0.22	0.355
		At Bti3-At Bti1	**0.322**	**4.1**	**0.0002**	**0.001**
		After3-At Bti1	**0.40**	**4.01**	**0.0004**	**0.002**
		At Bti2-After1	0.158	1.62	0.12	0.229
		After2-After1	**0.242**	**2.591**	**0.0167**	**0.039**
		At Bti3-After1	**0.437**	**5.652**	**2.44e-06**	**5.124e-05**
		After3-After1	**0.505**	**5.815**	**7.52e-06**	**7.896e-05**
		After2-At Bti2	0.045	0.387	0.703	0.777
		At Bti3-At Bti2	**0.24**	**2.623**	**0.013**	**0.034**
		After3-At Bti2	**0.308**	**2.756**	**0.0115**	**0.034**
		At Bti3-After2	0.097	1.199	0.239	0.358

Variables	Contrast					
		After3-After2	0.166	1.756	0.093	0.195
		After3-At Bti3	0.109	1.289	0.206	0.355
CH_4 concentration-seasonal		Pairwise (lme)				
	Season	**Summer - Spring**	**0.22**	**3.32**	**0.0012**	**0.0024**
		Autumn - Spring	**-0.42**	**-7.27**	**<.00001**	**<.00001**
		Winter - Spring	-0.06	-0.75	0.457	0.457
		Autumn - Summer	**-0.69**	**-8.11**	**<.00001**	**<.00001**
		Winter - Summer	**-0.34**	**-2.88**	**0.006**	**0.008**
		Winter - Autumn	**0.2**	**1.88**	**0.066**	**0.079**
CH_4 emissions -Short term		Contrasts (lme)				
	Zone / Treatment	Aquatic Control - Aquatic Bti	0.2	1	0.340	0.340
		Aquatic-Terrestrial Control - Aquatic-Terrestrial Bti	**-0.42**	**-2.65**	**0.024**	**0.048**
	Aquatic-Terrestrial transition zone / Timepoint	Contrasts (lm)				
		Before Bti 1 C – Before Bti 1 Bti	-0.55	-1.39	0.195	0.364
		After 1 C – After 1 Bti	-0.22	-0.99	0.334	0.364
		After 2 C – After 2 Bti	**-0.66**	**-3.65**	**0.004**	**0.018**
		After 3 C – After 3 Bti	-0.23	-0.95	0.36	0.364
CH_4 emissions-seasonal		Pairwise (lme)				
	Zone / Treatment	Aquatic Control - Aquatic Bti	0.11	0.74	0.476	0.476
		Aquatic-Terrestrial Control - Aquatic-Terrestrial Bti	**-0.47**	**-3.70**	**0.004**	**0.008**
		Pairwise (lme)				

Variables	Contrast					
	Aquatic-Terrestrial transition zone/ Season	**Spring C – Spring Bti**	**-0.44**	**-2.83**	**0.02**	**0.07**
		Summer C – Summer Bti	**-0.61**	**-2.15**	**0.057**	**0.08**
		Autumn C – Autumn Bti	**-0.55**	**-2.13**	**0.06**	**0.08**
		Winter C – Winter Bti	-0.35	-0.97	0.356	0.356
CH_4 oxidative fraction		Pairwise (lme)				
	Season	Summer - Spring	-0.14	-1.61	0.182	0.273
		Autumn - Spring	-0.19	-2.03	0.291	0.349
		Winter - Spring	-0.19	-3.06	0.018	0.110
		Autumn - Summer	-0.19	-1.6	0.155	0.273
		Summer - Winter	-0.18	-2.29	0.071	0.213
		Autumn - Winter	-0.06	-0.74	0.492	0.492

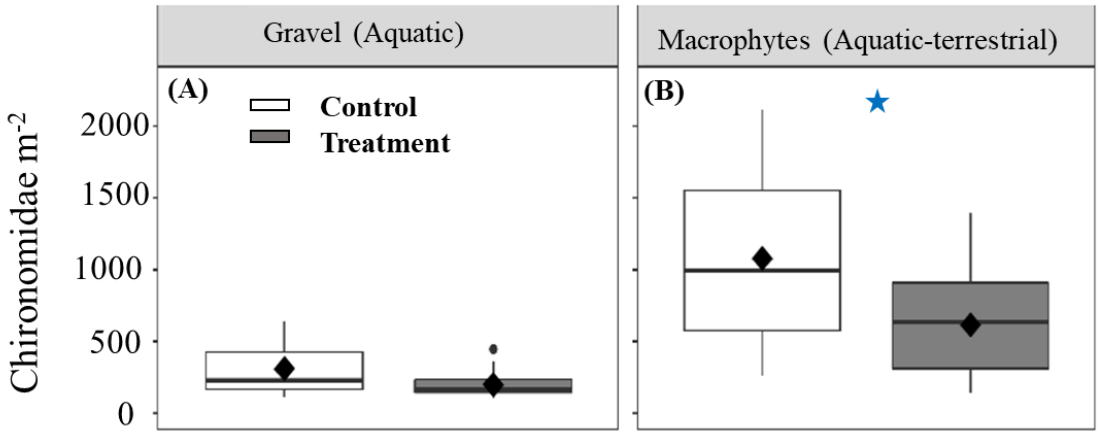

SI Figure S7: Abundance (number m^{-2}) of Chironomidae taxa in gravel (**A**) and macrophytes (**B**) habitat, respectively corresponding to aquatic and aquatic-terrestrial zone of FPMs in control (empty; n=6) and Bti-treated ponds (filled; n=6) collected two weeks after the three replicated Bti application. Lower and upper box boundaries show 25th and 75th percentiles, respectively, line inside box show medians, and black diamonds show mean density. Blue stars denote significant difference between treated and control groups. Data were log-transformed. Figure adopted from Gerstle et al. submitted manuscript.

SI Table S5: Average abundance of Chironomidae taxa in control (n=6) and treatment ponds (n=6) collected two weeks after the three replicated Bti application From April to June 2020. Table adopted from Gerstle et al. submitted manuscript

			Average abundance (m^{-2})	
Order	Family	Taxa	Control	Treatment
Diptera	Chironomidae	Chironominae	325	173

Order	Family	Taxa	Average abundance (m^{-2})	
			Control	Treatment
		Tanypodinae	207	171
		Orthocladiinae	131	49

Appendix II

Published paper

(Ganglo, C., Mendoza-lera, C., Manfrin, A., Bolpagni, R., Gerstle, V., Kolbenschlag, S., … Lorke, A. (2023). Science of the Total Environment Does biocide treatment for mosquito control alter carbon dynamics in floodplain ponds? *Science of the Total Environment*, *872*(2), 161978. https://doi.org/10.1016/j.scitotenv.2023.161978)

Science of the Total Environment 872 (2023) 161978

Contents lists available at ScienceDirect

Science of the Total Environment

journal homepage: www.elsevier.com/locate/scitotenv

Does biocide treatment for mosquito control alter carbon dynamics in floodplain ponds?

Caroline Ganglo [a,*], Clara Mendoza-Lera [a], Alessandro Manfrin [a], Rossano Bolpagni [b], Verena Gerstle [a], Sara Kolbenschlag [a], Eric Bollinger [a], Ralf Schulz [a], Andreas Lorke [a]

[a] RPTU Kaiserslautern-Landau, Institute for Environmental Sciences, Fortstr. 7, D-76829 Landau, Germany
[b] University of Parma, Department of Chemistry, Life Sciences and Environmental Sustainability, Parco Area delle Scienze 33/A, 43124 Parma, Italy

HIGHLIGHTS

- Implications of mosquito biocide on C dynamics in floodplain ponds are studied.
- Weak but long-lasting influence of biocide application on C pools and C fluxes.
- Increased CH_4 emissions in biocide-treated ponds.
- Weak reduction of dissolved organic C in treated ponds' porewater.
- Long-lasting effects of Bti on C budget components in ponds.

GRAPHICAL ABSTRACT

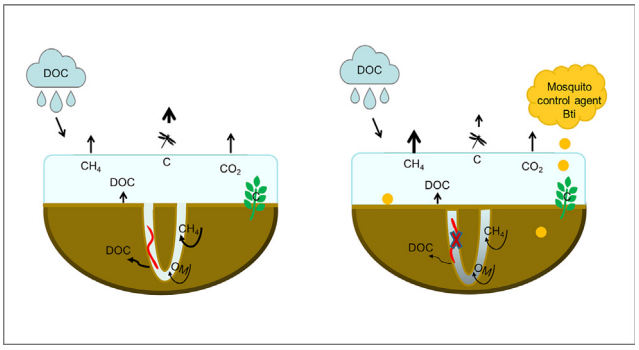

ARTICLE INFO

Editor: Jay Gan

Keywords:
Lentic
Carbon biogeochemistry
Bioturbation
Trophic interactions
Non-trophic interactions
Sediment oxygenation

ABSTRACT

Shallow lentic aquatic ecosystems, such as ponds, are important repositories of carbon (C) and hotspots of C cycling and greenhouse gas emission. Tube-dwelling benthic invertebrates, such as chironomids, may be key players in C dynamics in these water bodies, yet their role in the C-budget at ecosystem level remains unclear. We tested whether a 41 % reduction in chironomid abundance after application of the mosquito control biocide *Bacillus thuringiensis israelensis* (Bti) had implications for the C-fluxes to the atmosphere, C-pools, and C-transformation (i.e. organic matter decomposition) in ponds. Data were collected over one year in the shallow, deep and riparian zones of 12 experimental floodplain pond mesocosms (FPMs), half of them treated with Bti. C-fluxes were measured as CO_2 and CH_4 emissions, atmospheric deposition, and emerging insects. C-pools were measured as dissolved inorganic and organic C in surface and porewater, sediment organic C, C in plant and in macroinvertebrate biomass. Despite seasonal variability, treated FPMs, for which higher CH_4 emissions have been reported, showed a trend towards less dissolved organic C in porewater, while no effect was observed for all remaining components of the C-budget. We attribute the effect of Bti on the C-budget to the reduction in macroinvertebrates biomass, the increase in CH_4 emissions, and the input of C from the Bti excipients. This finding suggests that changes in tube-dwelling macroinvertebrates have a weak influence on C cycling in ponds and confirms the existence of long-lasting effects of Bti on specific components of C-budgets.

1. Introduction

Small, inland water bodies such as ponds have been recognized as a major component of the global carbon (C) budget (Holgerson, 2015; Downing, 2010). While globally small ponds (<0.001 km^2) comprise

* Corresponding author at: University of Kairserslautern-Landau, Fortstrasse 7, 76829 Landau, Germany.
E-mail address: carolineganglo20@gmail.com (C. Ganglo).

http://dx.doi.org/10.1016/j.scitotenv.2023.161978
Received 11 November 2022; Received in revised form 29 January 2023; Accepted 29 January 2023
Available online 3 February 2023

about 8.6 % of lentic inland water bodies by surface area, they contribute 41 % and 15 % to their diffusive emissions of carbon dioxide (CO_2) and methane (CH_4) (Holgerson and Raymond, 2016). Additionally, small ponds can store large amounts of organic C over extended periods, with areal burial rates up to 30 times higher than in other ecosystems (Taylor et al., 2019).

Benthic macroinvertebrates are important mediators of C biogeochemistry in ponds (Hölker et al., 2015), yet their role in C-budgets has received little attention (Colina et al., 2021; Vadeboncoeur et al., 2002; Covich et al., 1999). Benthic macroinvertebrates can directly or indirectly affect a large range of C cycling processes such as respiration and organic matter decomposition (Benelli and Bartoli, 2021; Baranov et al., 2016a, 2016b; Kajan and Frenzel, 1999). Among freshwater benthic macroinvertebrates, tube-dwelling taxa such as chironomid larvae (Diptera: Chironomidae) are among the most widely distributed and abundant ones (Hölker et al., 2015; Leeper and Taylor, 1998). Through their activity at the sediment-water interface, building U-shaped burrows in fine sediment (Nogaro and Steinman, 2014; De Haas et al., 2006), they connect oxic surface water with anoxic sediment modulating redox conditions and thus C-processing (Colina et al., 2021; Hölker et al., 2015; Murniati et al., 2017; Hodkinson and Williams, 1980; Mclachlan and Cantrell, 1976).

Tube-dwelling chironomids can potentially influence C cycling by altering three interrelated components of the C budget: (i) C-pools, (ii) C-transformation, and (iii) C-fluxes. The C-pools include particulate and dissolved organic C (DOC), dissolved inorganic C (DIC), and standing plant and living animal biomass. The activity of chironomids can affect the first three pools by feeding on particulate organic matter and by oxygenating the sediment, promoting aerobic decomposition of organic matter and respiration (Baranov et al., 2016a, 2016b). The C-fluxes mainly include CO_2 and CH_4 fluxes across the air-water interface, advective fluxes with inflowing and outflowing water, and the emergence of merolimnic insects. The activity of tube-dwelling chironomids can affect both CO_2 and CH_4 fluxes by promoting the transport of CO_2- and CH_4-rich porewater to the water column (Booth et al., 2021) and/or by modulating the processes that regulate their production and consumption (Colina et al., 2021), such as oxygenation of the sediment modulation of CH_4 production and oxidation (Baranov et al., 2016a, 2016b).

The effect of chironomid larvae on C cycling is conditioned by habitat suitability and season, which determine chironomid larval abundance (Baranov et al., 2016a, 2016b; Frouz et al., 2003; Jackson and Mclachlan, 1991). One key factor for habitat suitability is sandy sediment (grain size: < 0.06–0.5 mm, Nogaro and Steinman, 2014; De Haas et al., 2006). Besides habitat suitability, the abundance of chironomid larvae can be further affected by anthropogenic stressors such as micropollutants and larvicides. The biocide *Bacillus thuringiensis israelensis* (Bti, Brühl et al., 2020; Boisvert and Boisvert, 2000) is a widely applied mosquito control agent. Recent research conducted in the same experimental facility as our study revealed that Bti application reduced the abundance of chironomids (Gerstle et al., 2022), altered their emergence dynamics (Kolbenschlag et al., 2023), and increase CH_4 emissions (Ganglo et al., 2022).

Here we study whether the changes in chironomid abundance, caused by the application of Bti in the previously described mesocosm experiment (Ganglo et al., 2022), affected the pond-wide C-pools, −fluxes, and -transformations. We measured the components of the C-pool and C-flux during four seasons in the riparian zone, in the shallow and deep aquatic zone of twelve mesocosms, six of them treated with Bti. For the C-pools, we hypothesize that the reduced abundance of chironomids (Gerstle et al., 2022) results in reduced organic matter processing, leading to an increase in particulated and dissolved organic C in the sediment. For the C-fluxes, we hypothesize that the previously observed increase in CH_4 flux (Ganglo et al., 2022) is accompanied by a reduction in CO_2 flux due to reduced sediment aerobic respiration. We further expect that these effects are stronger in the shallow than in the deeper aquatic zones and more pronounced during spring and summer due to higher chironomid abundance and activity. To assess the implications of changes in chironomid abundance and Bti application for ecosystem C-budget, we incorporated additional C-flux and -pool measurements as wet C deposition and plant C biomass, as well as available data for the C biomass of benthic macroinvetebrates and emerged insects.

2. Material and methods

2.1. Experimental design

2.1.1. Floodplain pond mesocosms

The 12 floodplain pond mesocosms (FPMs, SI Fig. S1) used in our study were constructed in 2017 at the Eußerthal Ecosystems Research Station (EERES; Germany, 49°15′16“ N, 7°57′42” E) (Stehle et al., 2022). The FPMs are identical in shape and size (surface area: ~104 m^2, regular water volume: ~25 m^3, and regular water depth: ~0.30 m) and consist of a gradient in water depth divided into three zones: aquatic deep zone (surface area: ~43.5 m^2, volume: ~13 m^3, mean depth: ~0.30 m), aquatic shallow transition zone (surface area: ~30.25 m^2, volume: ~6 m^3, mean depth: ~0.20 m), and terrestrial riparian zone (surface area: ~30.25 m^2, SI Fig. S1). A hydrological separation between each FPM and groundwater is provided by a flexible rubber foil. The water level in each pond can be adjusted through overflows and inlets connected to the nearby stream Sulzbach. We monitored the water level in each FPM over the study period using pressure loggers (U20–001-03, Onset Computer Corporation, Hobo, USA).

In the aquatic deep zone, the bed consists of a ~ 13 cm thick layer of coarse pebbles (diameter 1–3 cm) and is populated by submerged macrophytes (*Elodea* sp. and *Ceratophyllum* sp., ~35 % areal coverage) and emergent plants (*Typha* sp., ~40 %) along the banks. In the aquatic shallow transition zone, the bed is characterized by a ~ 15 cm thick layer of medium to coarse sand (diameter: ~0.05 cm) and is covered by submerged macrophytes (~28 %) and emergent plants (*Typha* sp. ~46 %). The terrestrial riparian zone is characterized by ~20 cm of coarse sand, covered by spike rush grass (*Juncus* sp. ~50 %), and often covered by leaf litter (~18 %).

2.1.2. Bti application

We applied the biocide Bti three times during elevated water levels (i.e., flooding) following common practice (Becker, 2006). Before each application, we flooded each FPM by gradually increasing the water level by 0.20 m (from 0.30 ± 0.02 m to 0.50 ± 0.02 m at the deepest location) over two days. See Table S1 for a detailed description of application times. We applied Bti as a suspension (VectoBac WDG; Valent Biosciences, Illinois, USA) at a maximum field rate (2.88×10^9 ITU ha^{-1}, corresponding to ~118 mg VectoBac WDG m^{-2}) using a knapsack sprayer (Prima 5, Gloria, Germany) (see also Gerstle et al., 2022).

2.2. Sampling and data calculation

2.2.1. C-pools

We estimated the amount of total organic carbon (TOC) added as Bti (active component plus excipient) assuming it to be sucrose and corresponds to 0.136 g L^{-1}. The total amount of applied Bti product to each FPM (~354 mg m^{-2}) corresponds to 0.06 g C m^{-2}.

We sampled plant biomass (vascular plants and filamentous algae) in each zone for four seasons: spring, summer, autumn, and winter (see SI Table S2 for a detailed sampling design). In each zone, we determined area-specific biomass of above-ground plant material by counting the number of plants within a representative vegetated area (1.5 m × 1.5 m) (see picture in SI Fig. S2). To determine plant biomass, we collected two to four individuals of each plant species within the sampling area, unrooted, and washed with tap water before oven-dried at 60 °C for 96 h to obtain their dry mass. We sampled and counted *Typha* sp. in the deep and shallow transition zone, and *Juncus* sp. and *Typha* sp. in the riparian zone. In both aquatic zones, we visually assessed the area covered by submerged macrophytes and filamentous algae from a representative sampling area (0.25 m × 0.25 m). We collected all macrophytes and filamentous algae in the sampling area and further oven-dried at 60 °C for 96 h to obtain their dry

mass. We calculated the area-specific C as plant biomass (B_p in g C m^{-2}) in each zone as:

$$B_p = \frac{m_d}{A_s} c_p \quad (1)$$

where m_d is the total dry weight of plants (g) calculated as the sum of the product of the dry mass of each plant (*Typha* sp., *Juncus* sp., macrophytes, and filamentous algae) and the number of plants per area or the area covered, A_s is sum of the sampling area (m^2), and c_p is a conversion factor from dry mass to C (0.45; Fan et al., 2008).

We sampled sediment organic C in the deep, shallow transition and riparian zones for four seasons (SI Table S2). We sampled a sediment core in each zone using a sediment corer (length: ~13 cm, diameter: ~8 cm, area: ~50 cm^2). We weighed the samples before and after oven-drying at 60 °C for 96 h and then ground them (<0.5 mm grain size). From each sample, we fumigated a 15-mg subsample with hydrochloric acid (HCl) for organic C content determination using an elemental analyzer (Costech Elemental Combustion System, CHNS-O). We calculated the areal sediment C content in the sediment of each zone (S in g C m^{-2}) as:

$$S = (1-\varphi) h_s \rho_s c_s \quad (2)$$

where c_s is the measured mass fraction of organic C, φ is sediment porosity, h_s (m) is the thickness of the sediment layer (deep zone ~0.13 m, shallow ~0.15 m, and riparian zone ~0.2 m), and ρ_s is the density of solid sediment (2.6×10^6 g m^{-3}). We calculated sediment porosity from the ratio of dry to wet mass ($R = m_d/m_w$) as:

$$\varphi = \frac{\rho_s (1-R)}{\rho_s (1-R) + \rho_w R} \quad (3)$$

where ρ_w is the density of water (1.0×10^6 g m^{-3}).

We used macroinvertebrate abundance data reported in a companion study (Gerstle et al., 2022) and taxa-specific mean dry weight of individual organisms (5 samples per taxa dried at 60 °C for 96 h) of the three most abundant groups (95 % of the community abundance), i.e., Chironomidae (0.15 ± 0.03 mg (mean ± standard deviation)), Ephemeroptera (1.52 ± 0.38 mg), Odonata (41.15 ± 23.46 mg), to estimate total macroinvertebrate biomass. We measured the C mass fraction of each taxa using an elemental analyzer (Flash 2000 HT, Thermo Scientific, Bremen, Germany): Chironomidae (0.42 ± 0.02; $N = 47$), Ephemeroptera (0.51 ± 0.01; $N = 60$) and Odonata (0.44 ± 0.01; $N = 169$). We calculated the areal C content in macroinvertebrates B_{mc} (g C m^{-2}) for both the deep and shallow transition zone as:

$$B_{mc} = m_{Ch} N_{Ch} c_{Ch} + m_{Ep} N_{Ep} c_{Ep} + m_{Od} N_{Od} c_{Od} \quad (4)$$

Where m is the average taxa-specific dry weights (g), N is the abundance of each group per area from Gerstle et al. (2022), and c is the C mass fraction of each group. The subscripts correspond to *Ch* for Chironomidae, *Ep* for Ephemeroptera, and *Od* for Odonata.

In the shallow transition zone, we sampled porewater dissolved organic carbon (DOC) seasonally (SI Table S2). Due to the coarse bed and the low water content, respectively, we could not sample pore water in the deep and riparian zones. We assumed horizontal homogeneity of porewater DOC across zones. Porewater samples were collected over ~12 cm sediment depth using MacroRhizon samplers (pore size ~0.15 μm, Rhizosphere Research Products, Agro Business Park 7B, 6708 PV Wageningen, Netherlands). We analyzed the samples by catalytic combustion, after acidification with hydrochloric acid (HCl) to remove inorganic C (DIN EN ISO/IEC 17025:2018). We determined the areal DOC content in porewater ($D_{DOC,pw}$ in g C m^{-2}) of both aquatic zones as:

$$D_{DOC,pw} = \varphi C_{Doc,pw} h_s \quad (5)$$

Where $C_{DOC,pw}$ (g m^{-3}) is DOC concentration in porewater; h_S (0.16 m) is the mean sediment bed thickness.

We measured seasonally surface water DOC from 500 mL-water samples between deep and shallow transition zone, at the center of the aquatic area near the water surface (SI Fig. S1). We determined DOC by catalytic combustion, after acidification with hydrochloric acid (HCl) to remove inorganic C (DIN EN ISO/IEC 17025:2018). We estimated the areal content of DOC in surface water ($D_{DOC,sw}$ g C m^{-2}) for both the deep and shallow transition zone as:

$$D_{DOC,sw} = C_{DOC,sw} h_w \quad (6)$$

Where h_w (m) is the average FPM water depth and $C_{DOC,sw}$ (g m^{-3}) is the DOC concentration in surface water.

We determined dissolved inorganic C in surface water as CO_2 and CH_4, we took the values for the latter from Ganglo et al. (2022). We measured seasonal CO_2 concentration in the deep and shallow transition zone (SI Table S2) using the headspace method (International Hydropower Association, 2010; see Ganglo et al., 2022 for CH_4). We collected water samples at 5 to 10 cm depth using a 1.2-L Schott glass bottle (sample volume: ~0.9 L, headspace volume: ~0.3 L). Once the bottle was closed, we shook vigorously the bottle for two minutes to ensure gas equilibration between the water and the headspace. We then connected the bottle headspace to a gas analyzer (Ultra-portable Greenhouse Gas Analyzer; UGGA, Los Gatos Research Inc., Mountain View, CA, USA) in closed-loop to measure the molar fractions of CO_2 and CH_4. We calculated the areal C content as dissolved CO_2 and CH_4 in surface water ($D_{CH4,CO2}$ in g C m^{-2}) for each aquatic zone as:

$$D_{CH4,CO2} = 10^{-3} M_c h \left(X_{Final}\, p + (X_{Final} - X_{Initial}) \frac{V_{HS}}{V_s} \frac{p}{RT_k} \right) \quad (7)$$

Where X_{Final} and $X_{Initial}$ are the mole fractions of CO_2 or CH_4 (ppm_v) in the sample at equilibrium and in the atmosphere at the time of sampling, respectively, p is the atmospheric pressure (assumed constant at 1 atm), V_{HS} and V_s (in L) are headspace volume, including tubbing and gas analyzer internal volume, and water volume, respectively. R is the ideal gas constant (0.08 in L atm K^{-1} mol^{-1}). T_K is the sample temperature (K). Factor 10^{-3} is a unit conversion factor, M_C (12 g mol^{-1}) is the molar mass of C, and h is the mean water depth (m) of each zone. K is the Henry coefficient for CH_4 or CO_2 at the sampling temperature (mol L^{-1} atm^{-1}, calculated following International Hydropower Association (2010)). We measured water temperature and oxygen saturation at the time of sampling using a multiprobe (WTW 82362 Weilheim, multi 3430 Germany).

2.2.2. C-fluxes

We estimated the deposition of organic C as rainwater by repeated sampling of 500 mL of precipitation over each season (SI Table S2), which we analyzed for TOC ($c_{TOC,rw}$ in g C m^{-3}) concentration as described above for DOC (Eq. (6)). We calculated the wet deposition C flux ($F_{TOC,wd}$ in g C m^{-2} d^{-1}) for each FPM as:

$$F_{TOC,wd} = \frac{H_{wd}\, C_{TOC,wd}}{t} \quad (8)$$

Where H_{wd} is the total precipitation height during the season (in m) provided by a nearby (2 km) weather station, t is the duration of each season in days.

We performed seasonal measurements of atmospheric CO_2 flux from the shallow transition and deep zones simultaneously with those for CH_4 from Ganglo et al. (2022) (SI Table S2). We measured CO_2 and CH_4 emissions to the atmosphere in the deep, shallow transition, and riparian zone using transparent, floating, static chambers made of plastic polyethylene foil (allflex. E, 300 μm, PA/EVOH/PA/PE, allvac Folien GmbH, Germany). We used two chambers of different sizes depending on vegetation size: 72.5 × 72.5 × 54.6 cm and 72 × 72.5 × 147.2 cm (L x W x H SI Fig. S2). We placed two battery-powered fans inside each chamber to ensure uniform gas mixing and a logger for light intensity and temperature (UA-002-64, Onset Computer Corporation, Hobo, USA). We connected the chambers in a closed-loop with a gas analyzer (Ultra-portable Greenhouse

Gas Analyzer; UGGA, Los Gatos Research Inc., Mountain View, CA, USA) using 2 m Tygon tubing. Each chamber deployment lasted for about 5 min, or shorter if the relative humidity inside the chamber reached 90 % to avoid artifacts. We calculated the total flux of CO_2 and CH_4 based on the slope of a linear regression between the mean rate of change of gas mole fraction in the chamber headspace (α in ppm s^{-1}) as:

$$F_{CH4,CO2} = -\alpha\left(\frac{V}{A}\right)\left(\frac{p}{RT_K}\right)aM_C \quad (9)$$

where F (g C m^{-2} d^{-1}) represents the flux of C in form of CO_2 (F_{CO2}) and in form of CH_4 (F_{CH4}), V is the chamber volume including the tubbing (m^3); A is the chamber surface area (m^2), p is atmospheric pressure (kPa, assumed to be constant 101.325 kPa); R is the gas constant (8.31 m^3 Pa K^{-1} mol^{-1}), and T_K is the temperature in the chamber headspace (K); a is a unit conversion factor ($a = 10^{-3} \times 86{,}400$ s d^{-1}), and M_C (12 g mol^{-1}) the molecular weight of C.

We estimated the flux of C leaving the FPMs as emerging insects using data from Kolbenschlag et al. (2023). The emergent insects were collected using emergence traps between mid-April to the end of July (SI Table S2) and taxa-specific biomass of individuals was measured. The most abundant groups (by number) were Chironomidae and Baetidae, which accounted respectively for 87.8 % and 9.4 % of the total abundance of collected insects. Kolbenschlag et al. (2023) estimated dry-weight (by prior processing and drying at 60 °C) of Chironomidae (0.14 ± 0.006 mg) and Baetidae (0.93 ± 0.05 mg) for both control and treated FPMs. As for the C content in macroinvertebrate biomass, we determined C in emerged insects using an elemental analyzer (c_{E1} = 0.44 ± 1.05; N = 58 and c_{E2} = 0.50 ± 1.18; N = 52 for Chironomidae and Baetidae, respectively). We calculated the C flux as insect emergence (F_{mc} in g C m^{-2}) from both aquatic zones as:

$$F_{mc} = -\frac{m_{Ch}c_{Ch} + m_{Ba}c_{Ba}}{A_s\, t} \quad (10)$$

Where m_{Ch} (g) and m_{Ba} (g) are the total dry mass of emerged Chironomidae and Baetidae respectively, c_{Ch} and c_{Ba} are the respective C mass for each group. A_S is the emergence trap surface area (0.99 m^2) and t (d) is the time over which traps were deployed.

2.2.3. C-transformation: organic matter decomposition

We used the teabag method (Keuskamp et al., 2013) as a proxy for microbial decomposition of organic matter. Green tea (EAN: 87 22700 05552 5) and rooibos tea (EAN: 87 22700 18843 8) served as standardized organic matter, with green tea being more labile and rooibos more recalcitrant to biological decomposition. We deployed three pre-weighed teabags in the sediment of the deep, shallow transition, and riparian zones, (8 cm deep) and in the water column of both deep and shallow aquatic zones (5 cm below surface water) for four seasonal periods: spring (May to June 2020), summer (July to September 2020), autumn (September to December 2020), and winter (December 2020 to January 2021, SI Table S2). At the end of each incubation period (between 36 and 91 days; SI Table S2), we retrieved, cleaned, and oven-dried (70 °C for 48 h) the teabags to determine their final dry weight. The weight of the bag for each tea type was determined from 40 empty bags (0.126 ± 0.003 g and 0.133 ± 0.007 g; mean ± SD for green and rooibos, respectively). We calculated the decomposition rate (k in d^{-1}) and the stabilization factor (q) (the fraction of tea that is not decomposed but sequestered) following Keuskamp et al. (2013) (SI Eq. S1 - S3).

2.2.4. Statistical analysis

We assessed seasonal changes among zones and between treated and control FPMs for plant C biomass, sediment organic C, dissolved CO_2, CO_2 fluxes, CH_4 riparian fluxes, decomposition rates, and stabilization factor. We used mixed effect models (LMEMs) using the lme function in the package nlme (Pinheiro et al., 2022) for R (R Core Team, 2013). The model included zone (depending on where the response variable was collected, see above), treatment (Bti-treated and control FPM), season (spring, summer, autumn, and winter), and their interactions as fixed factors. For DOC in pore- and surface water, we could not distinguish between zones, therefore only treatment, season and their interactions were included as model fixed factors. In all models, the individual FPM was considered as a random factor to account for replicated sampling. By using likelihood ratios against reduced models, we performed a backward selection (Zuur et al., 2010). We assessed the residuals and normality of the initial and the final model using qqplots and model residual-fitted values plots. We log-transformed response variables to meet normality and homogeneity of residual assumptions when needed (Zuur et al., 2010). We log-transformed all variables except for CO_2 fluxes. We also considered potential temporal dependency by fitting the initial model with different temporal autocorrelation structures (corARMA, Zuur et al., 2010) and using Akaike Information Criterion assessment to select the best corARMA structure in the model (Zuur et al., 2010). When we found significant effects of model interactions, we ran a contrast analysis using linear models with adjusted p-values after applying a Benjamini-Hochberg correction for false positives due to multiple testing (Benjamini and Hochberg, 1995).

3. Results

3.1. C-pools

Bti did not affect any measured component of the C-pools. The different C components summed up to a mean total C-pool of 1159.2 ± 314.3 g C m^{-2} (mean ± standard deviation). The total C-pool varied seasonally, being the lowest in spring (1094.2 ± 294.6 g C m^{-2}) and the highest in winter (1270.0 ± 423.5 g C m^{-2}). These seasonal differences were associated with variations in water temperature during sampling, which ranged from 4 ± 3 °C in winter with few episodes of ice cover, to 21 ± 4 °C in summer.

Porewater and surface water DOC contributed ~0.1 % and ~ 0.2 % to the total C-pool, respectively (Fig. 2). DOC concentrations varied significantly between seasons (Table 1) with the highest concentrations in porewater in spring (1.7 ± 0.6 g C m^{-2}) and the lowest in winter (0.3 ± 0.1 g C m^{-2}, Fig. 1a). On average, porewater DOC tended to be lower in summer, autumn, and winter (0.6 ± 0.3 g C m^{-2}) in treated FPMs than in the control ones (0.9 ± 0.6 g C m^{-2}) (SI Table S4). Regardless of Bti treatment, surface water DOC was the lowest in autumn (1.1 ± 0.3 g C m^{-2}) and peaked in summer (1.7 ± 0.4 g C m^{-2} Fig. 1b).

For all seasons, the surface water was supersaturated in CO_2 and CH_4 with respect to atmospheric equilibrium concentration with a mean saturation of 217 ± 268 % and 6397 ± 5724 %, respectively. The dissolved gases

Table 1
F value for significant ($p \leq 0.05$) factors and their interactions for plant C biomass, sediment organic C, porewater DOC, surface water DOC, dissolved CO_2, decomposition rates and stabilization factor, CO_2 and CH_4 fluxes after linear mixed effect model backward selection. See SI Table S3 & S4 for further details.

Variables	Factors	F-value (numDF, denDF)	p-value
Plant C biomass	Zone	$F_{2,437}$ = 40.22	<0.0001
	Season	$F_{3,437}$ = 6.62	0.0002
Sediment total C	Zone	$F_{2,127}$ = 53.70	<0.0001
	Season	$F_{3,127}$ = 3.86	0.01
Porewater DOC	Season	$F_{3,33}$ = 36.41	<0.0001
Surface water DOC	Season	$F_{3,93}$ = 24.68	<0.0001
Dissolved CO_2	Season	$F_{3,274}$ = 15.73	<0.0001
Decomposition rate	Season	$F_{3,544}$ = 17.31	<0.0001
Stabilization factor	Season	$F_{3,525}$ = 49.39	<0.0001
	Zone	$F_{2,525}$ = 381.32	<0.0001
	Season × Zone	$F_{3,525}$ = 10.40	<0.0001
	Season × Zone × Treatment	$F_{3,525}$ = 3.15	0.005
CO_2 flux	Zone	$F_{2,341}$ = 51.42	<0.0001
	Season	$F_{3,341}$ = 9.84	<0.0001
	Zone × Season	$F_{6,341}$ = 6.67	<0.0001
CH_4 flux	Season	$F_{3,106}$ = 10.27	<0.0001

numDF = numerator degrees of freedom; denDF = denominator degrees of freedom.

made the smallest contribution to the total C-pool, ~0.03 % for CO_2 and ~ 0.001 % for CH_4 (Fig. 2), and varied strongly between seasons (Fig. 1c-d). For both treatments, dissolved CO_2 was the lowest in autumn (0.1 ± 0.2 g C m^{-2}) and the highest in spring (0.3 ± 0.3 g C m^{-2}, Table 1), while dissolved CH_4 was the lowest in autumn (0.003 ± 0.002 g C m^{-2}) and the highest in summer (0.09 ± 0.01 g C m^{-2}).

At the system level, sediment C made the largest contribution to the C-pool by comprising ~94 % (Fig. 2) and varied between seasons and zones (Table 1, Fig. 3a-c). Plant biomass made up to ~5 % of the C-pool (Fig. 2). Macroinvertebrates contributed ~0.08 % to the C-pool and the additional C from the Bti excipient represented ~0.007 % of the C-pool of the treated FPMs (Fig. 2). The C reduction as macroinvertebrates and C addition by Bti in treated ponds were of comparable magnitude (~0.02 % of the total C-pool).

3.2. C-fluxes

The CO_2 flux varied significantly between seasons and zones (Fig. 4 a-c, Table 1) with CO_2 evasion from the deep zone (−0.2 ± 0.6 g C m^{-2} d^{-1}) and uptake in the shallow zone (4.4 ± 4.9 g C m^{-2} d^{-1}), and riparian zone (2.1 ± 4.3 g C m^{-2} d^{-1}). CO_2 uptake was higher in summer (3.2 ± 5.9 g C m^{-2} d^{-1}) than in winter (0.3 ± 1.5 g C m^{-2} d^{-1}). Overall, the FPMs were oxygen saturated averaging 90 ± 21 % in spring and 108 ± 13 % in winter. As described in Ganglo et al. (2022), the CH_4 flux in the shallow transition zone was significantly higher in treated than in control FPMs (on average by 137 % overall seasons). Spatially, the CH_4 evasion flux were on average one order of magnitude lower in the riparian zone (−0.003 ± 0.1 g C m^{-2} d^{-1}), than in the deep (−0.05 ± 0.1 g C m^{-2} d^{-1}) and shallow transition zones (−0.1 ± 0.1 g C m^{-2} d^{-1}, Fig. 4 d-f); which were similar. Apart from the previously described effect of Bti treatment on CH_4 flux in the shallow transition zone (Ganglo et al., 2022), none of the remaining C fluxes was significantly affected by Bti treatment.

Regardless of treatment, the total C-input flux was 3.24 ± 3.26 g C m^{-2} d^{-1}. The largest C-input was the uptake of atmospheric CO_2 in the shallow transition and riparian zones accounting for up to ~99 %. Over the seasons, the C-input as wet deposition was lower than as CO_2 uptake (~0.1 %, Fig. 2). The total C-output flux was −0.23 ± 0.32 g C m^{-2} d^{-1}. C-output as emerging insects constituted the smallest loss by ~0.9 % (Fig. 2). The output as CH_4 for all zones represented ~24 %, whereas CO_2 evasion from the deep zone shared the largest loss percentage of ~75 % of the total C-output.

3.3. C-transformation: organic matter decomposition

Over the seasons, mean teabag decomposition rate was 0.009 ± 0.004 d^{-1} and varied similarly among zones. The decomposition rates were faster in winter (0.012 ± 0.003 d^{-1}) than in autumn (0.006 ± 0.004 d^{-1}, Fig. 5 a-c, Table 1). The stabilization factor, which describes the fraction of the tea that cannot be decomposed and is sequestered, was 0.28 ± 0.16 and varied both among zones and over the seasons (Fig. 5 d-f, Table 1). The stabilization factor was higher in the sediment (0.4 ± 0.01) than in the water column of the deep (0.2 ± 0.01) and in the shallow zones (0.3 ± 0.01). Over the seasons, the stabilization factor was slightly higher in winter (0.3 ± 0.1) than in autumn (0.2 ± 0.1, Fig. 5 d-f, Table 1). Neither the decomposition rates nor the stabilization factors were significantly affected by Bti treatment.

4. Discussion

Our study provides seasonal snapshots of the C-budget of floodplain pond mesocosms (FPMs) and the effect of Bti application on the C-budget. Overall, the FPMs were a net C sink for the atmosphere through high primary productivity. This is supported by the large amounts of C that have accumulated as organic matter in the sediments during the four years since the construction of the mesocosms. The organic C in the sediment is most likely a mixture of microorganisms, macroinvertebrates, and plant material (Sobek et al., 2006). However, established C-budgets include large uncertainties. As expected, C-fluxes and -pools varied strongly among seasons and zones. Our seasonal measurements of CO_2 and CH_4 concentrations and fluxes, and the single sampling of macroinvertebrate biomass, can only provide a hint of the highly dynamic C cycling in the FPMs. Additional unresolved variations, including night-time respiration, prevent us from completing the C mass balance. Furthermore, the macroinvertebrate flux is expected to be underestimated, as emerging insects were sampled with floating traps and do not capture large organisms that leave the water by climbing up vegetation, such as Odonata (Cadotte and Williams, 2014), which made a large contribution to macroinvertebrate biomass in the FPMs (Gerstle et al., 2022).

The application of Bti resulted in reduced chironomid abundance by 41 % (Gerstle et al., 2022) and their emergence by 26 % and a 10-day shift in the peak of emergence (Kolbenschlag et al., 2023). We hypothesized that these changes in chironomid abundance would alter the C-budget by (i) changes in the C-pool by increasing organic C and DOC in the sediment due to the reduction of organic matter processing, and (ii) changes in the C-

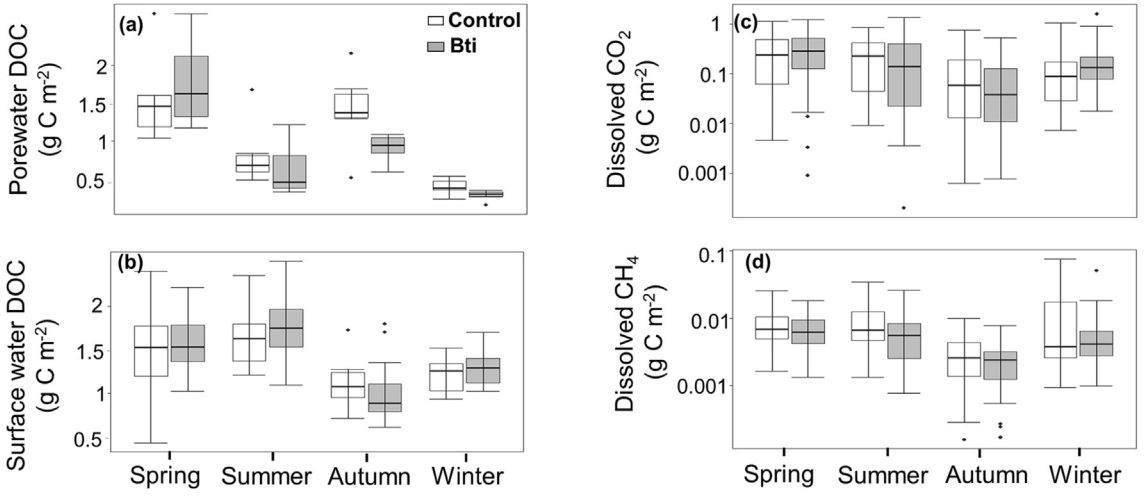

Fig. 1. Box plots of (a) surface water dissolved organic carbon (DOC), (b) porewater DOC, (c) dissolved CO_2, and (d) dissolved CH_4 in the surface water of control floodplain pond mesocosms (FPMs) (white boxes) and FPMs treated with Bti (grey boxes) at different seasons ($N = 6$). The lower and upper limits of the boxes represent the 25th and 75th percentiles, respectively; with the horizontal line inside the box as the median, and lower and upper whiskers show the 10th and 90th percentiles, respectively. Note that filled black circles are data falling outside the 10th and 90th percentiles. Note that the y-axis in c and d are log-scaled.

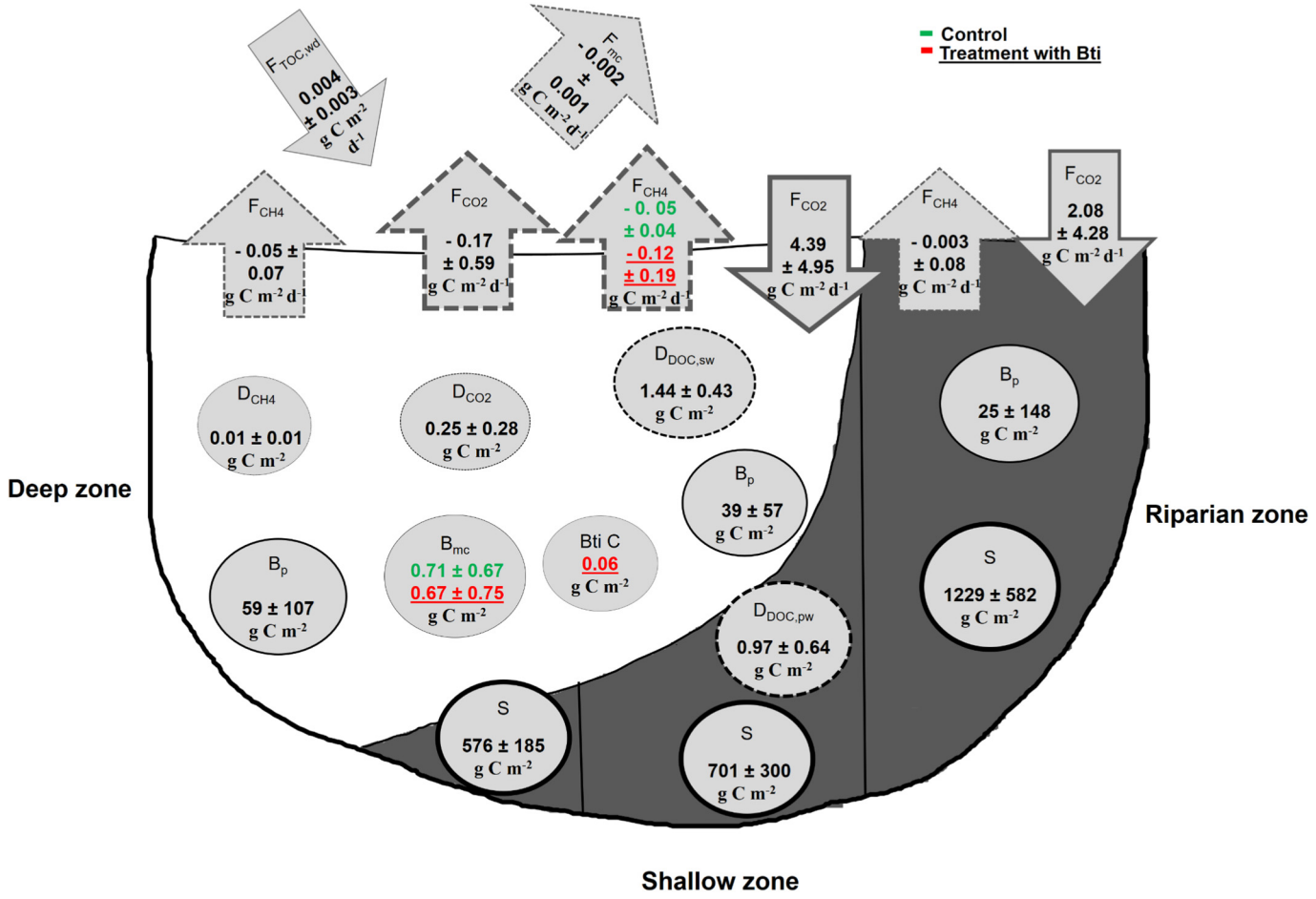

Fig. 2. Graphical representation of the average C-budget comprising the C-pool components (numbers in circles in g C m^{-2}) and C-flux components (numbers in arrows in g C m^{-2} d^{-1}) in the deep, shallow transition, and riparian zones of the 12 FPMs (mean ± standard deviation). If significant differences were observed between FPMs treated with Bti and control FPMs, numbers in red (underlined) and green represent mean values for both treatments, respectively, while numbers in black represent the global average (if no significant differences were observed). Total C in plant biomass (B_p), and sediment organic C (S) were measured in all three zones. Macroinvertebrate C (B_{mc}) was measured in macrophytes and gravel zones of the FPMs. Surface water DOC ($D_{DOC,sw}$), porewater DOC ($D_{DOC,pw}$), dissolved CO_2 (D_{CO2}), and dissolved CH_4 concentration (D_{CH4}) were measured in between the deep aquatic and shallow transition zones, assuming horizontal homogeneity in the FPMs. Wet deposition TOC influx ($F_{TOC,wd}$) was obtained from precipitation water collection and annual precipitation data. CO_2 flux (F_{CO2}) and CH_4 flux (F_{CH4}) were measured in all three zones, and insect biomass efflux (F_{mc}) was measured in the deep and shallow transitions zones of FPMs during spring and summer. Note that particulate C-pools (in sediment, plants, Bti C, and macroinvertebrates) are outlined by solid lines, dissolved C (in porewater and surface water, CO_2 and CH_4 concentration in water) outlined with dashed lines. Arrows indicating C-input (wet deposition DOC and CO_2 flux) are continuous and pointing downwards, whereas C-output (CH_4 flux, CO_2 flux, and emerging insects) is shown as dashed arrows pointing upwards. The width of the circles and arrows indicates the magnitude of the contribution (not to scale). (For interpretation of the references to colour in this figure legend, the reader is referred to the web version of this article.)

fluxes as a result of the redution in aerobic sediment respiration CH_4 flux would increase attributed to increased in anaerobic processing (Ganglo et al., 2022) and CO_2 flux decrease. In our study, we did not detect any changes in the C-pool components measured. Except for the reported increase in CH_4 flux during three seasons after Bti treatment in the shallow transition zone (Ganglo et al., 2022), none of the measured C-fluxes was significantly affected by treatment. The shallow transition zone was densely covered by macrophytes and had finer sediment compared to the deep zone, being the preferred habitat of chironomids. Gerstle et al. (2022) found a higher abundance of chironomid larvae in the macrophyte habitat, where conditions are comparable to our shallow transition zone. The deep zone was dominated by coarse pebbles and less vegetation, with generally fewer chironomid larvae density, limiting their contribution to C cycling in the deep zone (about 28 % of the total FPM area). Most chironomid species are tube dwellers that feed on sediment organic matter and increase the transport of oxygen into the sediment (Murniati et al., 2017) promoting sediment respiration (Baranov et al., 2016a, 2016b; Kajan and Frenzel, 1999). We expected these interactions to result in increased CO_2 production and atmospheric CO_2 flux. However, potential effects on dissolved CO_2 and flux of CO_2 may have been masked by the large uptake of CO_2 by primary producers in the shallow zone and by horizontal mixing of the surface water. This finding is in line with our previous study in the same system, which showed that the concentrations of dissolved CH_4 in surface water were not affected by Bti application (Ganglo et al., 2022). Our measurements suggest a trend towards a 33 % reduction in porewater DOC in treated FPMs, though not significant. This trend suggests a potential long-lasting effect of Bti application on chironomid densities. However, the large variability of porewater DOC in treated FPMs may have masked a potentially significant effect of the Bti application. Non-trophic interactions, such as bioturbation and oxygen transport into the sediment, may explain the reduction in porewater DOC in treated FPMs because of the reduced abundance of chironomid larvae. Chironomid bioturbation promotes the exchange of highly concentrated DOC porewater with oxygenated surface water (Booth et al., 2021; Oliveira Junior et al., 2019; Murniati et al., 2017; Hölker et al., 2015), promoting respiration and decomposition of organic matter, thus increasing DOC (Hölker et al., 2015). However, no

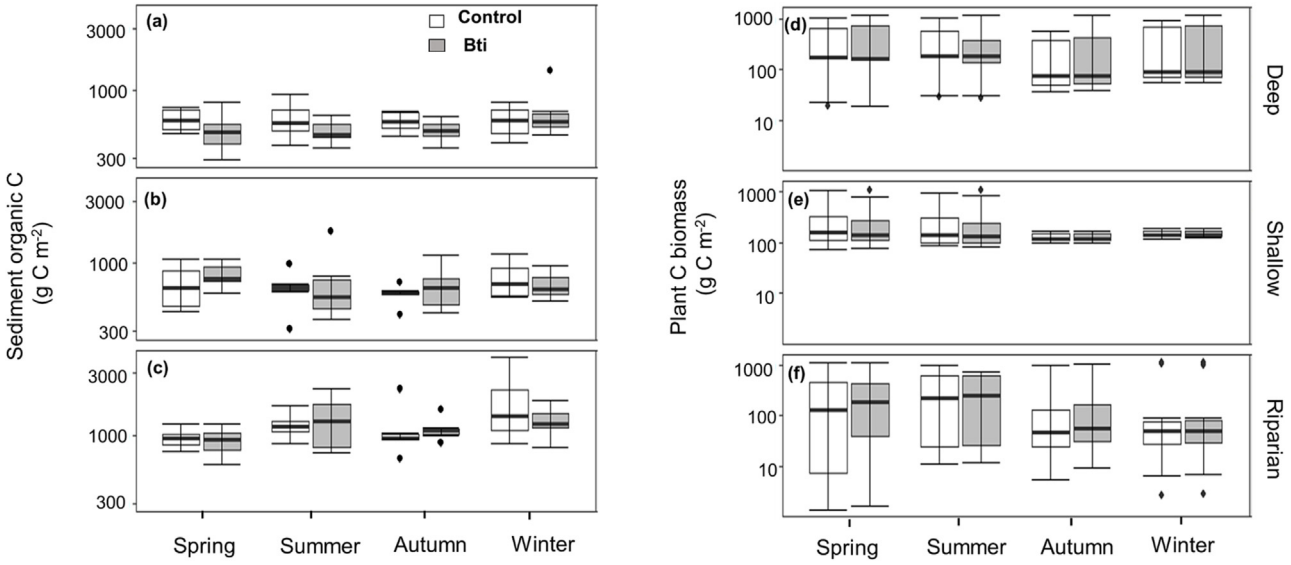

Fig. 3. Box plots of sediment organic C in g C m^{-2} in (a) the deep, (b) the shallow, (c) the riparian zones of control (white boxes), and Bti-treated FPMs (grey boxes) at different seasons. Box plot of plant C biomass in g C m^{-2} in (d) aquatic, (e) shallow transition, and (f) riparian zones of control and treated FPMs at different seasons ($N = 6$). The lower and upper limits of the boxes represent the 25th and 75th percentiles, respectively; with the horizontal line inside the box as the median, and lower and upper whiskers show the 10th and 90th percentiles, respectively. Note that filled black circles are data falling outside the 10th and 90th percentiles. The *y*-axes are log-scaled.

differences were observed in teabag decomposition rates, which may also depend on the depth of burrowing activity of the chironomids (Hölker et al., 2015).

It should be noted here that the Bti excipients are not fully known (Brühl et al., 2020) and part of the amount of Bti product applied may be available as a labile source of C source (~20 %) to microbial communities. We estimated this to be a minor contribution of ~0.007 % to the total C-pool in treated FPMs, less than the observed increase in C-fluxes in the form of CH_4, but indistinguishable in CO_2. Additionally, the reduced number of macroinvertebrates in treated FPMs may be an additional source of C source (as detritus) to the total C-pool in the treated FPMs. Dead organisms could be an addition of labile C to aquatic systems where Bti is applied. Furthermore, in many floodplains that are treated with Bti, dead mosquito detritus could contribute to the C-budget. However, in the FPMs no changes in sediment C (which is the largest contribution to C-pool) were detected. Under field conditions in the FPMs, the variability of processes that control C biogeochemistry may have covered a potential effect of treatment on the organic C-pool in sediment. Although the contribution of Bti treatment to the system level C budget in the treated FPMs is rather weak, its effect on the C components through chironomid reduction persists over an extended period. The mechanisms behind the long-lasting effect of Bti on CH_4 emissions in the FPMs remain an open question. In a microcosm study, a higher dose of Bti had long-lasting effects on the composition of microbial communities in the water column (Duguma et al., 2015). Additionally, upon its application, Bti spores can persistently recycle and regenerate over an extended period of at least four years in wetlands before the spores

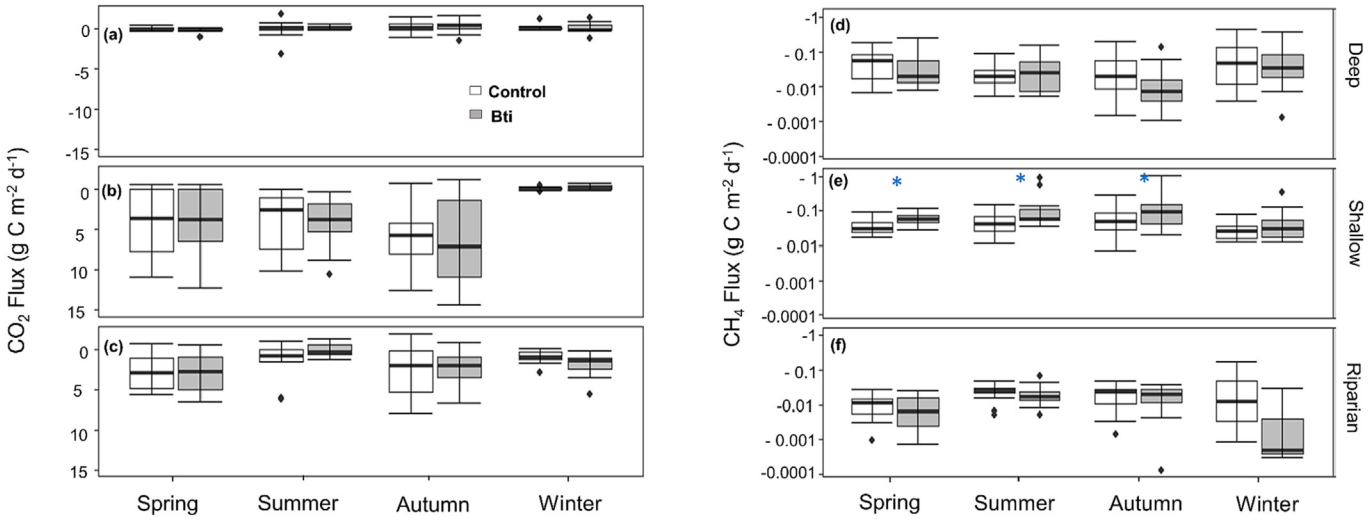

Fig. 4. Box plots of CO_2 flux in g C m^{-2} d^{-1} from the (a) deep, (b) shallow, and (c) riparian zones of control (white boxes) and treated FPMs (grey boxes) at different seasons. Box plots of CH_4 flux in g C m^{-2} d^{-1} from the (d) deep, (e) shallow transition, and (f) riparian zones of control FPMs and treated FPMs at different seasons. The asterisk indicates significant differences ($p \leq 0.05$) between the control and treatment ($N = 6$). The lower and upper limits of the boxes represent the 25th and 75th percentiles, respectively; with the horizontal line inside the box as the median, and lower and upper whiskers show the 10th and 90th percentiles, respectively. Note that filled black circles are data falling outside the 10th and 90th percentiles. The y-axis of d, e, and f are log-scaled.

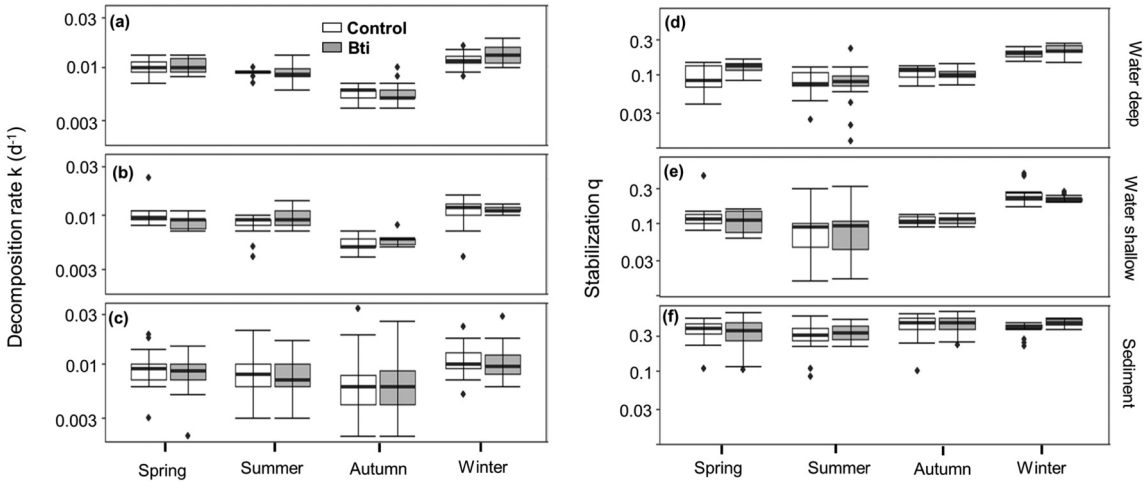

Fig. 5. Box plots of decomposition rates (k) in the (a) water column of the deep zone, the (b) shallow zone, and (c) in the sediment of the deep, shallow transition, and riparian zones of control FPMs (white boxes) and treated FPMs (grey boxes) at different seasons (teabag index) ($N = 6$). Box plots of stabilization factors (q) for tea decomposition in the (d) water column of the deep zone, (e) shallow zone, and (f) in the sediment of the deep, shallow, and riparian zones. The lower and upper limits of the boxes represent the 25th and 75th percentiles, respectively; with the horizontal line inside the box as the median, and lower and upper whiskers show the 10th and 90th percentiles, respectively. Note that filled black circles are data falling outside the 10th and 90th percentiles. The y-axes are log-scaled.

degenerate (Poulin et al., 2022). Such a persistent effect of Bti could have resulted in the long-term seasonal effect observed on the C-budget components in the FPMs. Given the important role of inland waters as the largest natural source of CH_4 (Peacock et al., 2021; Rosentreter et al., 2021) and the widespread use of Bti for mosquito control, follow-up studies are urgently needed.

5. Conclusions

Our study is the first to investigate the potential effects of the mosquito control biocide Bti on C dynamics in shallow lentic ecosystems. In the same replicated floodplain pond mesocosms (FPMs), we previously found that CH_4 flux increased significantly in response to the application of Bti. Here we see no additional effect on the seasonal C-budget, except for a trend towards lower porewater DOC in treated FPMs. These were potentially caused by non-target adverse effects of Bti on chironomid larvae, which can affect C cycling by both trophic and non-trophic interactions. The findings highlight the need to improve current knowledge on the role of benthic invertebrates in the regulation of C cycling in aquatic ecosystems under environmental conditions, as well as under the influence of biological and anthropogenic stressors. Our study provides empirical evidence that suggests a causal relationship between the reduction of chironomid abundance by Bti and C biogeochemistry at the ecosystem scale. However, these findings are limited to observation and call for more detailed studies under controlled environmental conditions to reveal the underlying process.

CRediT authorship contribution statement

Caroline Ganglo: Conceptualization, Experimental design, Methodology, Data collection, Data analysis, Writing; **Clara Mendoza-Lera**: Conceptualization, Experimental design, Methodology, Data analysis, Writing; **Alessandro Manfrin**: Methodology, Data analysis, Writing; **Rossano Bolpagni**: Methodology, Writing; **Verena Gerstle**: Experimental design, Data collection, Writing; **Sara Kolbenschlag**: Experimental design, Data collection, Writing; **Eric Bollinger**: Data collection, Writing; **Ralf Schulz**: Writing; **Andreas Lorke**: Conceptualization, Experimental design, Methodology, Data analysis, Writing.

Data availability

Data will be made available on request.

Declaration of competing interest

The authors declare no conflict of interest either financially or personally related to this work.

Acknowledgments

This work was financially supported by the Deutsche Forschungsgemeinschaft (DFG, German Research Foundation) – 326210499/GRK2360, Systemlink. We acknowledge the support of EERES for access to facilities and data. We also acknowledge the support of Christoph Bors, Housam Ismaeli, Oluwafunke Fagbule, Sandhya Magesh, Eliana Bohorquez Bedoya, Mayra Ishikawa, Gerrit Rau, Lorenzo Rovelli, Lediane Marcon, Anja Knäbel, Simone von Schlichtegroll, and Viktor Baranov through the discussion and implementation of this experiment. We further thank Thomas Mehner who provided valuable support during the conceptualization of the manuscript. We thank Jay Gan for editing this work. We further thank the two anonymous reviewers for their comments that improved our manuscript.

Appendix A. Supplementary data

Supplementary data to this article can be found online at https://doi.org/10.1016/j.scitotenv.2023.161978.

References

Baranov, V., Lewandowski, J., Krause, S., 2016a. Bioturbation enhances the aerobic respiration of lake sediments in warming lakes. Biol. Lett. 12 (8), 8–11. https://doi.org/10.1098/rsbl.2016.0448.

Baranov, V., Lewandowski, J., Romeijn, P., Singer, G., Krause, S., 2016b. Effects of bioirrigation of non-biting midges (Diptera: Chironomidae) on lake sediment respiration. Sci. Rep. 6 (January), 1–10. https://doi.org/10.1038/srep27329.

Becker, N., 2006. Biological control mosquitoes: management of the upper rhine mosquito population as a model programme. In: Eilenberg, J., Hokkanen, H.M.T. (Eds.), An Ecological and Societal Approach to Biological Control. 2. Springer, pp. 227–245. https://doi.org/10.1007/978-1-4020-4401-4_11.

Benelli, S., Bartoli, M., 2021. Worms and submersed macrophytes reduce methane release and increase nutrient removal in organic sediments. https://doi.org/10.1002/lol2.10207.

Benjamini, Y., Hochberg, Y., 1995. Controlling the false discovery rate: a practical and powerful approach to multiple testing. J. R. Stat. Soc. Ser. B Methodol. 57 (1), 289–300. https://doi.org/10.1111/j.2517-6161.1995.tb02031.x.

Boisvert, M., Boisvert, J., 2000. Effects of Bacillus thuringiensis var. Israelensis on target and nontarget organisms: a review of laboratory and field experiments. Biocontrol Sci. Technol. 10 (5), 517–561. https://doi.org/10.1080/095831500750016361.

Booth, M.T., Urbanic, M., Wang, X., Beaulieu, J.J., 2021. Bioturbation frequency alters methane emissions from reservoir sediments. Science of the Total Environment 789, 1–9. https://doi.org/10.1016/j.scitotenv.2021.148033.

Brühl, C.A., Després, L., Frör, O., Patil, C.D., Poulin, B., Tetreau, G., Allgeier, S., 2020. Environmental and socioeconomic effects of mosquito control in Europe using the biocide Bacillus thuringiensis subsp. israelensis (Bti). Science of the Total Environment 724, 1–16. https://doi.org/10.1016/j.scitotenv.2020.137800.

Cadotte, T.A.S.M.W., Williams, D.D., 2014. HowHydroperiod and Species Richness Affect the Balance of Resource Flows AcrossAquatic-terrestrial Habitats, pp. 131–143. https://doi.org/10.1007/s00027-013-0320-9.

Colina, M., Meerhoff, M., Pérez, G., Veraart, A.J., Bodelier, P., Horst, A.Van Der, Kosten, S., 2021. Trophic and non-trophic effects of fish and macroinvertebrates on carbon emissions. Freshwater Biology 66 (9), 1–15. https://doi.org/10.1111/fwb.13795.

Covich, A.P., Palmer, M.A., Crowl, T.A., 1999. The role of benthic invertebrate species in freshwater ecosystems: zoobenthic species influence energy flows and nutrient cycling. Bioscience 49 (2), 119–127. https://doi.org/10.2307/1313537.

De Haas, E.M., Wagner, C., Koelmans, A.A., Kraak, M.H.S., Admiraal, W., 2006. Habitat selection by chironomid larvae: fast growth requires fast food. J. Anim. Ecol. 75 (1), 148–155. https://doi.org/10.1111/j.1365-2656.2005.01030.x.

Downing, J.A., 2010. Emerging global role of small lakes and ponds: little things mean a lot. Limnetica 29 (1), 9–24. https://doi.org/10.23818/limn.29.02.

Duguma, D., Hall, M.W., Rugman-Jones, P., Stouthamer, R., Neufeld, J.D., Walton, W.E., 2015. Microbial communities and nutrient dynamics in experimental microcosms are altered after the application of a high dose of bti. J. Appl. Ecol. 52 (3), 763–773. https://doi.org/10.1111/1365-2664.12422.

Fan, J., Zhong, H., Harris, W., Yu, G., Wang, S., Hu, Z., Yue, Y., 2008. Carbon storage in the grasslands of China based on field measurements of above- and below-ground biomass. Clim. Chang. 86 (3–4), 375–396. https://doi.org/10.1007/s10584-007-9316-6.

Frouz, J., Matěna, J., Ali, A., 2003. Survival strategies of chironomids (diptera : chironomidae) living in temporary habitats : a review. Eur. J. Entomol. 100, 459–465. https://doi.org/10.14411/eje.2003.069.

Ganglo, C., Manfrin, A., Mendoza-Lera, C., Lorke, A., 2022. Biocide treatment for mosquito control increases CH4 emissions in floodplain pond mesocosms. Front. Water 10. https://doi.org/10.3389/frwa.2022.996898.

Gerstle, V., Manfrin, A., Kolbenschlag, S., Gerken, M., Islam, A.S.M.M.U., Entling, M.H., Brühl, C.A., 2022. Benthic macroinvertebrate community shifts based on bti-induced chironomid reduction also decrease odonata emergence. Environ. Pollut. 316 (P1), 120488. https://doi.org/10.1016/j.envpol.2022.120488.

Hodkinson, I.D., Williams, K.A., 1980. Tube formation and distribution of Chironomus plumosus L. (Diptera : Chironomidae) in a eutrophic woodland pond. Chironomidae https://doi.org/10.1016/b978-0-08-025889-8.50051-9.

Holgerson, M.A., 2015. Drivers of carbon dioxide and methane supersaturation in small, temporary ponds. Biogeochemistry 124 (1–3), 305–318. https://doi.org/10.1007/s10533-015-0099-y.

Holgerson, M.A., Raymond, P.A., 2016. Large contribution to inland water CO2 and CH4 emissions from very small ponds. Nat. Geosci. 9 (3), 222–226. https://doi.org/10.1038/ngeo2654.

Hölker, F., Vanni, M.J., Kuiper, J.J., Meile, C., Grossart, H.P., Stief, P., Lewandowski, J., 2015. Tube-dwelling invertebrates: tiny ecosystem engineers have large effects in lake ecosystems. Ecol. Monogr. 85 (3), 333–351. https://doi.org/10.1890/14-1160.1.

International Hydropower Association (IHA), 2010. GHG Measurement Guidelines for Freshwater Reservoirs.

Jackson, J.M., Mclachlan, A.J., 1991. Rain-pools on peat moorland as island habitats for midge larvae. Hydrobiologia 209, 59–65.

Kajan, R., Frenzel, P., 1999. The effect of chironomid larvae on production, oxidation and fluxes of methane in a flooded rice soil. FEMS Microbiol. Ecol. 28 (2), 121–129. https://doi.org/10.1016/S0168-6496(98)00097-X.

Keuskamp, J.A., Dingemans, B.J.J., Lehtinen, T., Sarneel, J.M., Hefting, M.M., 2013. Tea bag index: a novel approach to collect uniform decomposition data across ecosystems. Methods Ecol. Evol. 4 (11), 1070–1075. https://doi.org/10.1111/2041-210X.12097.

Kolbenschlag, S., Gerstle, V., Eberhardt, J., Bollinger, E., Schulz, R., Brühl, C.A., Bundschuh, M., 2023. A temporal perspective of aquatic subsidy: bti affects the emergence of chironomidae. Ecotoxicol. Environ. Saf. 250, 114503. https://doi.org/10.1016/j.ecoenv.2023.114503.

Leeper, D.A., Taylor, B.E., 1998. Insect emergence from a South Carolina (USA) temporary wetland pond, with emphasis on the chironomidae (diptera). Retrieved fromChicago J. 17 (1), 54–72.. http://www.jstor.org/stable/1468051.

Mclachlan, A.J., Cantrell, M.A., 1976. Sediment development and its influence on the distribution and tube structure of *Chironomus plumosus* L. (Chironomidae, Diptera) in a new impoundment. Freshw. Biol. 6 (5), 437–443. https://doi.org/10.1111/j.1365-2427.1976.tb01632.x.

Murniati, E., Gross, D., Herlina, H., Hancke, K., Lorke, A., 2017. Effects of bioirrigation on the spatial and temporal dynamics of oxygen above the sediment-water interface. Freshw. Sci. 36 (4), 784–795. https://doi.org/10.1086/694854.

Nogaro, G., Steinman, A.D., 2014. Influence of ecosystem engineers on ecosystem processes is mediated by lake sediment properties. Oikos 123 (4), 500–512. https://doi.org/10.1111/j.1600-0706.2013.00978.x.

Oliveira Junior, E.S., Temmink, R.J.M., Buhler, B.F., Souza, R.M., Resende, N., Spanings, T., Kosten, S., 2019. Benthivorous fish bioturbation reduces methane emissions, but increases total greenhouse gas emissions. Freshw. Biol. 64 (1), 197–207. https://doi.org/10.1111/fwb.13209.

Peacock, M., Audet, J., Bastviken, D., Cook, S., Evans, C.D., Grinham, A., Futter, M.N., 2021. Small artificial waterbodies are widespread and persistent emitters of methane and carbon dioxide. Glob. Chang. Biol. 27 (20), 5109–5123. https://doi.org/10.1111/gcb.15762.

Pinheiro, J., Bates, D., DebRoy, S., Sarkar, D., 2022. nlme: Linear and Nonlinear Mixed Effects Models. https://CRAN.R-project.org/package=nlme.

Poulin, B., Lefebvre, G., Hilaire, S., Després, L., 2022. Long-term persistence and recycling of Bacillus thuringiensis israelensis spores in wetlands sprayed for mosquito control. Ecotoxicol. Environ. Saf. 243 (August). https://doi.org/10.1016/j.ecoenv.2022.114004.

R Core Team, 2013. R: A Language and Environment for Statistical Computing.

Rosentreter, J.A., Borges, A.V., Deemer, B.R., Holgerson, M.A., Liu, S., Song, C., Eyre, B.D., 2021. Half of global methane emissions come from highly variable aquatic ecosystem sources. Nat. Geosci. 14, 225–230. https://doi.org/10.1038/s41561-021-00715-2.

Sobek, S., Söderbäck, B., Karlsson, S., Andersson, E., Brunberg, A.K., 2006. A carbon budget of a small humic lake: an example of the importance of lakes for organic matter cycling in boreal catchments. Ambio 35 (8), 469–475. https://doi.org/10.1579/0044-7447(2006)35[469:ACBOAS]2.0.CO;2.

Stehle, S., Manfrin, A., Feckler, A., Graf, T., Joschko, T.J., Jupke, J., Schulz, R., 2022. Structural and functional development of twelve newly established floodplain pond mesocosms. Ecol. Evol. 12 (3), 1–15. https://doi.org/10.1002/ece3.8674.

Taylor, S., Gilbert, P.J., Cooke, D.A., Deary, M.E., Jeffries, M.J., 2019. High carbon burial rates by small ponds in the landscape. Front. Ecol. Environ. 17 (1), 25–31. https://doi.org/10.1002/fee.1988.

Vadeboncoeur, Y., Vander Zanden, M.J., Lodge, D.M., 2002. Putting the lake back together: reintegrating benthic pathways into lake food web models. Bioscience 52 (1), 44–54. https://doi.org/10.1641/0006-3568(2002)052[0044:PTLBTR]2.0.CO;2.

Zuur, A.F., Ieno, E.N., Elphick, C.S., 2010. A protocol for data exploration to avoid common statistical problems. Methods Ecol. Evol. 1 (1), 3–14. https://doi.org/10.1111/j.2041-210x.2009.00001.x.

Supporting information for:

Does biocide treatment for mosquito control alter carbon dynamics in floodplain ponds?

Caroline Ganglo[a1], Clara Mendoza-Lera[a], Alessandro Manfrin[a], Rossano Bolpagni[b], Verena Gerstle[a], Sara Kolbenschlag[a], Eric Bollinger[a], Ralf Schulz[a], and Andreas Lorke[a]

[a]RPTU Kaiserslautern-Landau, Institute for Environmental Sciences, Fortstr. 7, D-76829 Landau, Germany

[b]University of Parma, Department of Chemistry, Life Sciences and Environmental Sustainability, Parco Area delle Scienze 33/A, 43124 Parma, Italy

[1]Email: carolineganglo20@gmail.com

Present address: University of Kairserslautern-Landau, 76829, Landau, Germany

Science of the Total Environment

26 pages, 3435 words, 5 Tables, 2 Figures

2. Methods

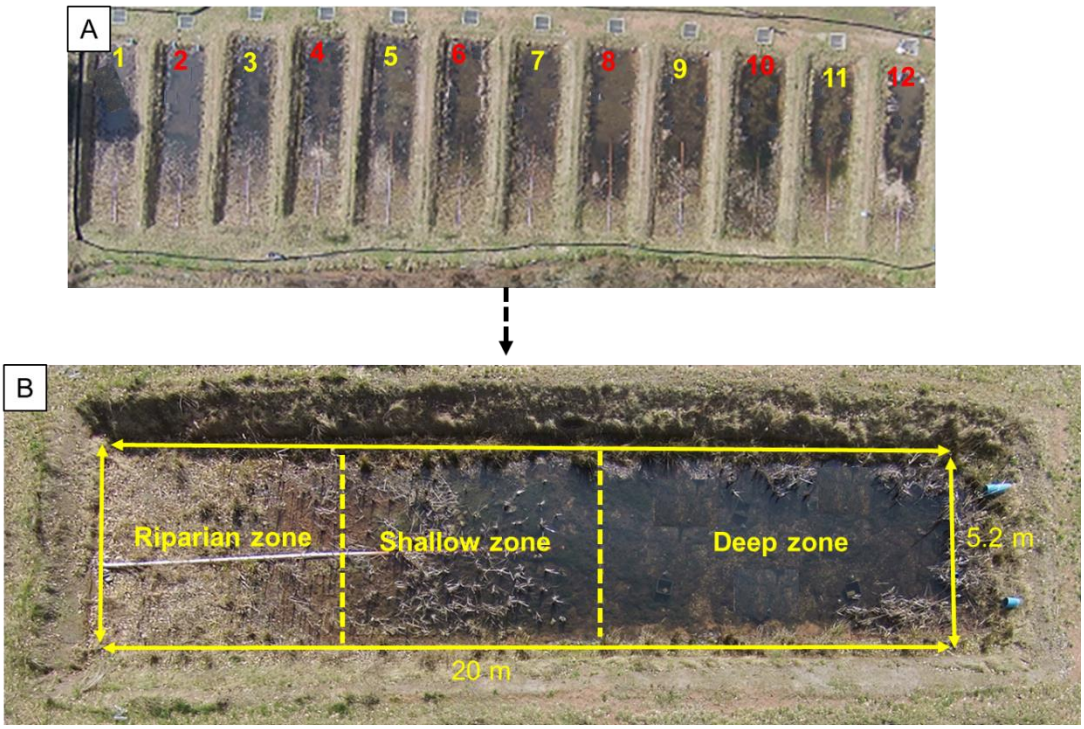

SI Figure S1 Areal image of the 12 floodplain pond mesocosms (FPMs) (panel A), with ponds treated with Bti labeled with yellow numbers and control ones labeled in red. Detailed view of a single pond (panel B) with the riparian and deep zones, and the shallow zone (transition between the deep and riparian zone) delimitated by yellow dashed lines. The width and length of the ponds are 5.2 m and 20 m respectively (images from Ganglo et al. 2022).

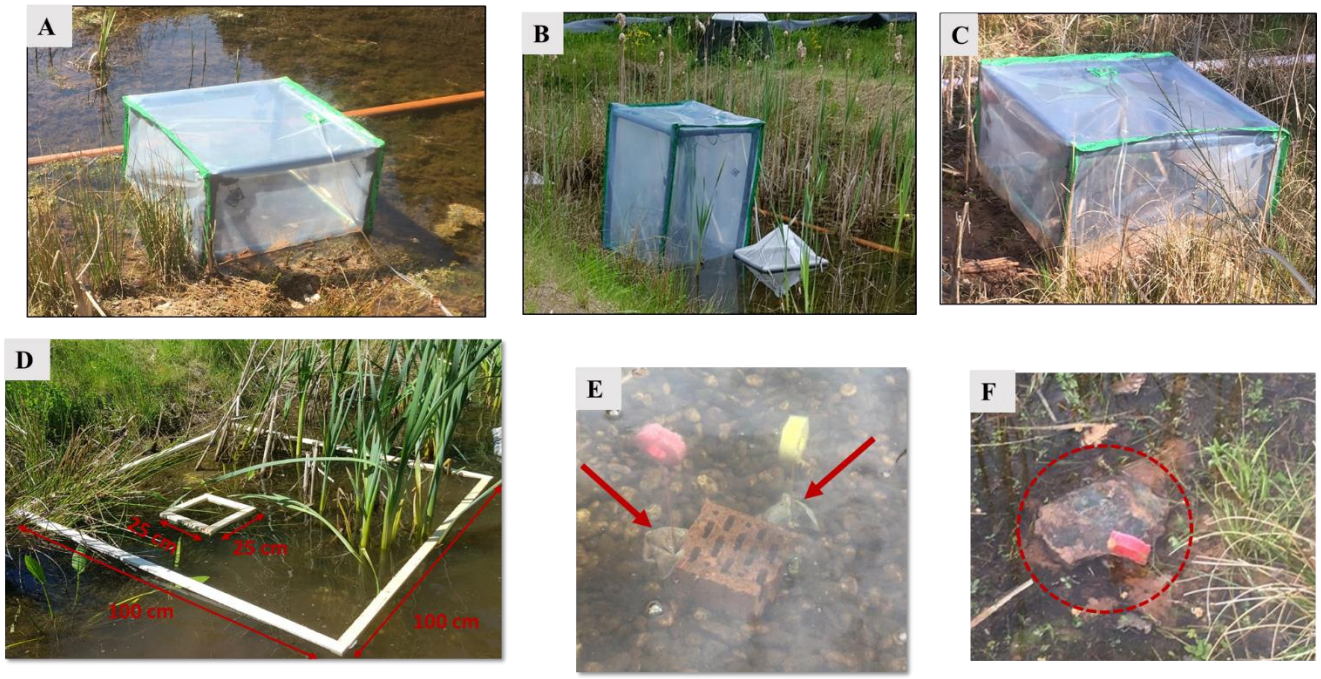

SI Figure S2 Transparent chambers used for CH_4 and CO_2 flux measurements in the deep zone (**A**), the shallow transition zone (**B**) (Ganglo et al. 2022), and the riparian zone (**C**) of each FPM. (**D**) Image of the frames used during plant biomass sampling (100 cm quadrats) and submerged macrophyte and filamentous algae sampling (25 cm). Teabags deployed in the water column (**E**), and in the sediment (**F**) (source C. Ganglo).

SI Table S1: Schedule for flooding and Bti application.

Date	Flooding/ Bti	Water level (m)
11 April 2020	**Flooding**	**0.3 → 0.4**
12 April 2020	**Flooding**	**0.4 → 0.5**
14 April 2020	**1st Bti application**	**0.5**
21 April 2020	**Drawdown**	**0.5 → 0.4**
22 April 2020	**Drawdown**	**0.4 → 0.3**
02 May 2020	**Flooding,**	**0.3 → 0.4**
03 May 2020	**Flooding,**	**0.4 → 0.5**
04 May 2020	**2nd Bti application**	**0.5**
12 May 2020	**Drawdown**	**0.5 → 0.4**
13 May 2020	**Drawdown**	**0.4 → 0.3**
23 May 2020	**Flooding**	**0.3 → 0.4**
24 May 2020	**Flooding**	**0.4 → 0.5**
25 May 2020	**3rd Bti application**	**0.5**
02 June 2020	**Drawdown**	**0.5 → 0.4**
03 June 2020	**Drawdown**	**0.4 → 0.3**

SI Table S2: Sampling schedule of each C pools and fluxes component, and transformation in the three zones of the FPMs (deep, shallow transition and riparian zones). References refer to data taken from previous publications.

Sampling date	Time during & after Bti application	Sample number FPMs	Season	Deep zone	Shallow transition zone	Riparian zone	References
			C-pools				
18-19 May 2020	After 2nd application	6 × 2 (emerged & submerged) per zone	Spring				This study
17 August 2020	After 3rd application	6 × 2 per zone	Summer	Plant biomass	Plant biomass	Plant biomass	
16-17 November 2020		6 × 2 per zone	Autumn				
22 February 2021		6 × 2 per zone	Winter				
30 April – 01 May 2020	After 2nd application	6 × 2 per zone	Spring	Sediment	Sediment organic C	Sediment	This study
07 July 2020	After 3rd application	6 × 2 per zone	Summer	organic C		organic C	
17 September 2020		6 × 2 per zone	Autumn				
17 December 2020		6 × 2 per zone	Winter				
10-13 June 2020	After 3rd application		Summer	Macroinvertebrates		-	Gerstle et al. (2022)
14 & 24 April 2020	During & after 1st application	6 per sampling date	Spring			-	This study
06 & 20 May 2020	During 2nd & after application	6 per sampling date	Spring	Surface water DOC taken at the border between deep and shallow transition, assuming horizontal homogeneity			
05 June 2020		6	Summer				
17 July 2020		6	Summer				
04 &17 November 2020		6	Autumn				
11 February 2021		6	Winter				

Sampling date	Time during & after Bti application	Sample number FPMs	Season	Deep zone	Shallow transition zone	Riparian zone	References
20 May 2020	After 2nd application	6	Spring	Porewater DOC sampled in the shallow transition zone assuming horizontal homogeneity		-	This study
06 August 2020	After 3rd application	6	Summer				
03 November 2020		6	Autumn				
29 March 2021		6	Winter				
20 & 27 April 2020	After 1st application	6 per sampling date & per zone	Spring	Dissolved CH_4	Dissolved CH_4	-	Ganglo et al (2022)
14-16 & 28-29 May 2020	After 2nd & 3rd application	6 per sampling date & per zone	Spring				
08 June 2020	After 3rd application	6 per zone	Summer				
21 & 22 July 2020		6 per sampling date & per zone	Summer				
21 September 2020		6 per zone	Autumn				
09 November 2020		6 per zone	Autumn				
09 January 2021		6 per zone	Winter				
21 & 23 March 2021		6 per zone	Winter				
14-16 & 28-29 May 2020	After 2nd 3rd & application	6 per sampling date & per zone	Spring	Dissolved CO_2	Dissolved CO_2	-	This study
08 June 2020	After 3rd application	6 per zone	Summer				
21 & 22 July 2020		6 per zone	Summer				

Sampling date	Time during & after Bti application	Sample number FPMs	Season	Deep zone	Shallow transition zone	Riparian zone	References
21 September 2020		6 per zone	Autumn				
09 November 2020		6 per zone	Autumn				
09 January 2021		6 per zone	Winter				
21 & 23 March 2021		6 per zone	Winter				
			C-fluxes				
11 & 23 May 2020	During & after 2nd application	6 per sampling date	Spring				This study
05 &17 June 2020	After 3rd application	6 per sampling date	Summer				
14 & 17 July 2020		6 per sampling date	Summer				
09 October 2020		6	Autumn		Wet deposition DOC		
02, 17 & 27 November 2020		6 per sampling date	Autumn				
01, 08 & 17 December 2021		6 per sampling date	Winter				
04 January 2020		6 per sampling date	Winter				
02 & 17 February 2021		6 per sampling date	Winter				
28, 29 April 2020	After 1st application	6 per zone	Spring	CH_4 & CO_2 fluxes	CH_4 & CO_2 fluxes	CH_4 & CO_2 fluxes	See Ganglo et al. (2022) for CH_4 in the deep
14-16 May 2020	After 2nd application	6 per zone	Spring				
08-09 June 2020	After 3rd application	6 per zone	Summer				

Sampling date	Time during & after Bti application	Sample number FPMs	Season	Deep zone	Shallow transition zone	Riparian zone	References
06-08 & 21 July 2021		6 per sampling date & per zone	Summer				and shallow transition zones
21-22 & 24 September 2020	After 3rd application	6 per sampling date & per zone	Autumn				
09 November 2020		6 per zone	Autumn				
09 January 2021		6 per zone	Winter				
20-21 March 2021		6 per zone	Winter				
15 April 2020-31 July 2020	During and after the 3 replicated Bti application		Spring & summer	Emerging insects	Emerging insects	-	(Kolbenschlag et al. 2023)
C-transformation: organic matter decomposition							
01 May - 30 June 2020	During and after 2nd application	3 Green tea (GT) + 3 Red tea (RT) per site (water column of deep & shallow zones & sediment of all three zones)	Spring	Tea bag incubation	Tea bag incubation	Tea bag incubation	This study
02 July - 09 September 2020	After 3rd application	3 (GT) + 3 (RT) per site	Summer				
17 September -17 December 2020		3 (GT) + 3 (RT) per site	Autumn				

Sampling date	Time during & after Bti application	Sample number FPMs	Season	Deep zone	Shallow transition zone	Riparian zone	References
17 December 2020 - 22 January 2021		3 (GT) + 3 (RT) per site	Winter				

2.4.3 Tea bag index

The stabilization factor (q) and the decomposition rate (k in d^{-1}) of tea were calculated using the two-phase decomposition model described in Keuskamp et al (2013):

$$q = 1 - \frac{1}{H_g}\left(1 - \frac{m_{f,g}}{m_{i,g}}\right) \quad \text{Eq. S1}$$

$$a_r = H_r(1 - q) \quad \text{Eq. S2}$$

$$k = -\frac{1}{t_I}\ln\left(\frac{1}{a_r}\left(\frac{m_{f,r}}{m_{i,r}} + a_r - 1\right)\right) \quad \text{Eq. S3}$$

a_r (-) is the decomposable fraction of rooibos tea, $m_{f,r}$ and $m_{i,r}$ (g) are the final and initial dry weight of rooibos tea, $m_{f,g}$ and $m_{i,g}$ (g) are those of green tea. H_r (0.552 g g^{-1}) and H_g (0.842 g g^{-1}) are the hydrolysable fraction of rooibos tea and green tea, respectively. t_I (d) is the incubation time and q the stabilization factor.

3. Results

SI Table S3: Linear mixed effect model selection using likelihood ratio tests (LRT) against reduced models: interactions among individual factors (:), effect of individual factor and significant factor of the final model on plant C biomass, sediment organic C, Porewater DOC, Surface water DOC, Dissolved CO_2, tea bag decomposition rate and stabilization factor, CO_2 and CH_4 fluxes. Numbers marked in bold highlight significant effects ($p \leq 0.05$).

Variables	R^2 marginal Full/Final	Factors	Statistical test	*p*-value
	Model Selection (Likelihood ratio test, LRT)		LRT	
Plant C biomass	0.11	Zone : Season : Treatment	0.25	0.99
		Zone : Season	12.46	0.06
		Zone : Treatment	0.57	0.75
		Treatment : Season	0.51	0.92
		Treatment	0.19	0.66
	Final model		F-stat	
	0.09	**Zone**	**$F_{2,437} = 40.22$**	**<.0001**
		Season	**$F_{3,437} = 6.62$**	**0.0002**
Sediment organic C	0.51	Zone : Season : Treatment	7.71	0.26

Variables	R^2 marginal Full/Final	Factors	Statistical test	*p*-value
		Zone : Season	12.11	0.06
		Zone : Treatment	1.72	0.42
		Treatment : Season	0.48	0.92
		Treatment	0.14	0.71
	Final model		*F*-stat	
	0.48	**Zone**	$\mathbf{F_{2,127} = 53.76}$	**<.0001**
		Season	$\mathbf{F_{3,127} = 3.86}$	**0.01**
Porewater DOC	Model Selection (LRT)		LRT	
	0.68	Season: Treatment	5.51	0.14
		Treatment	1.80	0.18
	Final model		*F*-stat	
	0.65	**Season**	$\mathbf{F_{3,33} = 36.41}$	**<.0001**
Surface water DOC	Model Selection (LRT)		LRT	
	0.26	Treatment	4.57	0.21
	Final model		*F*-stat	
	0.25	**Season**	$\mathbf{F_{3,93} = 24.68}$	**<.0001**
Dissolved CO_2	Model Selection (LRT)		LRT	
	0.15	Treatment: Season	1.89	0.59
		Treatment	0.05	0.82

Variables	R^2 marginal Full/Final	Factors	Statistical test	*p*-value
	Final model		*F*-stat	
	0.15	**Season**	$\boldsymbol{F_{3, 274} = 15.73}$	**<.0001**
Organic matter decomposition	Model Selection (LRT)		LRT	
rate	0.05	Season: Treatment: Zone	0.78	0.99
		Season: Treatment	0.85	0.84
		Treatment: Zone	0.15	0.93
		Site: Season	0.93	0.33
		Zone	0.004	0.95
		Treatment	0.04	0.98
	Final model		*F*-stat	
	0.04	**Season**	$\boldsymbol{F_{3, 544} = 17.31}$	**<.0001**
Stabilization factor	Model Selection (LRT)		LRT	
	0.77	Treatment: Season	4.08	0.25
		Treatment: Zone	2.30	0.32
		Treatment	0.19	0.66
	Final model		*F*-stat	
	0.77	**Season: Treatment: Zone**	$\boldsymbol{F_{3, 525} = 3.15}$	**0.005**
		Season: Zone	$\boldsymbol{F_{3, 525} = 10.40}$	**<.0001**
		Zone	$\boldsymbol{F_{2, 525} = 381.32}$	**<.0001**

Variables	R^2 marginal Full/Final	Factors	Statistical test	*p*-value
		Season	**$F_{3, 525}$ =49.39**	**<.0001**
CO_2 flux	Model Selection (LRT)		LRT	
	0.33	Zone : Season : Treatment	2.22	0.90
		Zone : Treatment	3.84	0.15
		Treatment : Season	2.35	0.50
		Treatment	0.07	0.79
	Final model		*F*-stat	
	0.32	**Zone**	**$F_{2, 341}$= 51.42**	**<.0001**
		Season	**$F_{3,341}$= 9.84**	**<.0001**
		Zone: Season	**$F_{6, 341}$= 6.67**	**<.0001**
CH_4 flux	Model Selection (LRT)		LRT	
	0.14	Treatment	1.06	0.79
	Final model		*F*-stat	
	0.13	**Season**	**$F_{3, 106}$= 10.27**	**<.0001**

SI Table S4: Post-hoc pairwise comparisons of factors or interaction on plant C biomass C, sediment organic C, porewater DOC, surface water DOC, dissolved CO_2, organic matter decomposition rate and stabilization factor, CO_2 and CH_4 fluxes using linear model (lm)/ linear mixed effect model (lme). Estimate represents the mean difference between pairwise factors and t-ratio is the ratio of Estimate to standard error. Statistically significant P values are printed in bold and P adjusted (adj) correct for multiple factor statistical significance.

Variables	Contrast					
Plant C biomass	Pairwise structure	Pairwise (lme)	Estimate	t.ratio	p	p-adj
	Zone	Deep–Shallow	0.03	0.22	0.8298	0.8298
		Shallow -Riparian	**-0.71**	**-3.24**	**0.0015**	**0.0022**
		Riparian -Deep	**-0.76**	**-3.66**	**4e-04**	**0.0012**
	Season	Summer – Spring	-0.21	-0.85	0.3971	0.4765
		Autumn – Spring	-0.34	-1.39	0.16	0.26
		Winter – Spring	-0.33	-1.36	0.17	0.26
		Autumn – Summer	**-0.56**	**-2.54**	**0.01**	**0.04**
		Winter – Summer	**-0.55**	**-2.47**	**0.01**	**0.04**
		Winter – Autumn	-0.003	-0.01	0.98	0.98
Sediment organic C		Pairwise (lme)	Estimate	t.ratio	p	p-adj
	Zone	Deep–Shallow	-0.15	-1.61	0.1154	0.1154
		Deep-Riparian	**-0.62**	**-7.40**	**<0.0001**	**<0.0001**

Variables	Contrast					
		Riparian -Deep	**0.51**	**4.53**	**1e-04**	**0.00015**
	Season	Summer – Spring	-0.047	-0.746	0.548	0.878
		Autumn – Spring	0.005	0.078	0.938	1.000
		Winter – Spring	**-0.188**	**-2.673**	**0.026**	**0.042**
		Autumn – Summer	0.052	0.832	0.548	0.839
		Winter – Summer	-0.142	-2.049	0.085	0.176
		Winter – Autumn	**-0.194**	**-3.093**	**0.015**	**0.013**
Porewater DOC		Pairwise (lme)	Estimate	t.ratio	p	p-adj
	Season	**Summer – Spring**	**-0.46**	**-3.75**	**0.0038**	**0.0063**
		Autumn – Spring	**0.278**	**2.920**	**0.0153**	**0.01836**
		Winter – Spring	**-0.672**	**-7.54**	**<0.0001**	**<0.0001**
		Autumn – Summer	**0.064**	**0.668**	**0.5192**	**0.5192**
		Winter – Summer	**-0.329**	**-3.686**	**0.0042**	**0.0063**
		Winter – Autumn	**-0.603**	**-5.903**	**2e-04**	**6e-04**
Surface water DOC		Contrast (lm)	Estimate	t.ratio	p	p-adj
	Season	Summer – Spring	-0.103	-1.53	0.1561	0.2092
		Autumn – Spring	**-0.206**	**-2.584**	**0.0272**	**0.0816**
		Winter – Spring	0.070	0.786	0.4501	0.4501
		Autumn – Summer	**-0.270**	**-3.55**	**0.0053**	**0.0318**
		Winter – Summer	-0.134	-2.15	0.0573	0.4501

Variables	Contrast					
		Winter – Autumn	0.10	1.46	0.1743	0.2092
Dissolved CO_2		Pairwise (lme)	Estimate	t.ratio	p	p-adj
	Season	Summer – Spring	-0.08	-1.69	0.09	0.11
		Autumn – Spring	**-0.23**	**-6.91**	**<0.0001**	**<0.0001**
		Winter – Spring	**0.15**	**3.33**	**0.0015**	**0.003**
		Autumn – Summer	**-0.18**	**-4.99**	**<0.0001**	**<0.0001**
		Winter – Summer	**-0.11**	**-2.45**	**0.02**	**0.03**
		Winter – Autumn	0.05	1.17	0.23	0.23
Organic matter		Pairwise (lme)	Estimate	t.ratio	p	p-adj
decomposition	Season	Summer – Spring	-0.0007	-1.54	0.1247	0.1247
rate						
		Autumn – Spring	**-0.0028**	**-6.5279**	**<0.0001**	**<0.0001**
		Winter – Spring	**0.00257**	**4.274**	**<0.0001**	**<0.0001**
		Autumn – Summer	**-0.00226**	**-5.20**	**<0.0001**	**<0.0001**
		Winter – Summer	**-0.0031**	**-5.188**	**<0.0001**	**<0.0001**
		Winter – Autumn	**0.0051**	**6.478**	**<0.0001**	**<0.0001**
Stabilization		Pairwise (lme)	Estimate	t.ratio	p	p-adj
factor	Season/ Zone	Autumn Deep - Spring Deep	-0.001	-0.071	0.970	1.000
		Autumn Deep - Summer Deep	0.017	1.183	0.285	0.990
		Autumn Deep - Winter Deep	**-0.084**	**-4.890**	**<0.0001**	**<0.0001**
		Autumn Deep - Autumn shallow	0.001	0.056	0.970	1.000

Variables	Contrast				
	Autumn Deep - Autumn Sediment	**-0.271**	**-19.066**	**<.0001**	**<.0001**
	Spring Deep - Summer Deep	0.018	1.288	0.242	0.980
	Spring Deep - Winter Deep	**-0.083**	**-5.454**	**<.0001**	**<.0001**
	Spring Deep - Spring Shallow	-0.015	-0.835	0.430	1.000
	Spring Deep - Spring Sediment	**-0.218**	**-15.025**	**<.0001**	**<.0001**
	Spring Deep - Winter Sediment	**-0.247**	**-14.953**	**<.0001**	**<.0001**
	Summer Deep - Winter Deep	**-0.101**	**-6.485**	**<.0001**	**<.0001**
	Summer Deep water - Summer Sediment	**-0.202**	**-14.601**	**<.0001**	**<.0001**
	Winter Deep - Winter Shallow water	-0.030	-1.674	0.118	0.879
	Winter Deep - Winter Sediment	**-0.165**	**-9.512**	**<.0001**	**<.0001**
	Autumn Shallow - Spring Shallow	-0.017	-1.014	0.360	0.997
	Autumn Shallow - Summer Shallow	0.016	0.973	0.370	0.998
	Autumn Shallow - Winter Shallow	**-0.115**	**-6.849**	**<.0001**	**<.0001**
	Autumn Shallow - Autumn Sediment	**-0.272**	**-17.979**	**<.0001**	**<.0001**
	Spring Shallow - Summer Shallow	0.033	2.288	0.030	0.487
	Spring Shallow - Winter Shallow	**-0.098**	**-6.756**	**<.0001**	**<.0001**
	Spring Shallow - Spring Sediment	**-0.203**	**-13.732**	**<.0001**	**<.0001**
	Summer Shallow - Winter Shallow	**-0.130**	**-9.175**	**<.0001**	**<.0001**
	Summer Shallow **- Summer Sediment**	**-0.201**	**-14.545**	**<.0001**	**<.0001**
	Winter Shallow - Winter Sediment	**-0.135**	**-8.355**	**<.0001**	**<.0001**
	Autumn Sediment - Spring Sediment	**0.052**	**6.112**	**<.0001**	**<.0001**

Variables	Contrast					
		Autumn Sediment - Summer Sediment	**0.086**	**10.444**	**<.0001**	**<.0001**
		Autumn Sediment - Winter Sediment	0.022	1.891	0.075	0.765
		Spring Sediment - Summer Sediment	**0.034**	**3.997**	**0.000**	**0.004**
		Spring Sediment - Winter Sediment	-0.030	-2.504	0.017	0.340
		Summer Sediment - Winter Sediment	**-0.064**	**-5.296**	**<.0001**	**<.0001**
	Season/ Zone/ Treatment	Autumn Bti Deep - Spring Bti Deep	-0.015	-0.654	0.603	1.000
		Autumn Bti Deep - Summer Bti Deep	0.017	0.811	0.510	1.000
		Autumn Bti Deep - Winter Bti Deep	**-0.090**	**-3.623**	**0.001**	**0.056**
		Autumn Bti Deep - Autumn Control Deep	0.002	0.099	0.933	1.000
		Autumn Bti Deep - Autumn Bti Shallow	-0.009	-0.326	0.797	1.000
		Autumn Bti Deep - Autumn Bti Sediment	**-0.274**	**-13.728**	**<.0001**	**<.0001**
		Spring Bti Deep - Summer Bti Deep	0.032	1.522	0.172	0.998
		Spring Bti Deep - Winter Bti Deep	**-0.075**	**-3.246**	**0.002**	**0.167**
		Spring Bti Deep - Spring Control Deep	0.030	1.211	0.327	0.999
		Spring Bti Deep - Spring Bti Sediment	**-0.188**	**-8.912**	**<.0001**	**<.0001**
		Summer Bti Deep- Winter Bti Deep	**-0.106**	**-4.600**	**<.0001**	**0.001**
		Summer Bti Deep - Summer Control Deep	0.004	0.166	0.905	1.000
		Summer Bti Deep - Summer Bti Shallow	0.007	0.277	0.827	1.000
		Summer Bti Deep - Summer Bti Sediment	**-0.205**	**-10.343**	**<.0001**	**<.0001**
		Winter Bti Deep - Winter Control Deep	0.015	0.541	0.679	1.000

Variables	Contrast					
		Winter Bti Deep - Winter Bti Shallow	0.004	0.137	0.912	1.000
		Winter Bti Deep - Winter Bti Sediment	**-0.191**	**-7.591**	**<.0001**	**<.0001**
		Autumn Control Deep - Spring Control Deep	0.013	0.554	0.661	1.000
		Autumn Control Deep - Summer Control Deep	0.018	0.862	0.480	1.000
		Autumn Control Deep - Winter Control Deep	**-0.078**	**-3.287**	**0.002**	**0.150**
		Autumn Control Deep - Autumn Control Shallow	0.011	0.424	0.736	1.000
		Spring Control Deep - Summer Control Deep	0.005	0.266	0.833	1.000
		Spring Control Deep - Winter Control Deep	**-0.090**	**-4.597**	**<.0001**	**0.001**
		Spring Control Deep - Spring Control Shallow water	-0.041	-1.738	0.114	0.989
		Spring Control Deep - Spring Control Sediment	**-0.247**	**-12.457**	**<.0001**	**<.0001**
		Summer Control Deep - Summer Control Shallow	-0.008	-0.326	0.797	1.000
		Summer Control Deep - Summer Control Sediment	**-0.199**	**-10.306**	**<.0001**	**<.0001**
		Winter Control Deep - Winter Control Shallow	**-0.063**	**-2.612**	**0.014**	**0.588**
		Winter Control Deep - Winter Control Sediment	**-0.138**	**-5.815**	**<.0001**	**<.0001**
		Autumn Bti Shallow - Spring Bti Shallow	0.005	0.198	0.878	1.000
		Autumn Bti Shallow- Summer Bti Shallow	0.032	1.345	0.238	1.000
		Autumn Bti Shallow - Winter Bti Shallow	**-0.078**	**-3.105**	**0.003**	**0.236**
		Autumn Bti Shallow - Autumn Control Shallow	0.021630	0.801	0.526	1.000
		Autumn Bti Shallow **- Autumn Bti Sediment**	**-0.265**	**-11.976**	**<.0001**	**<.0001**
	Zone	Deep - Shallow	-0.011	-0.973	0.331	0.5943

Variables	Contrast					
		Deep - Sediment	**-0.214**	**-21.898**	**<.0001**	**<.0001**
		Shallow - Sediment	**-0.203**	**-20.754**	**<.0001**	**<.0001**
	Season	Autumn - Spring	0.0114	1.374	0.17	0.5161
		Autumn - Summer	**0.0397**	**5.135**	**<.0001**	**<.0001**
		Autumn - Winter	**-0.0586**	**-6.583**	**<.0001**	**<.0001**
		Spring - Summer	**0.0284**	**3.886**	**0.0001**	**0.0007**
		Spring - Winter	**-0.07**	**-8.724**	**<.0001**	**<.0001**
		Summer - Winter	**-0.0984**	**-12.155**	**<.0001**	**<.0001**
CO_2 flux		Pairwise (lme)	Estimate	t.ratio	p	p-adj
	Zone	**Deep– Shallow**	**4.73**	**6.83**	**0.000**	**0**
		Deep-Riparian	**1.99**	**5.34**	**0.0000**	**0**
		Riparian-Deep	**2.38**	**2.45**	**0.0159**	**0.0159**
	Season	Summer – Spring	1.74	1.80	0.07	0.11
		Autumn – Spring	0.72	1.12	0.26	0.32
		Winter – Spring	**-1.67**	**-2.99**	**0.004**	**0.01**
		Autumn – Summer	-0.5977	0.61	0.54	0.54
		Winter – Summer	**-2.98**	**-2.69**	**0.009**	**0.02**
		Winter – Autumn	**-2.33**	**-4.05**	**1e-04**	**6e-04**
	Zone / Season	**Deep Spring –Shallow Spring**	**5.001**	**3.19**	**0.007**	**0.014**
		Deep Spring –Riparian Spring	0.46	0.65	0.53	0.61
		Shallow Spring - Riparian Spring	**-4.09**	**-3.50**	**0.006**	**0.014**

Variables	Contrast				
	Deep Summer – Shallow Summer	**7.74**	**5.49**	**<.0001**	**<.0001**
	Deep Summer –Riparian Summer	**2.97**	**3.82**	**0.0007**	**0.00214**
	Shallow Summer - Riparian Summer	**-3.45**	**-2.48**	**0.02**	**0.03**
	Deep Autumn –Shallow Autumn	**4.001**	**4.35**	**0.0002**	**8e-04**
	Deep Autumn –Riparian Autumn	**2.96**	**6.22**	**<.0001**	**<.0001**
	Shallow Autumn - Riparian Autumn	-1.16	-1.11	0.28	0.42
	Deep Winter –Shallow Winter	0.073	0.53	0.61	0.61
	Deep Winter – Riparian Winter	0.48	0.64	0.53	0.61
	Shallow Winter - Riparian Winter	0.44	0.55	0.59	0.61
	Deep Spring-Deep Summer	0.457	1.572	0.131	0.2616
	Deep Spring- Deep Autumn	0.043	0.150	0.882	0.9771
	Deep Spring – Deep winter	0.255	0.661	0.522	0.6717
	Deep Summer- Deep Autumn	-0.269	-1.617	0.119	0.2616
	Deep Summer – Deep Winter	-0.048	-0.196	0.847	0.9342
	Deep Autumn- Deep Winter	0.230	1.276	0.219	0.3585
	Shallow Spring-Shallow Summer	-3.099	-1.520	0.146	0.2626
	Shallow Spring- Shallow Autumn	0.490	0.349	0.732	0.8779
	Shallow Spring – Shallow winter	**4.707**	**4.792**	**0.001**	**0.009**
	Shallow Summer- Shallow Autumn	2.404	1.609	0.121	0.2616
	Shallow Summer – Shallow Winter	**6.617**	**4.405**	**0.0004**	**0.0072**
	Shallow Autumn- Shallow Winter	**4.310**	**3.551**	**0.003**	**0.0162**

Variables	Contrast					
		Riparian Spring- Riparian Summer	-1.984	-1.880	0.074	0.2223
		Riparian Spring- Riparian Autumn	**-2.134**	**-3.168**	**0.005**	**0.02385**
		Riparian Spring – Riparian winter	0.373	0.406	0.691	0.8779
		Riparian Summer- Riparian Autumn	-0.061	-0.028	0.978	0.978
		Riparian Summer – Riparian Winter	2.572	0.970	0.344	0.4763
		Riparian Autumn- Riparian Winter	**2.492**	**2.706**	**0.016**	**0.05616**
CH_4 flux		Pairwise (lme)	Estimate	t.ratio	p	p-adj
	Season	**Summer – Spring**	**0.02**	**3.94**	**0.0007**	**0.004**
		Autumn – Spring	0.01	1.60	0.13	0.15
		Winter – Spring	-0.0	-1.3	0.22	0.22
		Autumn – Summer	**-0.01**	**-1.91**	**0.07**	**0.102**
		Winter – Summer	**-0.05**	**-2.68**	**0.01**	**0.04**
		Winter – Autumn	-0.04	-2.058	0.06	0.10

SI Table S5: Average abundance of macroinvertebrate taxa in control (*N*=6) and treatment ponds (*N*=6) collected in gravel (G) and macrophytes (M) zones in June 2020, two weeks after the three replicated Bti applications. Reduced species numbers potentially due to Bti application are highlighted in bold and differences are marked by a blue asterisk (*). The data from Gerstle et al. (2022) and Kolbenschlag et al. (2023).

Order	**Family**	**Taxa**	**Control FPMs**			**Bti FPMs**			**Grand Total**
			Macroinvertebrates						
			G	M	Total	G	M	Total	
Odonata	**Aeshnidae**	**Aeshnidae**	4	54	58	8	88	96	154
	Libellulidae	**Libellulidae**	**47**	**523**	**570**	**35**	**313**	**348**	**918**
	Coenagrionidae	**Coenagrionidae**	**10**	**249**	**259**	**17**	**140**	**157**	**416**
Diptera	**Chironomidae**	**Chironominae**	**916**	**2007***	**2923**	**510**	**1048***	**1558**	**4481**
		Chironomidae	**88**	**184***	**272**	**70**	**59***	**129**	**401**
		Tanypodinae	**299**	**1566***	**1865**	**277**	**1261***	**1538**	**3403**
		Orthocladiinae	**91**	**1085***	**1176**	**41**	**401***	**442**	**1618**
Ephemeroptera	Caenidae	Caenidae	14	97	111	32	65	97	208

Order	Family	Taxa	Control FPMs			Bti FPMs			Grand Total
	Baetidae	Baetidae	290	391	681	320	462	782	1463
			Emerging insects						
Diptera	**Chironomidae**	**Chironomidae**	**16492**	**-**	**-**	**14122***	**-**	**-**	**30614**
Ephemeroptera	Baetidae	Baetidae	1545	-	-	1729	-	-	3274

References

Ganglo, C., Manfrin, A., Mendoza-lera, C., & Lorke, A. (2022). Biocide treatment for mosquito control increases CH4 emissions in floodplain pond mesocosms. *Frontiers in Water*, 10. https://doi.org/10.3389/frwa.2022.996898

Gerstle, V., Manfrin, A., Kolbenschlag, S., Gerken, M., Islam, A. S. M. M. U., Entling, M. H., … Brühl, C. A. (2022). Benthic macroinvertebrate community shifts based on Bti-induced chironomid reduction also decrease Odonata emergence. *Environmental Pollution*, *316*(P1), 120488. https://doi.org/10.1016/j.envpol.2022.120488

Keuskamp, J. A., Dingemans, B. J. J., Lehtinen, T., Sarneel, J. M., & Hefting, M. M. (2013). Tea Bag Index: A novel approach to collect uniform decomposition data across ecosystems. *Methods in Ecology and Evolution*, *4*(11), 1070–1075. https://doi.org/10.1111/2041-210X.12097

Kolbenschlag, S., Gerstle, V., Eberhardt, J., Bollinger, E., Schulz, R., Brühl, C. A., & Bundschuh, M. (2023). A temporal perspective of aquatic subsidy: Bti affects the emergence of Chironomidae. *Ecotoxicology and Environmental Safety*, *250*, 114503. https://doi.org/10.1016/j.ecoenv.2023.114503

Appendix III

Submitted paper

(Ganglo, C., Manfrin, A., Mendoza-Lera, C. & Lorke, A. (2023). Effects of chironomids density and mosquito biocide on methane dynamics in freshwater sediments. Plos One (resubmitted 30 June 2023)

Effects of chironomid larvae density and mosquito biocide on methane dynamics in freshwater sediments

Caroline Ganglo[a1], Alessandro Manfrin[a], Clara Mendoza-Lera[a], Andreas Lorke[a]

[a]*iES Landau, Institute for Environmental Sciences, RPTU Kaiserslautern-Landau, Fortstr. 7, D-76829 Landau, Germany*

[1]Email: carolineganglo20@gmail.com

26 Pages, 3 Figures, 1 Table

Plos One

Abstract

Small lentic water bodies are important emitters of methane (CH_4), but the processes regulating CH_4 dynamics and their susceptibility to human-induced stressors are not fully understood. Bioturbation by chironomid larvae has been proposed as a potentially important factor controlling CH_4 dynamics in aquatic sediments. Chironomid abundance can be affected by the application of biocides for mosquito control, such as Bti (*Bacillus thuringiensis* var. *israelensis*). Previous research has attributed increases in CH_4 emissions after Bti application to reduced bioturbation by chironomids. In this study, we tested the effect of chironomid bioturbation and Bti addition on CH_4 production and emission from natural sediments. In a set of 15 microcosms, we compared CH_4 emission and production rates with high and low densities of chironomid larvae at the bioturbating stage, and standard and 5 x standard Bti dose, with sediments that contained neither larvae nor Bti. Regardless of larvae density, the chironomids did not affect CH_4 emission and production of the sediment, although both rates were more variable in the treatments with organisms. 5xBti dosage, however, led to a more than three-fold increase in CH_4 and CO_2 production rates, likely stimulated by bioavailable dissolved carbon in the Bti excipient.

Our results suggest weak effects of bioturbating chironomid larvae on the CH_4 dynamics in aquatic ecosystems. Furthermore, our results point out towards potential functional implications of Bti for carbon cycling beyond those mediated by changes in the macroinvertebrate community.

Keywords Bio-irrigation, Macroinvertebrates; Bio-engineers; Aquatic pollution, greenhouse gases, Ponds

1 Introduction

Freshwater ecosystems are the largest natural source of methane (CH_4) [1] and small, shallow aquatic systems are particular hotspots of carbon cycling [2], by contributing about 41% to the global diffusive CH_4 emissions from lentic water bodies [3]. CH_4 is mostly produced in anoxic sediments as a function of the availability of labile carbon and alternative terminal electron acceptors, and temperature [4-6]. Under aerobic conditions, CH_4 can be oxidized to carbon dioxide (CO_2) [7]. Tube-dwelling macroinvertebrates, such as the most widely distributed Chironomidae (hereafter referred to as chironomids), rework and ventilate sediments [8]. These bioturbating activities promote aerobic processes in the upper sediment [9-11], and potentially modulate CH_4 and CO_2 dynamics [8]. Burrow construction and ventilation is limited to the latest larval stage of chironomids (third to fourth instar) [12].

Experimental evidence for the effects of chironomid larvae density and activity on CH_4 production and emission across the sediment-water interface, however, is limited and findings are contrasting. Chironomids may affect CH_4 dynamics through trophic and non-trophic interactions [13]. Potential trophic interactions include the feeding on organic matter [14] and CH_4 oxidizing bacteria [15,16]. Non-trophic effects include enhanced transport of nutrients and oxygen (O_2) into the sediment, increasing the volume of oxic sediment, and aerobic respiration [13,17-19]. On the one hand, laboratory incubations of paddy soils showed that chironomids had no effect on CH_4 emission across the sediment-water interface, neither by diffusion nor by ebullition [20]. On the other hand, Booth et al. [17] mechanically mimicked different bioturbation frequencies and observed non-linear responses of CH_4 emissions, mostly related to the triggering of gas bubble release (i.e., CH_4 ebullition).

The widespread application of the biocide *Bacillus thuringiensis* var. *israelensis* (Bti) for mosquito control [21-24] has been reported to reduce the larval density of non-target organisms [25-27], including chironomids [28]. This reduction in chironomid larvae density could potentially cascade into CH_4 dynamics through changes in the bioturbating activity as suggested by Ganglo et al. [29]. Furthermore, Ganglo et al. [30] suggested that the excipient of Bti that contains bioavailable dissolved organic carbon (DOC) could potentially boost aerobic respiration and methanogenesis for a given limited time [31-33]. Experimental evidence for these conjectures from former studies, however, is lacking, as the specific effect pathway by which Bti addition has affected the CH_4 emissions in the mesocosm experiments could not be disentangled.

In laboratory microcosms, we tested the effect of bioturbation by chironomid larvae (*Chironomus riparius*) and Bti application on CH_4 dynamics in freshwater sediments. We hypothesized that increasing chironomid larvae density would result in a decrease in CH_4 production and emissions due to increased bioturbating activity that reduces anoxic sediment (increasing CO_2 emissions from aerobic respiration). We further hypothesized that the addition of Bti in absence of chironomids would stimulate the production and emission of CH_4 and CO_2 due to addition of labile organic carbon.

2 Material and Methods

2.1 Experimental design

We conducted the experiment in gas-tight microcosms (1-L glass bottles, height 17.8 cm, radius 4.5 cm, area 63.5 cm^2) containing 0.19 L of sediment (3 cm height), 0.2 L of overlying water (3 cm height), and 0.61 L of headspace (**Figure 1A**). We sampled the headspace gas for CH_4 and CO_2 through a connector in the lid and measured dissolved O_2 concentration in the water through contactless sensors

(PyroScience GmbH, Germany) at 2 cm above the sediment surface. The relatively large headspace volume provided sufficient oxygen for maintaining the concentrations of dissolved oxygen in the water well above 30% oxygen saturation, which has been reported as a threshold for alterations of the bioturbating activity of chironomid larvae [34,35]. To ensure gas equilibration between the water and the headspace, we continuously aerated the water with headspace air using an internal air pump and a submerged bubble diffusor (**Figure 1**). The gas recirculation rate (150 mL h^{-1}) generated gentle flows in the water, without causing sediment resuspension.

We collected sediment and water from a pond at the Eußerthal Ecosystem Research Station (49°15'16" N, 7°57'42" E, facility of the University of Kaiserslautern-Landau, Germany, no permits were required). We sieved the sediment (mesh size 0.2 mm) to remove debris and large organisms and acclimated it to the experimental conditions (25°C ± 2, in darkness) for 10 days.

The experimental design consisted of four treatments and a control (*n*=3, **Figure 1B-F**): i) low, and ii) high chironomid larvae density, iii) standard Bti concentration (no chironomids); iv) five-times standard Bti concentration (no chironomids). Finally, the control conditions consisted of sediment and overlying water without chironomids or Bti. The treatments with chironomid larvae contained 16 (Low larvae density) and 32 (High larvae density) *Chironomus riparius* third to fourth instar larvae (**Figure 1C-D**). These densities correspond to 2500 and 5000 individuals m^{-2}, which is in the mid-range of densities found in shallow lake sediments (70 – 11000 individuals m^{-2}, [36]. We cultured the larvae following OECD (Organisation for Economic Co-operation and Development) guidelines [37] for about three months until reaching third to fourth instar and the experiment required no special permission. *Chironomus riparius* third to fourth instar larvae (10-15 mm body length) bioturbate

before emerging as adults [20,38]. We cultured the larvae in three aquaria (4 L, height 8 cm, surface area 588 cm^2) containing 200 mL of a mixture of sediment consisting of peat, kaolin clay, and sand, purchased from a local garden center (OECD 2004) and a litter of Borgmann medium (174 mg $CaCl_2 \cdot 2H_2O$, 85.5 mg $NaHCO_3$, 61.5 mg $MgSO_4 \cdot 7H_20$, 1.03 mg NaBr and 3.8 mg KCl in 1 L of deionized water). Once per week, we replaced the culture medium, and fed the larvae with 23.52 g of fish food (Tetramin flakes).

The Bti treatments consisted of one at the standard field application rate (2.9 x 10^9 International Toxic Units (ITU; [39,40]) and another at five times that rate (hereafter referred to as Bti and 5xBti, respectively, **Figure 1**). To each treatment, we added 1 mL of a Bti stock solution containing 0.76 mg mL^{-1} and 3.84 mg mL^{-1} of VectoBac WDG (2400 ITU mg^{-1}) (Valent BioSciences Corporation, Illinois, USA) (**Figure 1**). We estimated the amount of dissolved organic carbon (DOC) contained in the Bti stock solutions by catalytic combustion, after acidification with hydrochloric acid (HCl) to remove inorganic carbon, following DIN EN ISO/IEC 17025:2018. We added 0.18 ± 0.02 mg DOC (15 ± 1.6 µmol carbon) to Bti and 0.84 ± 0.12 mg DOC (70 ± 10 µmol carbon, all values as mean ± standard deviation) to 5xBti. These additions correspond to increases in surface water DOC concentrations of 0.91 ± 0.10 mg L^{-1} and 4.24 ± 0.61 mg L^{-1}. We determined specific ultraviolet absorbance ($SUVA_{254}$) of filtered (pore size 0.45 µm, Altmann Analytik PA4525-100) Bti solution using a UV–VIS scanning spectrophotometer (T3,15A/H, 232B105 Analytik Jena AG Germany) with a 1 cm cuvette and a wavelength of 254 nm. We determined the $SUVA_{254}$ (3.18 ± 0.16 L mg^{-1} m^{-1}) as the ratio of the measured absorbance (0.29 ± 0.05 cm^{-1}) and the DOC concentration (9.15 ± 1.09 mg L^{-1}) in the sample multiplied by 100.

Prior to the start of the experiment, we filled all microcosms (plus three additional ones for initial concentration measurements, see below) with sediment and sterile-filtered pond water and let them settle for 72 hours open to the atmosphere. After 72 hours, we added the larvae and Bti to the corresponding microcosms (Figure 1b-f) and gas-tight closed them. We used the three additional microcosms to determine the total initial amount of CH_4 and CO_2 in the pore water and in the surface water of the microcosms, by measuring the headspace concentrations after vigorous shaking (to equilibrate the pore and surface water). These microcosms were subsequently discarded. At 24 h, 72 h, and 120 h after the start of the experiment, we measured dissolved O_2 concentration, the CO_2 and CH_4 mixing ratios in the headspace to determine O_2 consumption, CO_2 and CH_4 emission rates. We ended the experiment when we detected the first emerged adult chironomid at 120 h. After the last headspace sampling at 120 h, we vigorously shook all microcosms to ensure full equilibration between pore water, surface water, and the headspace, and collected gas samples from the headspace to determine the total amount of CH_4 and CO_2 in the microcosms (dissolved and gaseous). We used the difference between the total amount at the end and the beginning of the experiment to determine the net production of CO_2 and CH_4, which accounts for the gas that has accumulated in the pore water during the experiment.

2.2 CO_2 and CH_4 emission and net production and oxygen consumption

At each sampling (24 h, 72 h, and 120 h after the start of the experiment), we collected 100 µL of headspace gas from each microcosm using a gastight syringe (Hamilton, USA). he mixing ratios (ppmv) of CO_2 and CH_4 were measured by injecting the samples into a gas analyzer (Ultra-portable Greenhouse Gas Analyzer; UGGA, Los Gatos Research Inc., Mountain View, CA, USA) in closed-loop operation [41]. By

assuming full equilibration between the headspace and the overlying water, we determined the amount of CH_4 and CO_2 (µmol) in the headspace and overlying water at each sampling time. We estimated gas-specific Henry coefficients at incubation temperature using common parametrizations [42]. We then calculated the emissions rates of CH_4 and CO_2 as the difference in amount between two subsequent samplings divided by the elapsed time. The emission rates account for the fluxes across the sediment-water interface and potential oxidation of CH_4 and CO_2 production by respiration in the surface water.

After each headspace sampling, we measured dissolved O_2 concentration in the overlying water. We calculated the amount of O_2 (µmol) as the sum of O_2 gas in the headspace and dissolved O_2 in the overlying water by assuming equilibrium between the water and the headspace. We calculated O_2 consumption rates (i.e., respiration) from the difference between two subsequent samplings divided by the elapsed time.

We estimated the total net production rates of CH_4 and CO_2 as the difference between the mean initial total and final CH_4 and CO_2 amounts divided by the total experimental time (120 h). We calculated the initial total amount as the mean of the three additional microcosms. The net CH_4 and CO_2 production rates account for the emissions and gas was produced in the sediment but not emitted to the water and headspace during the incubation period.

2.3 Statistical analysis

We used a linear mixed effect model [43] implemented in the lme function for R [44] to test for differences in amount, emission, and net production rates of CH_4, CO_2, the ratios of emission to net production rate, and O_2 consumption rate among

treatments (control, low and high chironomid larvae density, Bti and 5 × Bti). For each variable, we considered treatment as a fixed factor, and replicated microcosms and sampling time as random factors (except for the net CH_4 and CO_2 production rates which were not replicated in time). We assessed model residuals using quantile-quantile plots and plots of residuals versus fitted values. When needed, we log-transformed dependent variables to meet assumptions of normality and homogeneity. For significant effects, we applied a post-hoc contrast analysis using the lsmeans function for R. To decrease the false discovery rate due to multiple testing, we adjusted p-values using the Benjamini-Hochberg correction [45].

3 Results

Throughout the experimental time, the surface water remained well oxygenated with a mean concentration of dissolved O_2 in the overlying water of 7.0 ± 0.7 mg L^{-1} (corresponding to 81 ± 8 % O_2 saturation, with a minimum value of 63 %) at the last sampling. Overall, we observed CH_4 and CO_2 production, and O_2 consumption in all treatments (**Figure 2**). For chironomid density treatments, the emission of both CO_2 and CH_4 were highly variable compared to the control and tended to increase with density, yet no differences were observed (**Figure 2A-B, Table 1, S1**). O_2 consumption was not affected by chironomid density (**Figure 2C**). Alike the emissions, net production rates of CO_2 and CH_4, which additionally consider gas that has accumulated in the sediment, were comparable between the control and both densities, which were more variable than the other treatments (**Figure 2D-E, Table 1, S1**).

The addition of Bti, did neither affect CO_2 and CH_4 emission, nor O_2 consumption compared to the control (**Figure 2A-C, Table 1, S1**). However, Bti

promoted net production of CH_4 and CO_2 at the 5x dose, whereas no effect was observed at the standard dose (**Figure 2 D-E, Table S1, S2**). Compared to the effect of chironomid density, Bti had an affect at the 5x dose for CH_4, but not for CO_2 (**Figure 2D-E, Table 1, S1, S2**).

The ratio of CO_2 emission to net production was comparable between control and any chironomid density (**Figure 3A, Table 1, S1, S2**), indicating that most of the CO_2 produced during the experiment was emitted to the overlying water and headspace. For Bti, the ratio of CO_2 emission and production rates was significantly lower than the control, and the net production rates exceeded the emission by a factor of three (**Figure 3A**). Overall, the ratio of CH_4 emission to net production was comparable among treatments (**Figure 3B, Table 1, S1**). For the control and the Bti treatments, the ratio of CH_4 emission to net production was smaller than 1% for both Bti treatments and control, indicating that most of the produced CH_4 had accumulated in the sediment (**Figure 3B**). While both chironomid densities had higher variability and the ratio tended to be above 10% (**Figure 3A-B, Table S2**).

Table 1: Linear mixed effect model for the effects of treatment on CH_4, CO_2 emission and net production, and O_2 consumption. Significant differences at $p < 0.05$ are indicated in bold letters (*F*-statistics, numDF: numerator degrees of freedom; denDF: denominator degrees of freedom). See the complete results of the statistical analysis in **SI, Table S1** and **S2.**

Variables	Factors	numDF	denDF	*F*	*p*
CH_4 emission (µmol d^{-1})	Treatment	4	10	0.93	0.48
CO_2 emission (µmol d^{-1})	**Treatment**	**4**	**10**	**3.55**	**0.04**

Variables	Factors	numDF	denDF	*F*	*p*
O_2 consumption (µmol d^{-1})	Treatment	4	10	0.47	0.75
Net CH_4 production (µmol d^{-1})	**Treatment**	**4**	**10**	**4.47**	**0.02**
Net CO_2 production (µmol d^{-1})	**Treatment**	**4**	**10**	**4.35**	**0.02**
Ratio CH_4 emission/ net production	Treatment	4	10	0.69	0.61
Ratio CO_2 emission/ net production	**Treatment**	**4**	**10**	**13.48**	**$5x10^{-4}$**

4 Discussion

4.1 Effects of bioturbation on methane dynamics in aquatic sediments

We hypothesized that higher density of chironomid larvae would result in lower net production and emission of CH_4 due to their bioturbating activity (pumping of oxygenated water into the sediment), which would reduce the volume of anoxic sediment and increase the volume of oxic sediment with aerobic metabolism. Contrary to our hypothesis, we found no effect of density on CH_4 emission and production. In presence of chironomids, CH_4 and CO_2 emission and production rates were highly variable and tended to increase with density.

Former studies simulated bioturbation by mechanical disturbances of the sediment surface and found an enhancement of CH_4 transport from porewater to overlying water associated with ebullitive emission but not for diffusive fluxes [17]. Our results with actual macroinvertebrate activity also indicate that bioturbation might not affect the total emissions (diffusive and ebullitive) as reported by [20], yet we have detected high variability associated with bioturbation, pointing towards some potential effect of bioturbation on emissions. We attribute this variability to the interplay of three main factors: (i) variability in chironomid activity, (ii) spatial distribution of the methane production in the sediment, and (iii) stochastic nature of bubble formation and ebullition. First, intraspecific variations, or different development speeds among

individuals that resulted in temporal and/or spatial variability of the carbon biogeochemistry of the sediments, as only mature larvae can bioturbate [10,46]. Additionally the bioturbating activity of chironomid larvae can be modulated by O_2 saturation and temperature, and higher activity can be expected at lower O_2 concentrations (Roskosch et al. 2012). Former studies found higher activity for burrow ventilation if the dissolved O_2 concentration on the overlying water decreased to values below 30% saturation [34,35], which is well above the lowest value observed at the end of our experiment.

Second, as suggested by the emission-to-net-production of CO_2 compared to that for CH_4, there was a spatial separation of aerobic respiration and methane production in the microcosms. While CO_2 produced by aerobic respiration in the oxygenated surface sediment was more rapidly transported to the overlying water, CH_4 production took place in deeper layers beyond the bioturbating activity, and CH_4 emission became limited by diffusion in the porewater. In addition to promoting microbial metabolism in the sediment, the respiration of the chironomid larvae contributed directly to net CO_2 production and emission rates, as well as to O_2 consumption. Chironomids respire between 2.9 and 6.5 µmol O_2 per day [9]. Assuming an average of 5 µmol per day and individual, the net O_2 consumption by chironomid larvae was 80 and 180 µmol O_2 per day for our low and high larvae densities, respectively. For a unity respiratory quotient, these rates fall in the range of observed increases in CO_2 emission in both treatments, suggesting that this increase was predominantly caused by larvae respiration rather than by microbial CO_2 production in the sediment. The observed changes in O_2 consumption rates were less pronounced, yet, as in other incubation experiments (e.g., Baranov et al. [10]), the variability

between different densities and replicates was high and may have offset the effect of chironomids.

Third, gas bubble formation and release from the sediment is controlled by small-scale heterogeneities in pore geometry and shows rather stochastic dynamics [47]. Although our experimental approach did not allow to distinguish ebullitive and diffusive fluxes and ebullition was not observed visually during the sampling, the release of single gas bubbles may have resulted in large changes in the headspace gas concentrations of the microcosms. We note that given the high net CH_4 production longer incubation periods might have resulted in gas bubble formation and transport by ebullition, which in turn could have led to higher and even more variable CH_4 emission rates during prolonged measurements. An additional influence of bioturbation on CH_4 emissions may occur through the influence on methane oxidation rates [20]. The lack of differences between the emission-to-net production ratio of CH_4 between the control and both larvae densities suggests that chironomids did not affect the overall balance between CH_4 production and oxidation rates. All in all, the potential of bioturbation by chironomid larvae to affect emission rates is strongly modulated by physical and biological factors.

4.2 Effects of Bti on methane dynamics in aquatic sediment

To the best of our knowledge, our study provides the first evidence of functional implications of the mosquito biocide Bti in biogeochemical cycling in freshwater aquatic ecosystems. Our second hypothesis stated that Bti excipients could represent a pulse of labile DOC, temporarily promoting aerobic (CO_2 dynamics) and anerobic carbon processing (CH_4 dynamics). Our results showed that the addition of Bti at high dose (5x standard dose) increased net CO_2 and CH_4 production, indicating that both aerobic

and anaerobic carbon metabolism might have been boosted by labile carbon availability upon Bti addition. The increase in net CO_2 production in Bti treatments was comparable to that due to chironomid activity. In comparison to the treatments with larvae and to the control, a larger fraction of the produced CO_2 was stored in the sediment, i.e., the emission to net production ratio was reduced.

The amount of carbon added with Bti was about one order of magnitude less than the difference in C-CO_2 (792 µmol) and C-CH_4 (321 µmol) produced in the 5xBti to the control. Consequently, the higher net CO_2 and CH_4 production rates in Bti treatments cannot be explained solely by the decomposition of the DOC added with Bti, even if it was completely metabolized during the five-day experimental period. The discrepancy could be explained by a stimulation of aerobic and anaerobic degradation of sediment organic carbon that was not available without the presence of Bti. This could either be through Bti-induced changes in the composition of the microbial community [48] or through priming effects [49] of the dissolved organic carbon in Bti excipients.

Increased CH_4 emissions upon treatment with Bti have also been observed in a mesocosm study [29]. There, the authors hypothesized that the increased emissions, which persisted for several months after Bti addition, were caused by a reduction in the density of chironomid larvae by Bti. Our results cannot confirm this conjecture and rather suggests that more direct effects of Bti on microbial communities and their activity were promoting the observed emission increase. Consequently, our study adds to the growing, yet very limited, evidence that chemical and microbial stressors can have adverse effects on CH_4 dynamics in affected aquatic ecosystems [29,50-52]. The biogeochemical implications of these stressors, including greenhouse

gas emissions, should receive more attention in assessments of their environmental impacts.

5 Author contributions

CG: conceptualization, methodology, data collection, data analysis, and original draft writing. AM: conceptualization, data analysis, and writing. CM-L and AL: conceptualization, methodology, data analysis, and writing. All authors contributed to the article and approved the submitted version.

6 Acknowledgments

This work was funded by the Deutsche Forschungsgemeinschaft (DFG, German Research Foundation) −326210499/GRK2360, SystemLink. We are grateful for the support of EERES for access to facilities. We acknowledge the support of Lorenzo Rovelli, Gerrit Rau, Christoph Bors, Rajdeep Roy, Karin Meyer, Simone von Schlichtegroll, Verena Gerstle, Sara Kolbenschlag, Sebastian Pietz, Nina Röder, Alexis P. Roodt, Anja Knäbel, Kennedy Anoka, Victoria Ayesu-Atsu, Housam Ismaeli, Sandhya Magesh, and Michael Schwarz during the planning and implementation of the experiment. We thank Viktor Baranov for valuable support during the planning of the experiments and the conceptualization of this manuscript.

7 Conflict of interest

The authors declare no commercial or financial conflict of interest.

8 References

1. Rosentreter, J. A., Borges, A. V, Deemer, B. R., Holgerson, M. A., Liu, S., Song,

C., et al. (2021). Half of global methane emissions come from highly variable aquatic ecosystem sources. *Nature Geoscience*, *14*, 225–230. https://doi.org/10.1038/s41561-021-00715-2

2. Downing, J. A. (2010). Emerging global role of small lakes and ponds: little things mean a lot. *Limnetica*, *29*(1), 9–24. https://doi.org/10.23818/limn.29.02
3. Holgerson, M. A., & Raymond, P. A. (2016). Large contribution to inland water CO2 and CH4 emissions from very small ponds. *Nature Geoscience*, *9*(3), 222–226. https://doi.org/10.1038/ngeo2654
4. Bastviken David. (2022). Methane. In: Tockner, Klement, Encyclopedia of Inland Waters 2nd edition. Oxford: Elsevier. 1,136-154. dx.doi.org/10.1016/B978-0-12-819166-8.00147-X
5. Grasset Charlotte, Mendonça Raquel, Villamor Saucedo Gabriella, Bastviken David, Roland Fabio, Sobek Sebastian (2018). Large but variable methane production in anoxic freshwater sediment upon addition of allochthonous and autochthonous organic matter. Limnology and Oceanography, 63 (4), 1488-1501. https://doi.org/10.1002/lno.10786
6. Segers, R. (1998). Methane Production and Methane Consumption: A Review of Processes Underlying Wetland Methane Fluxes. Berlin: Springer. p. 41, 23–51.
7. Borrel, G., Jezequel, D., Biderre-Petit, C., Morel-Desrosiers, N., Jean-Pierre Morel, Pierre Peyret, G. F., & Lehours, A.-C. (2011). Production and consumption of methane in freshwater lake ecosystems. *Research in Microbiology*, *162*, 832–847. https://doi.org/10.1016/j.resmic.2011.06.004
8. Hölker, F., Vanni, M. J., Kuiper, J. J., Meile, C., Grossart, H. P., Stief, P., et al. (2015). Tube-dwelling invertebrates: Tiny ecosystem engineers have large

effects in lake ecosystems. *Ecological Monographs*, *85*(3), 333–351. https://doi.org/10.1890/14-1160.1

9. Murniati, E., Gross, D., Herlina, H., Hancke, K., & Lorke, A. (2017). Effects of bioirrigation on the spatial and temporal dynamics of oxygen above the sediment-water interface. *Freshwater Science*, *36*(4), 784–795. https://doi.org/10.1086/694854
10. Baranov, V., Lewandowski, J., & Krause, S. (2016). Bioturbation enhances the aerobic respiration of lake sediments in warming lakes. Biology Letters, 12(8), 8-11. https://doi.org/10.1098/rsbl.2016.0448
11. Hodkinson, I. D., & Williams, K. A. (1980). Tube Formation and Distribution of Chironomus Plumosus L. (Diptera : Chironomidae) in a Eutrophic Woodland Pond. In *Chironomidae*. https://doi.org/10.1016/b978-0-08-025889-8.50051-9
12. Adámek, Z., & Maršálek, B. (2013). Bioturbation of sediments by benthic macroinvertebrates and fish and its implication for pond ecosystems: A review. Aquaculture International, 21(1), 1–17. https://doi.org/10.1007/s10499-012-9527-3
13. Colina, M., Meerhoff, M., Pérez, G., Veraart, A. J., Bodelier, P., Horst, A. Van Der, & Kosten, S. (2021). Trophic and non- - trophic effects of fish and macroinvertebrates on carbon emissions. *Freshwater Biology*, *66*(9), 1–15. https://doi.org/10.1111/fwb.13795
14. De Haas, E. M., Wagner, C., Koelmans, A. A., Kraak, M. H. S., & Admiraal, W. (2006). Habitat selection by chironomid larvae: Fast growth requires fast food. *Journal of Animal Ecology*, *75*(1), 148–155. https://doi.org/10.1111/j.1365-2656.2005.01030.x
15. Jones, R. I., & Grey, J. (2011). Biogenic methane in freshwater food webs.

Freshwater Biology, *56*(2), 213–229. https://doi.org/10.1111/j.1365-2427.2010.02494.x

16. Deines, P., Bodelier, P. L. E., & Eller, G. (2007). Methane-derived carbon flows through methane-oxidizing bacteria to higher trophic levels in aquatic systems. *Environmental Microbiology*, *9*(5), 1126–1134. https://doi.org/10.1111/j.1462-2920.2006.01235.x
17. Booth, M. T., Urbanic, M., Wang, X., & Beaulieu, J. J. (2021). Bioturbation frequency alters methane emissions from reservoir sediments. *Science of the Total Environment*, *789*, 1 9. https://doi.org/https://doi.org/10.1016/j.scitotenv.2021.148033
18. Lewandowski, J., Laskov, C., & Hupfer, M. (2007). The relationship between Chironomus plumosus burrows and the spatial distribution of pore-water phosphate, iron and ammonium in lake sediments. *Freshwater Biology*, *52*(2), 331–343. https://doi.org/10.1111/j.1365-2427.2006.01702.x
19. Andersen, F., Jørgensen, M., & Jensen, H. S. (2006). The influence of Chironomus plumosus larvae on nutrient fluxes and phosphorus fractions in aluminum treated lake sediment. *Water, Air, and Soil Pollution: Focus*, *6*(5–6), 465–474. https://doi.org/10.1007/s11267-006-9030-9
20. Kajan, R., & Frenzel, P. (1999). The effect of chironomid larvae on production, oxidation and fluxes of methane in a flooded rice soil. *FEMS Microbiology Ecology*, *28*(2), 121–129. https://doi.org/10.1016/S0168-6496(98)00097-X
21. Bordalo, M., Machado, A., Campos, D., Coelho, S., Rodrigues, A., Lopes, I., Pestana, J. (2021). Responses of benthic macroinvertebrate communities to a Bti-based insecticide in artificial microcosm streams.Environmental pollution (282) 117030. https://doi.org/10.1016/j.envpol.2021.117030

22. Brühl, C. A., Després, L., Frör, O., Patil, C. D., Poulin, B., Tetreau, G., & Allgeier, S. (2020). Environmental and socioeconomic effects of mosquito control in Europe using the biocide Bacillus thuringiensis subsp. israelensis (Bti). *Science of the Total Environment*, *724*, 1–16. https://doi.org/10.1016/j.scitotenv.2020.137800.

23. Jakob, C., & Poulin, B. (2016). Indirect effects of mosquito control using Bti on dragonflies and damselflies (Odonata) in the Camargue. *Insect Conservation and Diversity*, *9*(2), 161–169. https://doi.org/10.1111/icad.12155

24. Boisvert, M., & Boisvert, J. (2000). Effects of bacillus thuringiensis var. israelensis on target and nontarget organisms: A review of laboratory and field experiments. *Biocontrol Science and Technology*, *10*(5), 517–561.

25. Gerstle, V., Manfrin, A., Kolbenschlag, S., Gerken, M., Islam, A. S. M. M. U., Entling, M. H., … Brühl, C. A. (2023). Benthic macroinvertebrate community shifts based on Bti-induced chironomid reduction also decrease Odonata emergence. *Environmental Pollution*, *316*(P1), 2–8. https://doi.org/10.1016/j.envpol.2022.120488

26. Allgeier, S., Friedrich, A., & Brühl, C. A. (2019a). Mosquito control based on Bacillus thuringiensis israelensis (Bti) interrupts artificial wetland food chains. *Science of the Total Environment*, *686*, 1173–1184. https://doi.org/10.1016/j.scitotenv.2019.05.358

27. Allgeier, S., Kästel, A., & Brühl, C. A. (2019b). Adverse effects of mosquito control using Bacillus thuringiensis var. israelensis: Reduced chironomid abundances in mesocosm, semi-field and field studies. *Ecotoxicology and Environmental Safety*, *169*, 786–796. https://doi.org/10.1016/j.ecoenv.2018.11.050

28. Liber, K., K. L. Schmude and D. M. Rau (1998). "Toxicity of Bacillus thuringiensis var. Israelensis to Chironomids in Pond Mesocosms." Ecotoxicology 7(6): 343-354. DOI:10.1023/A:1008867815244

29. Ganglo, C., Manfrin, A., Mendoza-lera, C., & Lorke, A. (2022). Biocide treatment for mosquito control increases CH4 emissions in floodplain pond mesocosms. *Frontiers in Water*, 10. https://doi.org/10.3389/frwa.2022.996898

30. Ganglo, C., Mendoza-lera, C., Manfrin, A., Bolpagni, R., Gerstle, V., Kolbenschlag. S., Bollinger, E., Schulz, R., & Lorke, A. (2023). Does biocide treatment for mosquito control alter carbon dynamics in floodplain ponds? Science of the Total Environment. 872 (2), 161978. https://doi.org/10.1016/j.scitotenv.2023.161978

31. Berberich, M. E., Beaulieu, J. J., Hamilton, T. L., Waldo, S., & Buffam, I. (2020). Spatial variability of sediment methane production and methanogen communities within a eutrophic reservoir: Importance of organic matter source and quantity. *Limnology and Oceanography*, *65*(6), 1336–1358. https://doi.org/10.1002/lno.11392

32. Romeijn, P., Comer-Warner, S. A., Ullah, S., Hannah, D. M., & Krause, S. (2019). Streambed Organic Matter Controls on Carbon Dioxide and Methane Emissions from Streams. *Environmental Science and Technology*, *53*(5), 2364–2374. https://doi.org/10.1021/acs.est.8b04243

33. Grasset, C., Mendonça, R., Villamor Saucedo, G., Bastviken, D., Roland, F., & Sobek, S. (2018). Large but variable methane production in anoxic freshwater sediment upon addition of allochthonous and autochthonous organic matter. *Limnology and Oceanography*, *63*(4), 1488–1501. https://doi.org/10.1002/lno.10786

34. Roskosch, A., Hette, N., & Hupfer, M. (2012). Alteration of Chironomus plumosus ventilation activity and bioirrigation-mediated benthic fluxes by changes in temperature , oxygen concentration , and seasonal variations. *Freshwater Science*, *31*(2), 269–281. https://doi.org/10.1899/11-043.1

35. Walshe, B. (1950). The function of haemoglobin in Chironomus plumosus under natural conditions. Journal of experimental Biology,27 (1), 73-95. https://doi.org/10.1242/jeb.27.1.73

36. Mousavi, S. K. (2002). *Boreal chironomid communities and their relations to environmental factors — the impact of lake depth , size and acidity*. Boreal Environment Research. *7*,63-75.

37. OECD Guidelines for th etesting of chemicals. (2004). (April), 1–21.

38. Gallep, G. W. (1979). *Chironomid Influence on Phosphorus Release in Sediment-Water*. *60*(3), 547–556. https://doi.org/10.2307/1936075

39. Becker, N., (1997). Microbial control of mosquitoes: management of the upper Rhine mosquito population as a model programme. Parasitol. Today 13 (12), 485–487.

40. Becker, N. (2003). Ice granules containing endotoxins of microbial agents for the control of mosquito larvae - A new application technique. *Journal of the American Mosquito Control Association*, *19*(1), 63–66.

41. Wilkinson, J., Bors, C., Burgis, F., Lorke, A., & Bodmer, P. (2018). Measuring CO2 and CH4 with a portable gas analyzer: Closed-loop operation, optimization and assessment. *PLoS ONE*, *13*(4), 29617382. https://doi.org/10.1371/journal.pone.0193973

42. International Hydropower Association (IHA). (2010). GHG Measurement Guidelines for Freshwater Reservoirs.138.

43. Pinheiro, J., Bates, D., DebRoy, S., & Sarkar, D. (2022). *nlme: Linear and Nonlinear Mixed Effects Models*. https://doi.org/https://CRAN.R-project.org/package=nlme

44. R Core Team. (2013). R: A Language and Environment for Statistical Computing.

45. Benjamini, Y., & Hochberg, Y. (1995). Controlling the False Discovery Rate: A Practical and Powerful Approach to Multiple Testing. *Journal of the Royal Statistical Society: Series B (Methodological)*, *57*(1), 289–300. https://doi.org/10.1111/j.2517-6161.1995.tb02031.x

46. Lagauzère, S. Moreira, S. Koschorreck. M (2011). Influence of bioturbation on the biogeochemistry of littoral sediments of an acidic post-mining pit lake. Biogeosciences 8 (2), 339-352. doi:10.5194/bg-8-339-2011

47. Liu, L., T. De Kock, J. Wilkinson, V. Cnudde, S. Xiao, C. Buchmann, D. Uteau, S. Peth and A. Lorke (2018). "Methane Bubble Growth and Migration in Aquatic Sediments Observed by X-ray μCT." Environmental Science & Technology 52(4): 2007–2015. DOI:10.1021/acs.est.7b06061

48. Duguma, D., Hall, M. W., Rugman-Jones, P., Stouthamer, R., Neufeld, J. D., & Walton, W. E. (2015). Microbial communities and nutrient dynamics in experimental microcosms are altered after the application of a high dose of Bti. *Journal of Applied Ecology*, *52*(3), 763–773. https://doi.org/10.1111/1365-2664.12422

49. Kayler, Z. E., Premke, K., Gessler, A., Gessner, M. O., Griebler, C., Hilt, S., et al. (2019). Integrating aquatic and terrestrial perspectives to improve insights into organic matter cycling at the landscape scale. *Frontiers in Earth Science*, *7*(June), 1–14. https://doi.org/10.3389/feart.2019.00127

50. Wang, B., Stirling, E., He, Z., Ma, B., Zhang, H., Zheng, X., et al. (2021). Pollution

alters methanogenic and methanotrophic communities and increases dissolved methane in small ponds. *Science of the Total Environment*, *801*, 149723. https://doi.org/10.1016/j.scitotenv.2021.149723

51. Bollinger, E., Zubrod, J. P., Lai, F. Y., Ahrens, L., Filker, S., Lorke, A., & Bundschuh, M. (2021). Antibiotics as a silent driver of climate change? A case study investigating methane production in freshwater sediments. *Ecotoxicology and Environmental Safety*, *228*(113025), 2–11. https://doi.org/10.1016/j.ecoenv.2021.113025
52. Tong, T., & Xie, S. (2019). Impacts of sulfanilamide and oxytetracycline on methane oxidation and methanotrophic community in freshwater sediment. *Ecotoxicology*, *28*(4), 392–398. https://doi.org/10.1007/s10646-019-02026-0

Figure 1. Experimental microcosms (A), and experimental design (B) with four treatments and control: Control, Low**,** and High chironomid larvae density, Bti, and 5 x Bti (*n* = 3)**.**

Figure 2. Mean ± Standard Deviation emission rates of CH_4 (**A**), CO_2 (**B**), and O_2 consumption (**C**) (*n* = 6), and net production rates of CH_4 (**D**) and CO_2 (**E)** (*n* = 3) for each treatment (Control, Low larvae density, High larvae density, Bti, and 5 x Bti). Significant differences between treatments are indicated by different letters ($p \leq 0.05$).

Figure 3. Mean ± Standard Deviation ratios of emission-to-net production rates of CO_2 (**A**) and CH_4 (**B**) for each treatment (Control, Low larvae density, High larvae density,

Bti, and 5 x Bti). (n = 6). Significant differences ($p \leq 0.05$) between treatments are indicated by different letters.

SI Figure S1: Mean ± Standard Deviation of amount (µmol) of (**A**) CH, (**B**) CO_2, and (**C**) O_2 emitted for Control, Low and High Density, Bti and 5xBti at 24 h, 72 h, and 120 h during the incubation period (n=9), and the total final amount produced over the experiment (including dissolved and gaseous component in the sediment porewater) of (**D**) CH_4 and (**E**) CO_2 (n=3). Different letters above bar indicate significant differences within treatment at the same timepoint ($p \leq 0.05$).

SI Table S1: Linear mixed effect model selection using likelihood ratio tests (LRT) against reduced models. Treatment effect on CH_4 and CO_2 emission and net production, and O_2 consumption. Statistically significant differences are marked in bold ($p \leq 0.05$).

SI Table S2: Post-hoc pairwise comparisons of CH_4 and CO_2 emission and net production, and O_2 consumption. The estimates represent the mean difference between pairwise factors and t-ratio is the ratio of the estimate and the standard error. Statistically significant differences are marked in bold ($p \leq 0.05$).

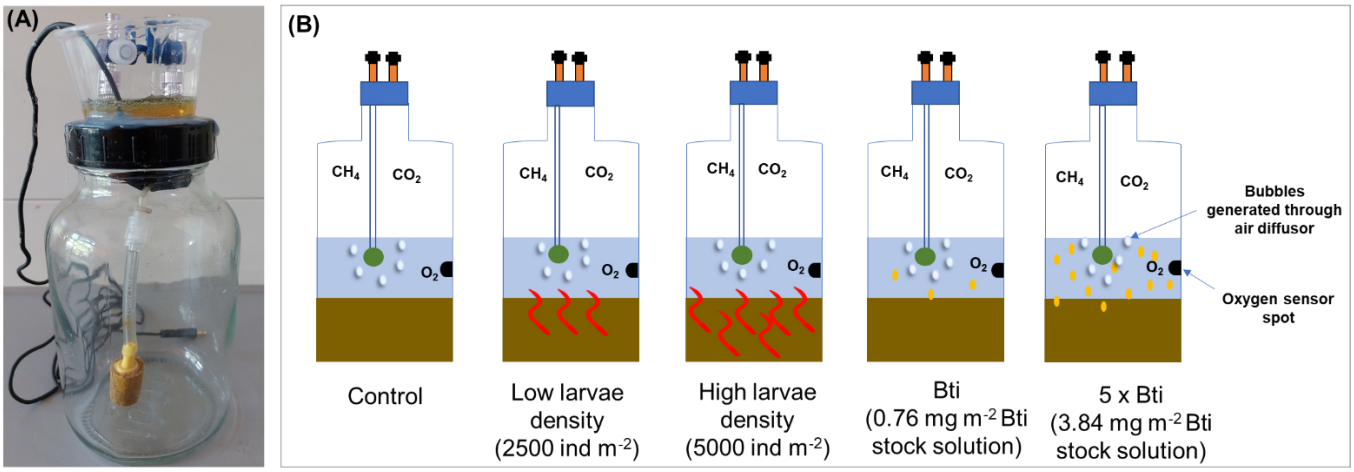

Figure 1. Experimental microcosms (A), and experimental design (B) with four treatments and control: Control, Low**,** and High chironomid larvae density, Bti, and 5 x Bti (*n* = 3)**.**

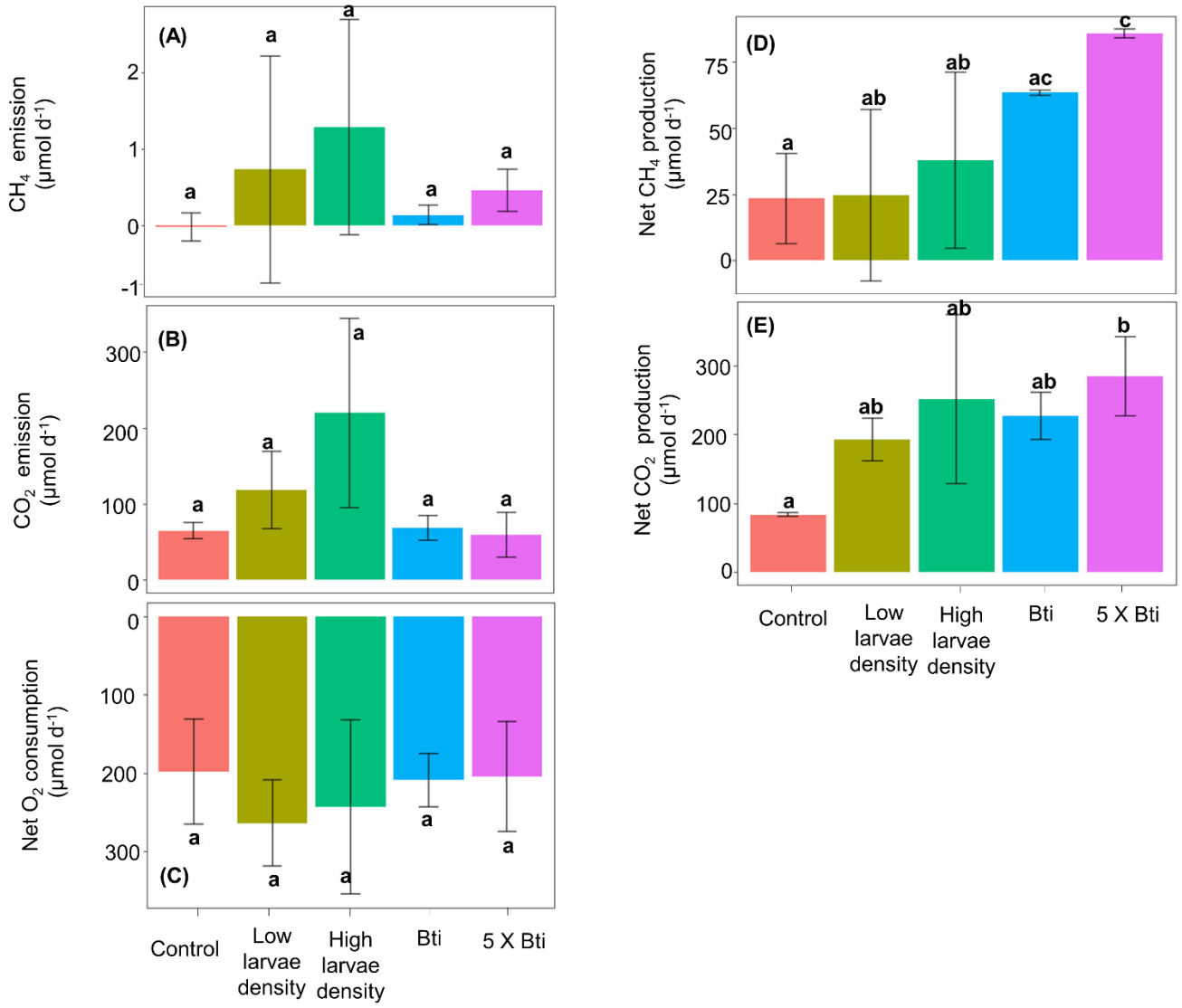

Figure 2. Mean ± Standard Deviation emission rates of CH_4 (**A**), CO_2 (**B**), and O_2 consumption (**C**) (n = 6), and net production rates of CH_4 (**D**) and CO_2 (**E**) (n = 3) for each treatment (Control, Low larvae density, High larvae density, Bti, and 5 x Bti). Significant differences between treatments are indicated by different letters ($p \leq 0.05$).

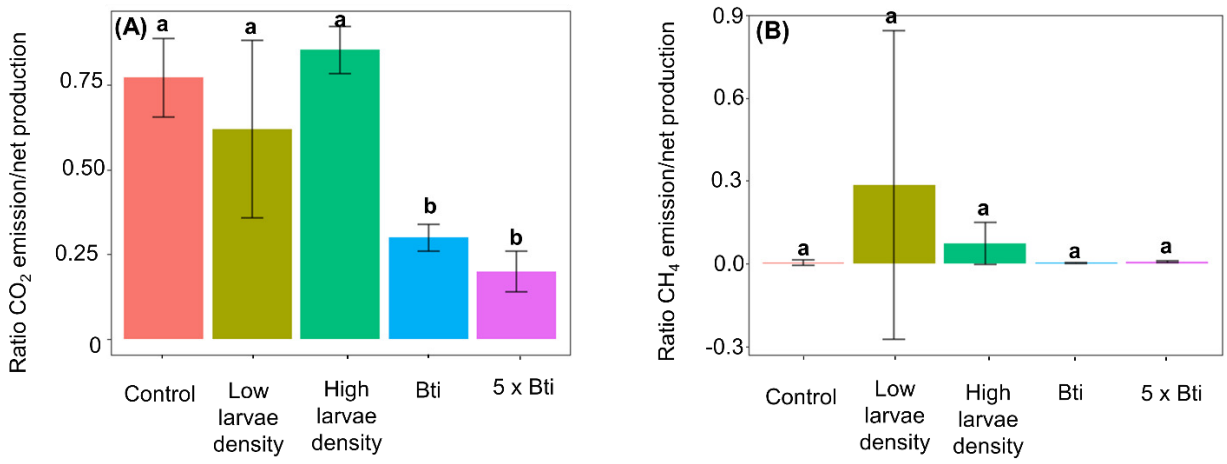

Figure 3. Mean ± Standard Deviation ratios of emission-to-net production rates of CO_2 (**A**) and CH_4 (**B**) for each treatment (Control, Low larvae density, High larvae density, Bti, and 5 x Bti). (n = 6). Significant differences ($p \leq 0.05$) between treatments are indicated by different letters.

Supporting information for:

Effects of chironomid larvae density and mosquito biocide on methane dynamics in freshwater sediments

Caroline Ganglo[a1], Alessandro Manfrin[a], Clara Mendoza-Lera[a], Andreas Lorke[a]

[a] *iES Landau, Institute for Environmental Sciences, RPTU Kaiserslautern-Landau, Fortstr. 7, D-76829 Landau, Germany*

[1]Email: carolineganglo20@gmail.com

6 Pages, 1 Figure, 2 Tables

Plos One

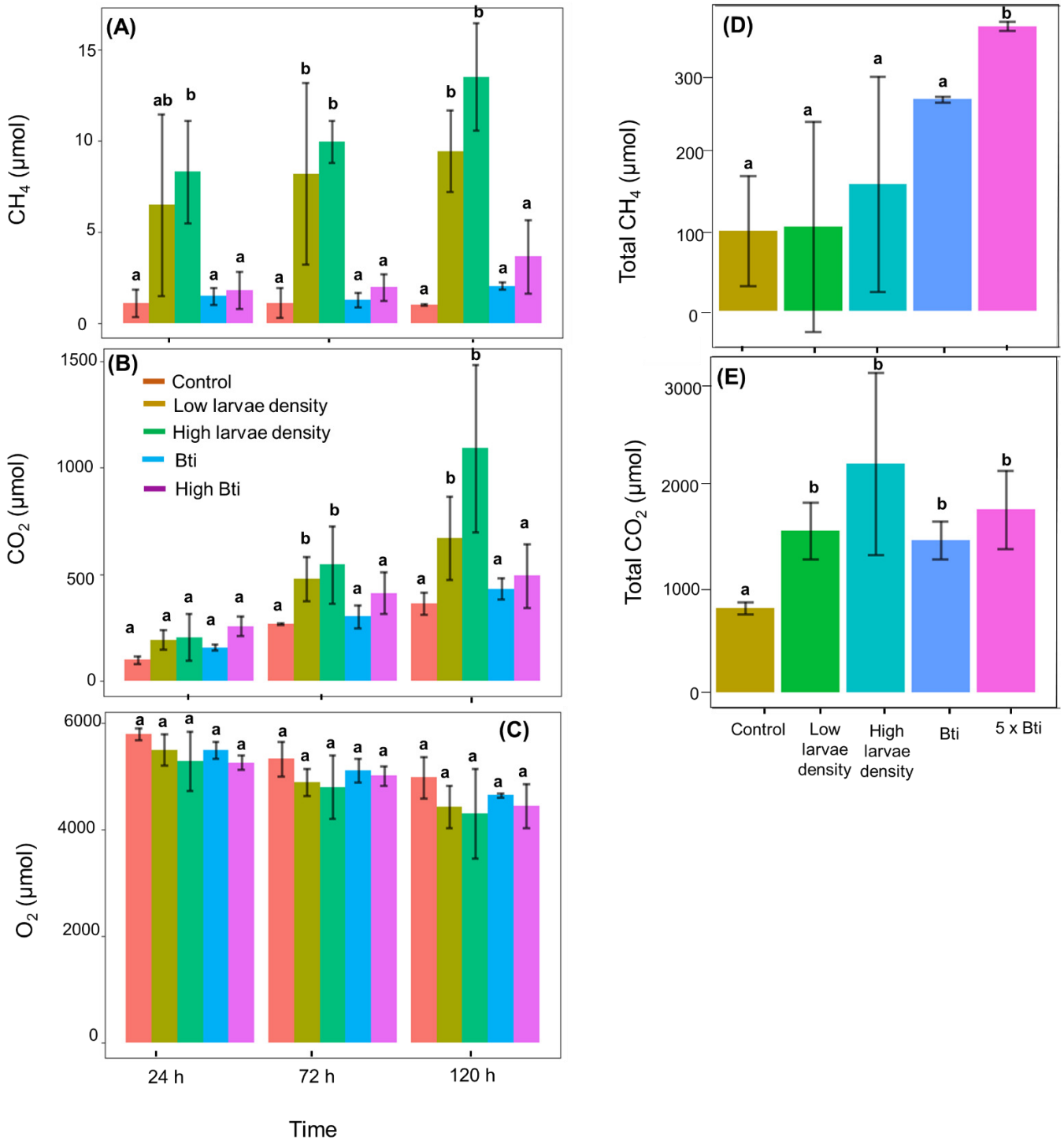

SI Figure S1: Mean ± Standard Deviation of amount (µmol) of (**A**) CH_4, (**B**) CO_2, and (**C**) O_2 emitted for Control, Low and High Density, Bti and 5xBti at 24 h, 72 h, and 120 h during the incubation period (n=9), and the total final amount produced over the experiment (including dissolved and gaseous component in the sediment porewater) of (**D**) CH_4 and (**E**) CO_2 (n=3).

Different letters above bar indicate significant differences within treatment at the same timepoint ($p \leq 0.05$)

SI Table S1: Linear mixed effect model selection using likelihood ratio tests (LRT) against reduced models. Treatment effect on CH_4 and CO_2 emission and net production, and O_2 consumption. Statistically significant differences are marked in bold ($p \leq 0.05$).

Variables	R^2 marginal	Factors	*F*-value ($_{numDF, denDF}$)	*p*-value
	Likelihood ratio test (LRT) against reduced model	LRT		
CH_4 emission (µmol d^{-1})	0.21	Treatment	7.72	0.10
			$F_{4,10}$=0.93	0.48
CO_2 emission (µmol d^{-1})	**0.50**	**Treatment**	**49.31**	**<.0001**
			$F_{4,10}$=3.55	**0.04**
O_2 consumption (µmol d^{-1})	0.11	Treatment	7.72	0.10
			$F_{4,10}$=0.47	0.75
Net CH_4 production (µmol d^{-1})	**0.56**	**Treatment**	**42.97**	**<.0001**
			$F_{4,10}$=4.47	**0.02**
Net CO_2 production (µmol d^{-1})	**0.55**	**Treatment**	**51.25**	**<.0001**
			$F_{4,10}$=4.35	**0.02**
Ratio CH_4 emission/ net production	0.16	Treatment	3.71	0.44
			$F_{4,10}$=0.69	0.61
Ratio CO_2 emission/ net production	**0.79**	**Treatment**	**13.87**	**0.007**
			$F_{4,10}$=13.48	**5e-04**

SI Table S2: Post-hoc pairwise comparisons of CH_4 and CO_2 emission and net production, and O_2 consumption. The estimates represent the mean difference between pairwise factors and t-ratio is the ratio of the estimate and the standard error. Statistically significant differences are marked in bold ($p \leq 0.05$).

Variables	Contrast	Pairwise structure	Estimate	*t*-value	*p*	*p*-adjusted
CO_2 emission (µmol d^{-1})	Treatment	Low larvae density - Control	53.59	1.053	0.4992	0.8256
		High larvae density - Control	155.13	3.048	0.0463	0.0729
		Bti - Control	3.62	0.071	0.9446	1
		5 x Bti - Control	-5.68	-0.112	0.9446	1
		High larvae density - Low larvae density	-101.54	1.995	0.185	0.3338
		Bti - Low larvae density	-49.96	-0.982	0.4992	0.8576
		5 x Bti – Low larvae density	-59.27	-1.164	0.4992	0.7704
		Bti – High larvae density	-151.51	-2.977	0.0463	0.0813
		5 x Bti – High larvae density	-160.81	-3.159	0.0463	0.0613
		5 x Bti - Bti	-9.3	-0.183	0.9446	0.9997
Net CH_4 production (µmol d^{-1})	Treatment	Low larvae density - Control	1.16	0.064	0.9499	1
		High larvae density - Control	14.39	0.798	0.5333	0.9253
		Bti - Control	39.97	2.217	0.1137	0.2487
		5 x Bti - Control	62.29	3.455	0.0344	**0.0388**
		High larvae density - Low larvae density	13.23	0.734	0.5333	0.9435
		Bti - Low larvae density	38.81	2.152	0.1137	0.2715
		5 x Bti – Low larvae density	61.13	3.39	0.0344	**0.0429**
		Bti – High larvae density	25.58	1.419	0.3107	0.6306
		5 x Bti – High larvae density	47.9	2.656	0.0801	0.1321
		5 x Bti - Bti	22.32	1.238	0.3486	0.7314
Net CO_2 production (µmol d^{-1})	Treatment	Low larvae density - Control	109.6	2.095	0.1565	0.293
		High larvae density - Control	168.1	3.214	0.0464	0.0564
		Bti - Control	143.5	2.744	0.069	0.1159

Variables	Contrast	Pairwise structure	Estimate	*t*-value	*p*	*p*-adjusted
		5 x Bti - Control	200.9	3.841	0.0213	**0.0326**
		High larvae density - Low larvae density	58.5	1.118	0.426	0.7938
		Bti - Low larvae density	33.9	0.648	0.6049	0.963
		5 x Bti – Low larvae density	91.3	1.746	0.2229	0.4512
		Bti – High larvae density	-24.6	-0.47	0.6485	0.9885
		5 x Bti – High larvae density	32.8	0.627	0.6049	0.9671
		5 x Bti - Bti	57.4	1.097	0.426	0.8043
Ratio net CO_2 emission /net production		Low larvae density - Control	-0.1526	-1.374	0.2493	0.6558
		High larvae density - Control	0.0818	0.736	0.4786	0.9429
		Bti - Control	-0.4731	-4.26	0.0042	**0.0113**
		5 x Bti - Control	-0.5731	-5.16	0.0018	**0.003**
		High larvae density - Low larvae density	0.2344	2.11	0.0872	0.2872
		Bti - Low larvae density	-0.3205	-2.886	0.027	0.0934
		5 x Bti – Low larvae density	-0.4205	-3.786	0.0071	**0.0232**
		Bti – High larvae density	-0.5548	-4.996	0.0018	**0.0038**
		5 x Bti – High larvae density	-0.6548	-5.896	0.0015	**0.0011**
		5 x Bti - Bti	-0.1	-0.9	0.4323	0.8904